

**ELUCIDATION OF THE ROLES AND FUNCTIONAL IMPLICATIONS  
OF THE RET RECEPTOR TYROSINE KINASE IN CANCER**

by

Piriya Yoganathan

A thesis submitted to the Department of Pathology and Molecular Medicine

In conformity with the requirements for

the degree of Doctor of Philosophy

Queen's University

Kingston, Ontario, Canada

(December, 2017)

Copyright © Piriya Yoganathan, 2017

## Abstract

RET is a receptor tyrosine kinase that plays important roles in normal development of the kidney, spermatogonia, and neuroendocrine tissues. RET is also implicated in various diseases, including tumors of the breast, prostate and thyroid. Normally, RET is activated through the formation of a tri-molecular complex involving its co-receptor, GFR $\alpha$ 1, and its ligand, GDNF. The formation of this tri-molecular complex leads to the activation of many signaling pathways that induce cellular processes such as cell survival, differentiation and proliferation. RET is expressed in approximately 30-70% breast cancer cases. While initial work suggested that RET was associated with luminal forms of breast cancer, more recent data suggest that this receptor tyrosine kinase may be more broadly implicated with multiple subtypes of breast cancer. Here, we used *in vitro* cell-based models to further investigate the role of RET in breast cancer. Through our analysis, we found five RET-positive breast cancer cell lines, and confirmed the suitability of these models to explore the role of RET in breast cancer. Further, our data suggest that RET activation through GDNF treatment increases proliferation of most of these breast cancer cells. In a high throughput screen using a protein domain microarray dataset, a potential interaction between RET and the BCAR3 adaptor protein was previously identified. To gain a more mechanistic understanding of RET's contribution to cancer, we characterized and explored the functional implications of RET's interaction with the adaptor protein, BCAR3. Here, we confirm that RET and BCAR3 interact, and that it is a direct interaction between the SH2 domain of BCAR3 and RET. As we were not able to identify in our studies a suitable breast cancer cell model in which RET and BCAR3 were co-expressed, we used SH-SY5Y neuroblastoma cells, a cell line that co-expresses RET and BCAR3, for our functional analyses. Our data suggest that BCAR3 knockdown in SH-SY5Y neuroblastoma cells has a broad role in proliferation and adhesion, independent of RET. Further research is required to fully elucidate the functional relevance of the RET-BCAR3 association.

## Acknowledgements

“When we try to pick out anything by itself, we find it hitched to everything else in the Universe.”

– John Muir

I would like to begin by acknowledging Lois for providing an opportunity to perform graduate studies in her lab. Her unwavering guidance, intellectual inspiration and positive encouragement have been instrumental in the completion of this thesis. As a great mentor, she has continually challenged me to think critically, and to strive to become a better researcher.

I would also like to thank my other two supervisory committee members, Drs. Bruce Elliott and Xiaolong Yang, for constant support and guidance. Additionally, fellow labmates in the Mulligan Lab (both past and present) have fostered a positive, enjoyable graduate training atmosphere during my time at Queen’s. Further, I would like to thank my friends for support, conversations, and laughs over sushi dinners, volleyball games, and camping adventures.

I would also like to acknowledge the Canadian Breast Cancer Foundation, and the Terry Fox Foundation Training Program in Transdisciplinary Cancer Research in Partnership with CIHR for support for my graduate work.

Finally, I would like to acknowledge my family, especially my parents and my sister, Jamuna, for the endless love, support and motivation from the very beginning, and throughout my graduate studies. My mom – thank you for always believing in me, and for reminding me to enjoy and cherish every moment in life. My dad – thank you for inspiring me to pursue a career in science. Jams – thanks for always being there for me and continuously brightening up my day with your humour.

## Table of Contents

Abstract.....	ii
Acknowledgements.....	iii
Table of Contents.....	iv
List of Figures.....	vii
List of Tables.....	viii
List of Abbreviations.....	ix
Chapter 1 Introduction.....	1
1.1 RET.....	1
1.1.1 RET and Development.....	4
1.1.2 RET Regulation.....	5
1.1.3 RET Isoforms.....	9
1.1.4 RET and Disease.....	10
1.1.5 RET-based Therapies.....	12
1.2 Breast Cancer.....	13
RET and Breast Cancer.....	17
1.3 Cell Migration.....	19
1.4 Integrins.....	19
1.4.1 Focal Adhesions.....	20
1.4.2 RET and Integrins.....	21
1.5 BCAR3.....	22
1.5.1 BCAR3 & Breast Cancer.....	24
1.5.2 BCAR3 and Breast Cancer Endocrine Resistance.....	26
1.5.3 Additional BCAR3 Functions in Breast Cancer.....	27
1.5.4 BCAR3 Implicated in Other Models.....	27
1.5.5 BCAR3 and RTKs.....	28
1.6 Rationale/Objective.....	29
Chapter 2 Elucidation of the Role of RET in Breast Cancer.....	31
2.1 Abstract.....	32
2.2 Introduction.....	33
2.3 Materials & Methods.....	36
2.3.1 Cell Culture.....	36
2.3.2 Protein Isolation.....	36

2.3.3 Western Blotting .....	37
2.3.4 RNA Isolation and Quantitative Real-Time PCR (qRT-PCR).....	38
2.3.5 Cell Adhesion Assays .....	41
2.3.6 Cell Proliferation Assays .....	41
2.3.7 Short Hairpin RNA Production.....	42
2.3.8 Generation of Stable RET-KD MCF7 Cell Lines .....	43
2.3.9 Statistical Analysis.....	43
2.4 Results.....	43
2.4.1 Endogenous RET Expression in Breast Cancer Cell Lines.....	43
2.4.2 Endogenous RET Co-Receptor Expression in Breast Cancer Cell Lines .....	47
2.4.3 RET Activation has an Effect on Breast Cancer Cell Proliferation, but not Adhesion.....	50
2.4.4 Quantification of RET Isoform-Specific Knockdown in MCF7 Breast Cancer Cells .....	54
2.4.5 Effects of RET KD on Cell Proliferation.....	54
2.5 Discussion.....	57
Chapter 3 Characterization of the novel RET-BCAR3 interaction, and its functional implications .....	63
3.1 Abstract.....	64
3.2 Introduction.....	65
3.3 Materials and Methods.....	67
3.3.1 Cell Culture .....	67
3.3.2 Expression Constructs, DNA Isolation, Quantification and Transfection .....	68
3.3.3 BCAR3 shRNA KD.....	68
3.3.4 Purification of His and GST-tagged Recombinant Proteins .....	69
3.3.5 Far Western Blotting.....	70
3.3.6 Protein Harvest, Co-Immunoprecipitation and Western Blotting .....	71
3.3.7 RNA Isolation and Quantitative Real-time PCR (qRT-PCR).....	72
3.3.8 Cell Proliferation Assay.....	73
3.3.9 Cell Adhesion Assay .....	74
3.3.10 Single-Cell Migration Assay.....	74
3.3.11 Cell Morphology Assessment .....	75
3.3.12 Imaging of Focal Adhesion Proteins.....	75
3.3.13 Reverse Phase Protein Array (RPPA) Assays.....	76
3.3.14 Statistical Analyses .....	76
3.4 Results.....	80
3.4.1 The RET tyrosine kinase receptor interacts with the BCAR3 SH2 domain .....	80

3.4.2 BCAR3 contributes to SH-SY5Y neuroblastoma cell proliferation .....	82
3.4.3 RET-mediated migration is BCAR3-dependent .....	83
3.4.4 RET51-mediated focal adhesion formation .....	83
3.4.5 RET activation increases gene expression of Vimentin and MMP9 migratory markers .....	89
3.4.6 Effect of BCAR3 KD on RET-mediated <i>Cyclin D1</i> , <i>Vimentin</i> , and <i>MMP9</i> transcript expression .....	92
3.5 Discussion .....	97
Chapter 4 Discussion .....	101
4.1 RET's Contribution to Breast Cancer .....	102
4.2 Novel RET-BCAR3 interaction .....	106
4.3 Significance.....	109
4.4 Conclusions.....	112
References.....	

## List of Figures

Figure 1-1. Diagrammatic structure of the RET gene .....	2
Figure 1-2. Schematic diagram of the RET protein structure. ....	3
Figure 1-3. Diagram of RET activation.....	6
Figure 1-4. Signaling pathways mediated downstream of RET activation. ....	8
Figure 1-5. Schematic diagram of a breast cancer classification system. ....	16
Figure 1-6. Diagrammatic structure of BCAR3. ....	23
Figure 2-1. RET expression in breast cancer cell lines.....	45
Figure 2-2. Transcription expression of RET co-receptors, & RET target genes after induction with RET ligands, GDNF & Artemin. ....	49
Figure 2-3. Detectable levels of integrin beta subunit expression in breast cancer cell lines. ....	51
Figure 2-4. Collagen is the preferred extracellular matrix for RET-positive breast cancer cell lines. ....	52
Figure 2-5. RET activation via GDNF treatment does not affect MCF7 2D cell adhesion. ....	53
Figure 2-6. GDNF-mediated RET activation increases cell proliferation in MCF7, T47D, MDA-MB-453 & BT20 breast cancer cells. ....	55
Figure 2-7. Validation of RET knockdown in MCF7 cells, & effect of RET knockdown in MCF7 breast cancer cell proliferation. ....	56
Figure 3-1. RET receptor interacts with the BCAR3 adaptor protein .....	81
Figure 3-2. BCAR3 plays a role in SH-SY5Y neuroblastoma cell proliferation .....	84
Figure 3-3. BCAR3 plays a role in cell migration .....	85
Figure 3-4. RET isoforms differentially contribute to focal adhesion formation.....	87
Figure 3-5. RET51 differentially contributes to focal adhesion formation than RET9 .....	88
Figure 3-6. BCAR3 contributes to RET51-mediated focal adhesion formation .....	90
Figure 3-7. RET plays a role in SH-SY5Y cell adhesion and flattened cell morphology.....	91
Figure 3-8. Vimentin and MMP9 expression increases following RET activation in SH-SY5Y cells .....	93
Figure 3-9. Cyclin D1, Vimentin & MMP9 expression in BCAR3 KD cells.....	94
Figure 3-10. Levels of phosphorylated signaling proteins in SH-SY5Y BCAR3 KD cells.....	96
Figure 4-1. Model of downstream effects of receptor tyrosine kinase-BCAR3 interaction .....	108

## List of Tables

Table 2-1. Primer sequences used for qRT-PCR.....	39
Table 2-2. PCR cycling conditions for one-step qRT-PCR.....	40
Table 2-3. Receptor status of ER, PR and HER2 in RET-expressing breast cancer cell lines .....	46
Table 3-1. Antibodies utilized for immunoblotting and immunoprecipitation .....	73
Table 3-2. Sequences for primer pairs used for qRT-PCR.....	74
Table 3-3. One-step quantitative real-time PCR cycling conditions .....	76

## List of Abbreviations

<b>AKT</b>	Protein kinase B
<b>ARC</b>	Activity-regulated cytoskeleton-associated
<b>ARTN</b>	Artemin
<b>ATCC</b>	American type culture collection
<b>BCAR3</b>	Breast cancer anti-estrogen resistance 3
<b>BSA</b>	Bovine serum albumin
<b>CBL</b>	Casitas B-lineage lymphoma
<b>CLD</b>	Cadherin-like domains
<b>CCND1</b>	Cyclin D1
<b>Ct</b>	Cycle threshold
<b>DAB2-PTB</b>	Disabled-2 phosphotyrosine binding
<b>DCIS</b>	Ductal carcinoma in situ
<b>DFS</b>	Disease-free survival
<b>DMEM</b>	Dulbecco's modified eagle's medium
<b>DMFS</b>	Distant metastasis-free survival
<b>EGR1</b>	Early growth response 1
<b>EGFR</b>	Epidermal growth factor receptor
<b>ER<math>\alpha</math></b>	Estrogen receptor alpha
<b>ERK</b>	Extracellular signal-regulated kinase
<b>ET-1</b>	Endothelin
<b>FBS</b>	Fetal bovine serum
<b>GAB1</b>	GRB2-associated binding protein 1
<b>GDNF</b>	Glial cell-line derived neurotropic factor
<b>GEF</b>	Guanine nucleotide exchange factor
<b>GOBO</b>	Gene expressed-based outcome for breast cancer online
<b>GFL</b>	GDNF family ligand
<b>GFR<math>\alpha</math></b>	GDNF family receptor alpha
<b>GM</b>	Glomerular Mesangial
<b>GRB2</b>	Growth factor receptor-bound protein 2
<b>GST</b>	Glutathione S-transferase
<b>GUSB</b>	$\beta$ -glucuronidase
<b>HEF1</b>	Human enhancer of filamentation 1
<b>HER</b>	Human epidermal growth factor receptor
<b>HER2</b>	Human epidermal growth factor receptor 2
<b>IGFR-1</b>	Insulin-like growth factor receptor-1

<b>IL11</b>	Interleukin 11
<b>IR</b>	Insulin receptor
<b>JNK</b>	Jun N-terminal kinase
<b>JUNB</b>	Transcription factor jun-B
<b>kDa</b>	Kilodaltons
<b>KD</b>	Knockdown
<b>LCIS</b>	Lobular carcinoma <i>in situ</i>
<b>MAPK</b>	Mitogen-activated protein kinase
<b>MEN2</b>	Multiple endocrine neoplasia type 2
<b>MSD</b>	Mean square displacement
<b>MTC</b>	Medullary thyroid cancer
<b>MTT</b>	3-(4,5-dimethylthiazol-2-yl)-2,5-diphenyltetrazolium bromide
<b>NRTN</b>	Neurturin
<b>NSP</b>	Novel SH2-containing protein
<b>PBS</b>	Phosphate buffered saline
<b>PKC</b>	Protein kinase C
<b>PI3K</b>	Phosphatidylinositol-3-kinase
<b>PR</b>	Progesterone receptor
<b>PSPN</b>	Persephin
<b>PTB</b>	Phosphotyrosine-binding
<b>PTC</b>	Papillary thyroid carcinoma
<b>PTP<math>\alpha</math></b>	Protein tyrosine phosphatase alpha
<b>PYK2</b>	Proline-rich tyrosine kinase 2
<b>qRT-PCR</b>	Quantitative real-time polymerase chain reaction
<b>RET</b>	REarranged during Transfection
<b>RFS</b>	Relapse-free survival
<b>RPMI</b>	Roswell park memorial institute
<b>RPPA</b>	Reverse phase protein array
<b>RTK</b>	Receptor tyrosine kinase
<b>S6</b>	Ribosomal protein S6
<b>SDS-PAGE</b>	Sodium dodecyl sulfate-polyacrylamide gel electrophoresis
<b>SEM</b>	Standard error of the mean
<b>SH2</b>	Src homology 2
<b>shRNA</b>	short hairpin RNAs
<b>SHC-PTB</b>	Src homology 2 domain containing-phosphotyrosine binding
<b>TBST</b>	Tris buffered saline with 0.1% Tween-20
<b>TFAP2C</b>	Transcription factor AP-2 gamma

<b>TIRF</b>	Total internal reflection fluorescence
<b>TNM</b>	Tumor, node & metastases
<b>WT</b>	Wild-type

# Chapter 1

## Introduction

### 1.1 RET

REarranged during Transfection (RET) is a proto-oncogene that encodes a receptor tyrosine kinase (RTK) that plays important roles in normal development of tissues including of the nervous system, kidneys and in spermatogenesis [1-4]. RET was initially identified in 1985 as a transforming gene in NIH 3T3 cells following transfection with human lymphoma DNA [1]. RET is found on chromosome 10q11.2, and consists of 21 exons that encompass a region of 55,000 base pairs [5, 6]. There are three splice variants of RET that share the first 19 exons, but differ in the 3' ends, resulting in three distinct protein isoforms (Figure 1-1) [7]. RET is conserved across different species - homologues of RET have been found in other vertebrates, including mouse, rat, chicken, zebrafish and Xenopus, and also in the invertebrate *Drosophila melanogaster* [8, 9]. As per other RTKs, RET is comprised of three main domains, including an extracellular domain, a hydrophobic transmembrane domain, and an intracellular tyrosine kinase domain (Figure 1-2) [10]. The extracellular domain of RET consists of four cadherin-like domains (CLD1-4) that are each approximately 110 residues, a cysteine-rich region consisting of 120 residues, and 9 N-glycosylation sites that are required for RET's localization to the cell surface [10-12]. Between CLD2 and CLD3, there is a Ca<sup>2+</sup> binding site, and interaction of Ca<sup>2+</sup> is crucial for both the functional protein stability of RET, and the ability of RET to associate with its ligands [10].

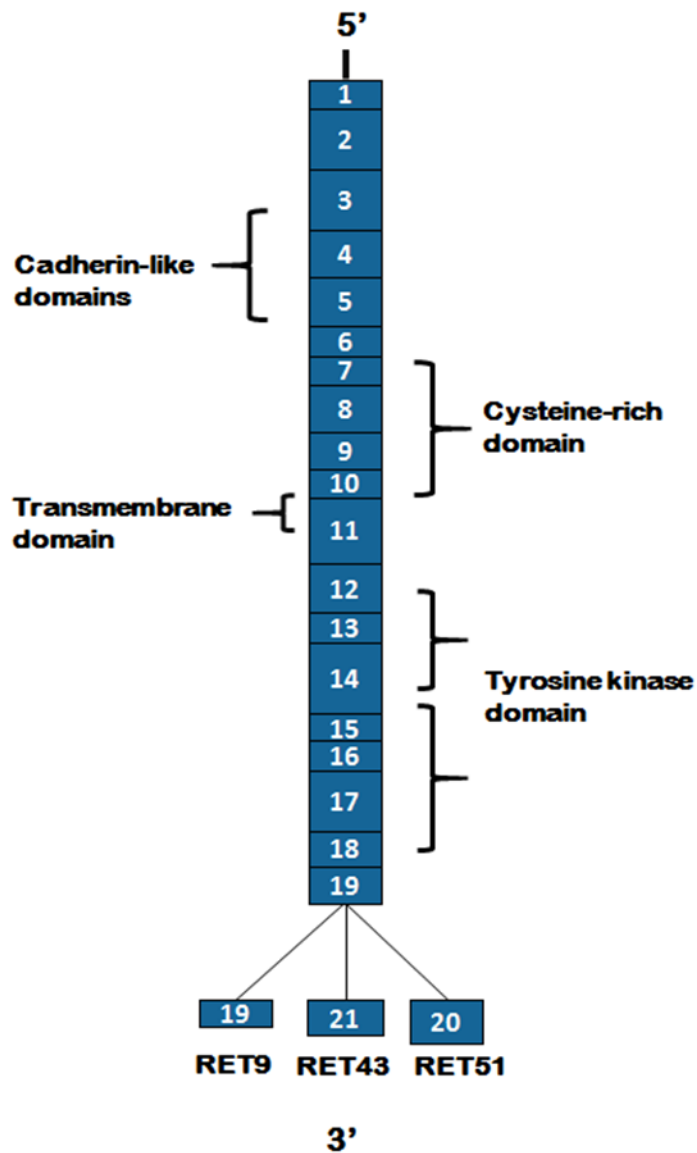


**Figure 1-1. Diagrammatic structure of the RET gene.**

*RET* is comprised of 21 exons. The three splice variants of *RET* share the first 19 exons, but vary in the 3' ends, resulting in three distinct protein isoforms. *RET9* is composed of the entire exon 19, *RET43* contains an incomplete exon 19 and the full exon 21, and *RET51* consists of a partial exon 19 and the entire exon 20.

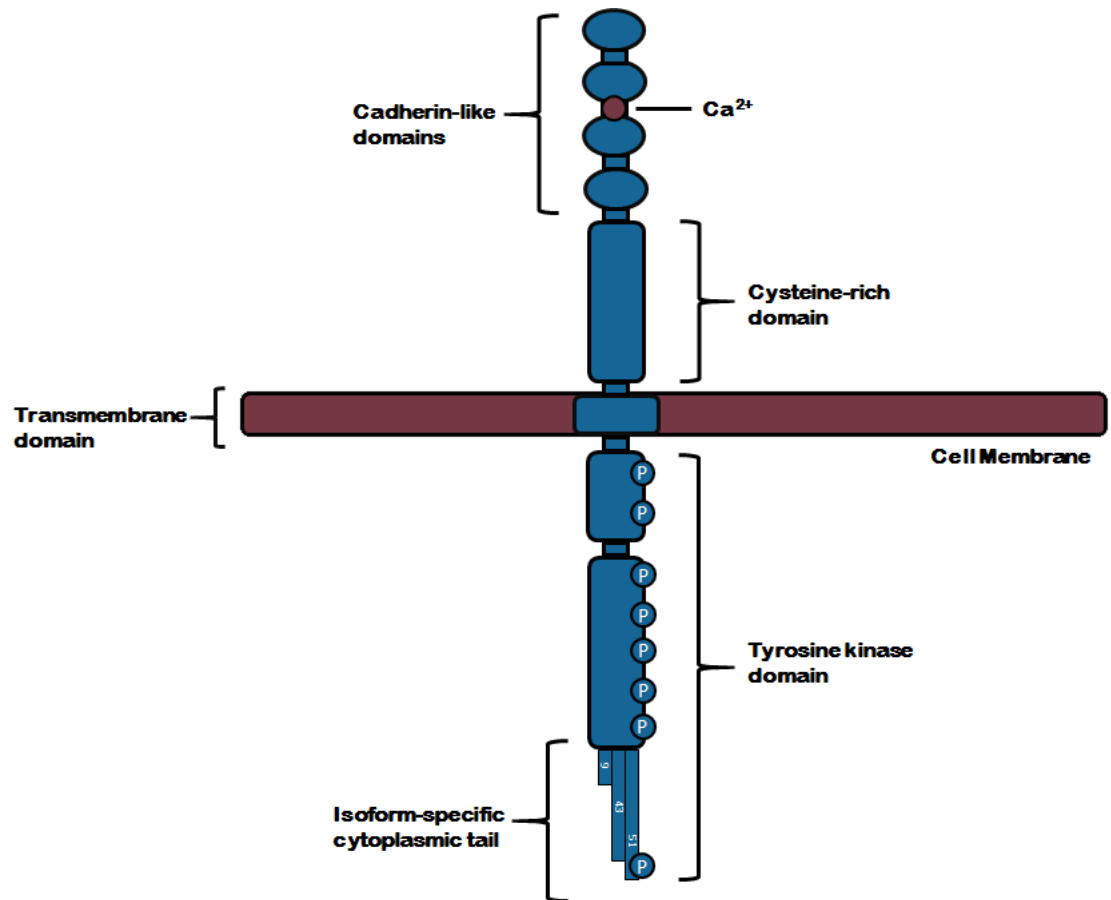


**Figure 1-2. Schematic diagram of the RET protein structure.**

RET is comprised of an extracellular region consisting of four cadherin-like domains, a  $\text{Ca}^{2+}$  binding site, a cysteine rich region and nine N-glycosylation sites, including N98 & N199, a transmembrane domain and an intracellular tyrosine kinase domain. RET has three distinct protein isoforms that share the first 1063 residues but differ in their C-terminal amino acids, termed RET9 (1072 amino acids), RET43 (1106 amino acids) and RET51 (1114 amino acids) after the numbers of unique amino acids.

The transmembrane domain is comprised of 22 residues, two of which, S649 and S653, regulate RET dimerization [13]. The cytoplasmic portion of RET includes a juxtamembrane region 50 amino acids in length, and a tyrosine kinase domain subdivided by a linker region [13]. RET can be found as either a 175kDa protein that is mature and fully glycosylated, and localized at the cell surface, or as a protein with a molecular weight of 155kDa that is immature and partially glycosylated, and contained in the Golgi [12].

### **1.1.1 RET and Development**

RET is found most highly expressed throughout early stages of embryogenesis, and reduces over time to much lower levels in normal adult tissues [14]. In particular, RET is expressed at high levels in tissues of neural crest origin, such as the kidney, during development [2]. Studies have demonstrated that mice null for RET die just after birth because of critical renal abnormalities, including renal agenesis, hypoplasia and ectopic ureter termination, and the lack of an enteric nervous system, highlighting the importance of normal RET signaling [15]. RET is involved in the growth and branching morphogenesis of the ureteric bud, and ureter maturation during the development of the kidney [16]. RET signaling also plays a crucial role in the growth and differentiation of certain peripheral neurons, including sympathetic, parasympathetic and enteric neurons, and in neurons of the central nervous system, such as motor and catecholaminergic neurons (Reviewed in [11]). Further, RET signaling contributes to normal spermatogenesis and spermatogonial stem cell self-renewal [17]. While RET expression

is much lower in adult tissues than during developmental stages, it remains present in spermatogonia, the C-cells of the thyroid gland, and nerve tissues [3, 4].

### **1.1.2 RET Regulation**

RET has four ligands, glial cell line-derived neurotrophic factor (GDNF), neurturin (NRTN), artemin (ARTN) and persephin (PSPN), all of which are collectively referred to as the GDNF family ligands (GFL), and has four co-receptors, GDNF Family Receptor alpha 1-4 (GFR $\alpha$ 1-4) (Figure 1-3) [18]. The GFLs contribute to the formation and maintenance of the nervous system [19]. For example, GDNF plays a role in the maintenance of dopamine-containing neurons - neurons that deteriorate in Parkinson Disease -, and is a therapeutic candidate for the disease [20, 21].

Like RET, GDNF also contributes to the formation and morphogenesis of the ureteric bud of the kidney during development, and the formation of enteric neurons [22, 23]. In fact, GDNF and GFR $\alpha$ 1 knockout mice both display a similar phenotype to that observed in RET null mice, emphasizing that RET signaling is dependent on the association of RET with its ligand and co-receptor [24]. While the ligands preferentially associate with a particular co-receptor (ie. GFR $\alpha$ 1-GDNF, GFR $\alpha$ 2-NRTN, GFR $\alpha$ 3-ARTN & GFR $\alpha$ 4-PSPN), cross-talk between the ligands and co-receptors was observed [25-28]. For instance, NRTN, ARTN and PSPN can also weakly interact with GFR $\alpha$ 1, and GDNF has been shown to cross-talk with GFR $\alpha$ 2 and GFR $\alpha$ 3 [25, 29, 30].

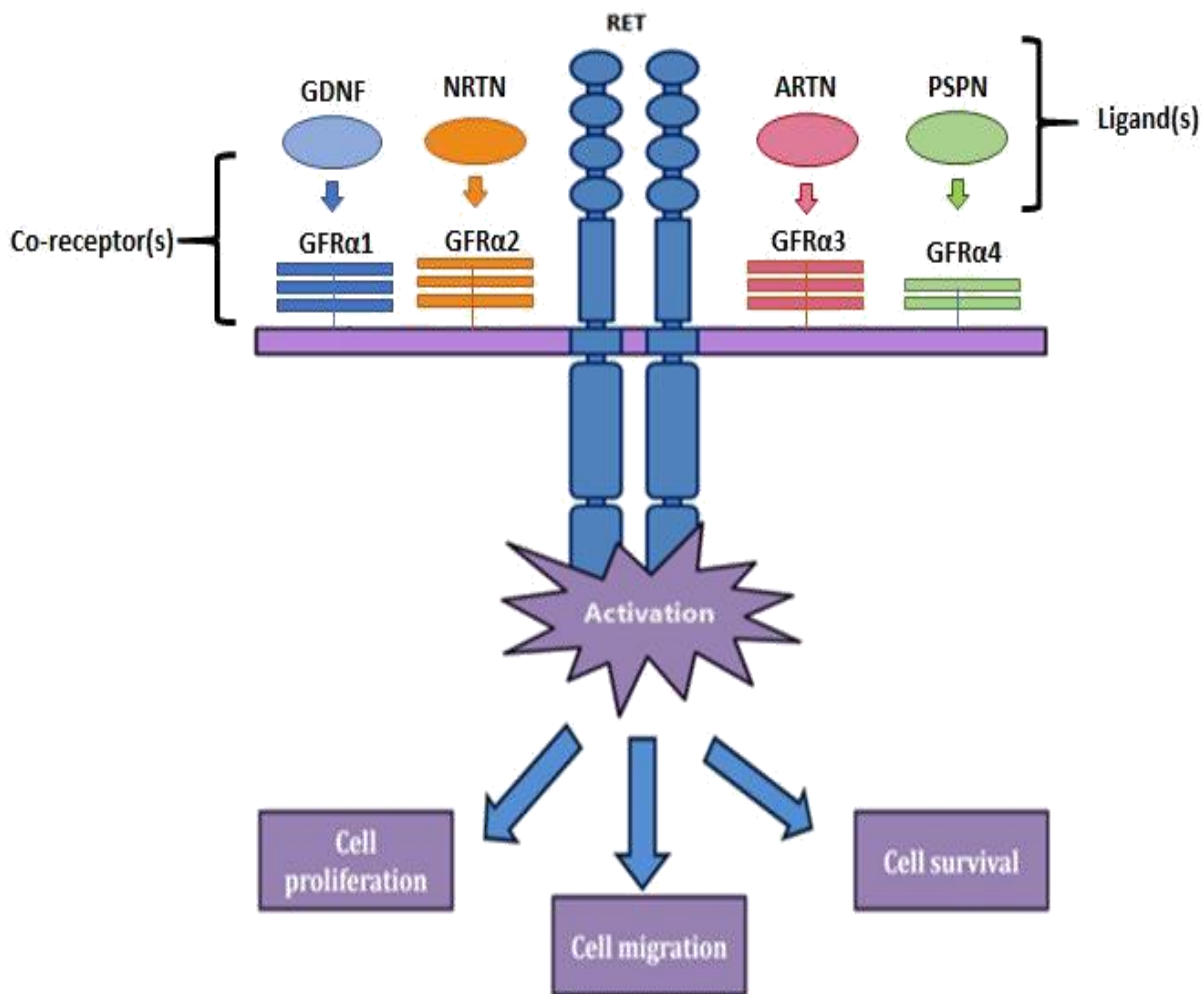


**Figure 1-3. Diagram of RET activation.**

RET is normally activated through the formation of a receptor complex consisting of a ligand of the glial cell line-derived neurotrophic factor (GDNF) family [GDNF, artemin (ARTN), persephin (PSPN) and neurturin (NRTN)], a membrane-anchored glycosylphosphatidylinositol-linked co-receptor of the GDNF family receptors (GFR $\alpha$ 1-4), and RET. The preferential ligand-GFR $\alpha$  receptor interactions are as follows: GDNF and GFR $\alpha$ 1, NRTN and GFR $\alpha$ 2, ARTN and GFR $\alpha$ 3 and PSPN and GFR $\alpha$ 4. Formation of this tri-molecular complex triggers multiple signal transduction pathways that result in cell survival, proliferation and migration.

Unlike other RTKs, activation of RET occurs through the formation of a tri-molecular complex comprised of two molecules of one of RET's ligands (GDNF, NRTN, ARTN & PSPN), two molecules of one of RET's co-receptors (GFR $\alpha$ 1-4), and two molecules of RET itself [10, 31]. RET is only able to bind to one of its ligands if it is in association with one of its co-receptors (Reviewed in [32]). Formation of the ligand-RET-co-receptor tri-molecular complex triggers RET dimerization and results in autophosphorylation of several key tyrosine residues in the intracellular region [33, 34]. This subsequently allows for binding of adaptor and signaling proteins containing Src homology 2 (SH2) or phosphotyrosine-binding (PTB) domains, leading to activation of multiple signal transduction pathways, including the phosphatidylinositol-3-kinase and protein kinase B (PI3K/AKT), Extracellular signal-regulated kinase (ERK), Mitogen-activated protein kinase (RAS/MAPK), Jun N-terminal kinase (JNK) and phospholipase C- $\gamma$  pathways (Figure 1-4) (Reviewed in [35]). Subsequent activation of these downstream pathways induces cell survival, differentiation, proliferation and migration (Figure 1-4) (Reviewed in [35]). RET-mediated induction of downstream signaling pathways regulates expression of various downstream target genes, including *Early Growth Response 1 (EGR1)*, *Interleukin 11 (IL11)*, *Activity-regulated cytoskeleton-associated (ARC)*, *cyclin D1 (CCND1)* and *transcription factor jun-B (JUNB)* [36, 37].

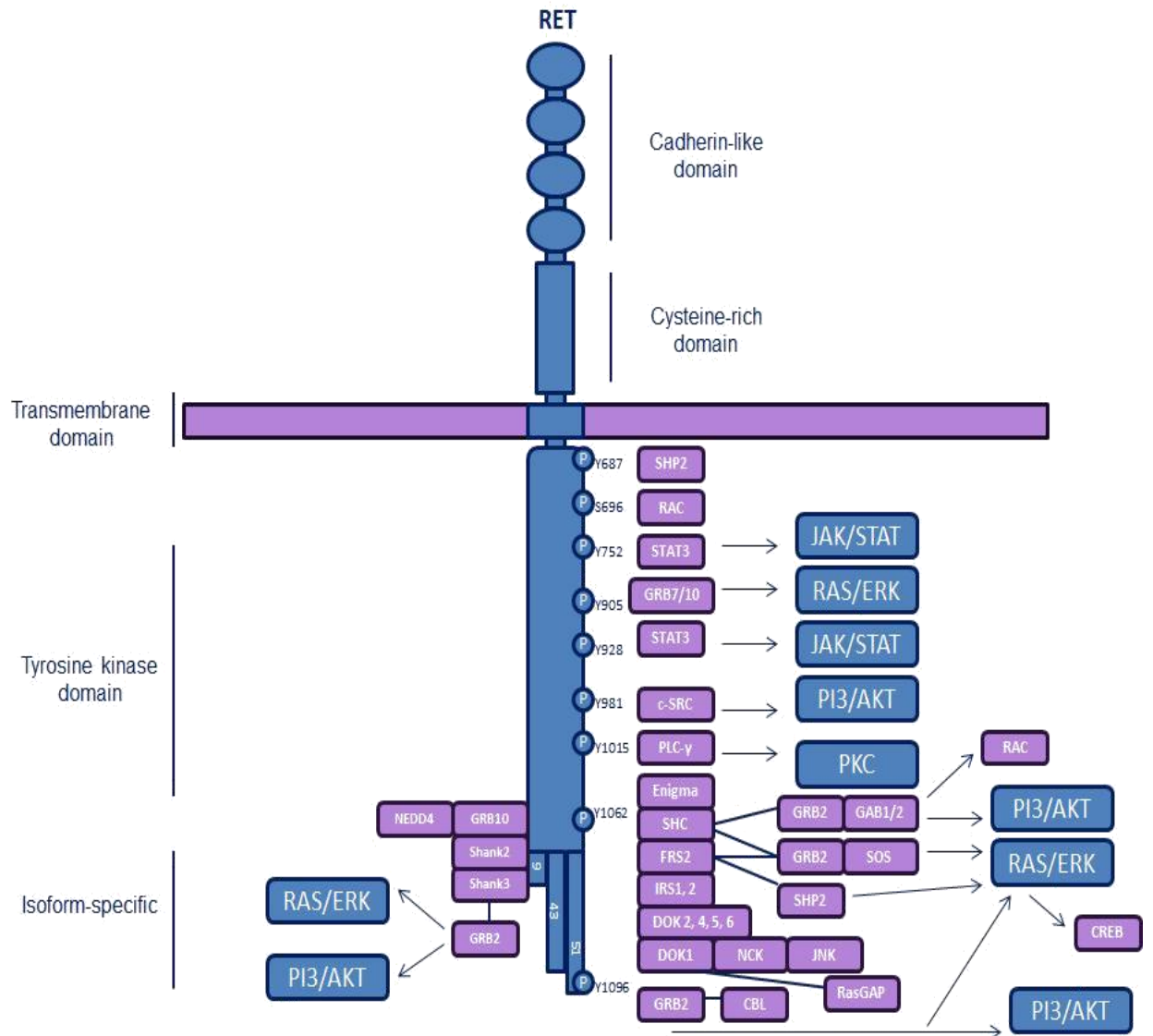


**Figure 1-4. Signaling pathways mediated downstream of RET activation.**

RET activation leads to the recruitment of adaptor proteins composed of either SH2 or PTB domains to interact with its phosphorylated tyrosine residues. Association of these adaptor proteins leads to the activation of several downstream signaling pathways. Known phosphotyrosine binding sites are indicated. The extracellular domain contains nine N glycosylation sites.

### 1.1.3 RET Isoforms

Due to alternative splicing at exon 19, there are three distinct protein isoforms of RET, RET9 (1072 amino acids), RET43 (1106 amino acids) and RET51 (1114 amino acids), which are named as per the number of unique amino acid residues at the C-terminal end after the shared 1062 amino acid residues [7]. In contrast to RET43, RET9 and RET51 are highly conserved across species, are abundantly expressed in the kidneys and in neural crest-derived tissues during development, and thus, are the two major isoforms of RET [8, 38]. Of note, RET9 is more highly expressed in most RET-expressing tissues tested to date than RET51 [39, 40]. The short isoform RET9 has 16 tyrosine residues, whereas, the longer RET51 isoform has two additional tyrosine residues, Y1090 and Y1096 (Reviewed in [35]).

Despite the slight sequence differences between the isoforms, major functional differences exist [41-46]. The functional differences between the isoforms have been explored in mouse and zebrafish models [41, 43]. RET9, rather than RET51, is required in the development of the enteric nervous system and the kidney – in fact, RET51 overexpression only partly compensates for the absence of RET9 in the development of these tissues [41, 47]. On the other hand, RET51 is necessary for the maturation of sympathetic neurons. Using *in vitro* assays, RET51 has been shown to have a greater transforming ability and an increased role in neurite outgrowth in comparison to RET9 [42, 44-46]. RET51 also contributes to a greater degree to cell survival, proliferation and

migration of both papillary (PTC) and medullary (MTC) thyroid carcinoma cells in comparison to RET9 [48]. These functional differences are likely due to the following isoform-specific differences including, distinct trafficking properties, differential recruitment of adaptor proteins, and unique target gene expression [33, 49-52]. RET51 is found at higher amounts as the mature form on the cell surface, and internalizes more rapidly following GDNF activation compared to RET9 [53]. Likewise, RET9 is found more abundantly as the immature form in the Golgi [53]. Interestingly, distinct trafficking between the isoforms results in a fast, sustained activation of the ERK/MAPK pathway downstream of RET51 compared to RET9 [53]. The tyrosine 1062 (Y1062) is situated very close to the splice site, leading to differences in the context of this tyrosine between the isoforms. RET51 has two additional tyrosines, Y1090 and Y1096, a major signaling hub, not found in the short isoform (Reviewed in [35]). Together, the differences in the sequences downstream of Y1062 and the additional tyrosines in RET51 result in differential binding of proteins between the isoforms (Reviewed in [35]). Of note, phosphorylation of Y1096 leads to the recruitment of GRB2, which subsequently interacts with GRB2-associated binding protein 1 (GAB1) and GAB2, promoting the downstream activation of the RAS/MAPK and PI3K/AKT pathways [54, 55], (Reviewed in [35]). Further, GRB2 that binds to Y1096 on RET51 also recruits CBL, mediating the downregulation of the longer isoform [52, 55]. Finally, the RET isoforms have been reported to differentially contribute to the induction of downstream target genes [49].

#### **1.1.4 RET and Disease**

RET has been implicated in various human diseases (Reviewed in [35]). In fact, mutations, gene fusions and wild-type expression of RET are associated with different disease phenotypes [35]. Germline loss-of-function *RET* mutations have been associated with approximately 50% of familial cases, and between 3 – 35% of sporadic cases of Hirschsprung disease, a congenital developmental disorder resulting in defects of the enteric nervous system [56, 57]. Hirschsprung-associated mutations result in various outcomes including, a lack of proper protein folding, inability to traffic to the cell surface, or an abrogation of functional activity [58]. Germline gain-of-function *RET* point mutations result in an inherited cancer syndrome that affects neuroendocrine tissues, multiple endocrine neoplasia type 2 (MEN 2) [59, 60]. There are two clinical sub-types of MEN 2, MEN 2A and MEN 2B, which are characterized by the occurrence of MTC, but differ in the presence of tumors affecting other tissues, including the parathyroid and the adrenal gland [61]. Somatic rearrangements of *RET* can result in PTC, lung adenocarcinoma and rarely chronic myelomonocytic leukemia [62-67]. These *RET* rearrangements in cancer involve the intracellular kinase domain of *RET* fused to sequences that include the N-terminal region of an unrelated gene, resulting in ligand-independent constitutive activation of RET [68].

Further, wild-type *RET* expression has been implicated in additional diseases, including tumors of the breast and pancreas [69-72]. RET is expressed in 30 – 70% of invasive breast cancers, with relatively more frequent expression in certain hormone receptor-positive sub-types [71-73]. RET expression is found in approximately 50 – 65%

of pancreatic ductal carcinomas, and associated with aggressiveness of the disease [69, 74].

RET is also expressed in other cancer types, including prostate, neuroblastoma, glioma, melanoma, renal cell and small-cell lung adenocarcinoma, and may act as a tumor suppressor in colon cancer [75-81]. While RET has been shown to be expressed in these cancers, its expression has not been associated with clinical parameters, such as age, stage, and histological type [75].

### **1.1.5 RET-based Therapies**

To date, clinically, there are no RET-specific inhibitors, but there are broad tyrosine kinase inhibitors that are used to treat cancers driven by the RET receptor. Vandetanib and Cabozantinib are both FDA-approved multi-tyrosine kinase inhibitors with selectivity for RET used in the treatment of MTC [82-84]. In addition to RET, Vandetanib also inhibits the vascular endothelial growth factor receptor-2 (VEGFR2), and the epidermal growth factor receptor, whereas, Cabozantinib, also blocks the VEGFR2 and the hepatocyte growth factor receptor [85-87]. Clinical trials are currently ongoing with several broad-based tyrosine kinase inhibitors in many tumor types, including thyroid and lung [88, 89]. The mechanisms of action of many of these tyrosine kinase inhibitors is competitive inhibition of ATP-binding at the catalytic site [90]. *In vitro* work suggests that subsets of luminal breast cancer patients may benefit from a combination of RET inhibition and endocrine therapy to prevent, or delay endocrine resistance [73, 91]. As high RET expression has been shown to be broadly associated

with decreased overall survival in breast cancer, RET inhibition may also have significance in non-luminal breast cancer subtypes [72].

## 1.2 Breast Cancer

Advances in early detection methods and treatment options have led to a reduction in breast cancer mortality rates. Yet, among women worldwide, breast cancer is the most frequently diagnosed cancer, with approximately 1.38 million new cancer cases annually, and the second leading cause of cancer death following lung cancer [92-94]. According to 2017 Canadian Cancer Society statistics, in Canada, 1 in 8 women are anticipated to develop breast cancer during her lifetime, and 1 in 31 are expected to succumb from the disease [95].

Breast cancer is regarded as a heterogeneous disorder, and can be characterized through various clinical and pathological factors, including patient age, histological type, tumor size, grade, lymph node involvement, hormone receptor status, and HER2 status [96-100]. Breast cancer is generally more frequent in older women – only 7% of women with breast cancer are diagnosed prior to age 40 [101]. The survival rates of breast cancer, however, are significantly better in older women than in women under the age of 40 years old [101]. Histological classification of breast cancer subtypes is based on cellular features and growth patterns, and can be broadly divided into either *in situ* carcinoma or invasive carcinoma [102]. The non-invasive classification of breast cancer can be further sub-divided into either ductal carcinoma *in situ* (DCIS) or lobular carcinoma *in situ* (LCIS) [102]. DCIS refers to the presence of abnormal cells exclusively in the lining of the milk ducts, and is more common than LCIS, which is characterized as

abnormal cell growth found within the lobules, or the milk-producing glands at the end of the ducts [102]. Invasive breast cancer can be sub-divided into multiple types – of which, infiltrating ductal carcinoma is the most prevalent subtype accounting for 70-80% of invasive forms of the disease [102].

Breast cancer can also be classified according to stage, a measure that indicates how far a cancer has spread [103]. The TNM system (refers to Tumor, Nodes and Metastases) is used to assess stage of disease through the evaluation of the size of the tumor, the number of lymph nodes affected, and whether the cancer has metastasized to other regions of the body [103]. Combined assessment of these three factors provides an overall stage ranging from 0-IV, and the lower values are correlated with a more favourable prognosis and outcome [103]. Another approach to categorize breast cancer is the utilization of tumor grade, a clinical parameter that takes into consideration the morphological appearance of cancer cells compared to normal cells, and provides insight into the growth rate, and metastatic potential of cancer [103]. Values for tumor grade range from 1 to 3, with 1 referring to low grade tumors that are well-differentiated, slow growing, and less likely to metastasize, 2 regarded as intermediate grade tumors that are moderately differentiated, and 3 describing tumors that are poorly differentiated, fast growing, and more likely to metastasize [103].

One well-accepted therapeutically-relevant classification system of breast cancer is based on the immunohistochemical detection of the estrogen receptor alpha (ER $\alpha$ ), progesterone receptor (PR), human epidermal growth factor receptor 2 (HER2) & Ki-67, a marker of cell proliferation [99]. Through this particular classification system, breast

cancer can be divided into broad, yet clinically relevant categories: Luminal A, Luminal B, Luminal B/Her2+, Her2+ and triple-negative [99]. The molecular characteristics of these subtypes are outlined in Figure 1-5. The general clinical recommendations stemming from this classification system are as follows: endocrine therapy for patients classified under the Luminal A subtype, endocrine therapy in combination with chemotherapy for Luminal B patients, Herceptin, a monoclonal antibody specific for Her2, for Her2+ patients, and chemotherapy alone for triple-negative breast cancer patients [104]. In comparison to Luminal A tumors, Luminal B breast cancers have a poorer prognosis, and are more likely to recur following endocrine therapy or chemotherapy [105-107].

Several studies have further characterized the molecular basis of the heterogeneous triple-negative form of breast cancer, and multiple sub-groups have emerged including, basal-like, and claudin-low [108-110]. Basal-like breast cancer is defined as tumors that are negative for hormone receptors, and positive for genes that characterize the basal epithelium, including epidermal growth factor receptor (EGFR), and cytokeratin 5/6, and is regarded as an aggressive subtype [111]. Claudin-low is a less frequent triple-negative breast cancer subtype and is correlated with low survival. Patients with claudin-low tumors are negative for the following markers, ER, PR, HER2, and claudins 3, 4 & 7 and E-cadherin [112, 113]. As per basal-like breast cancer, while claudin-low breast cancer generally displays a triple-negative phenotype, the opposite is not true – only a small proportion of triple-negative breast tumors are claudin-low [112, 113].

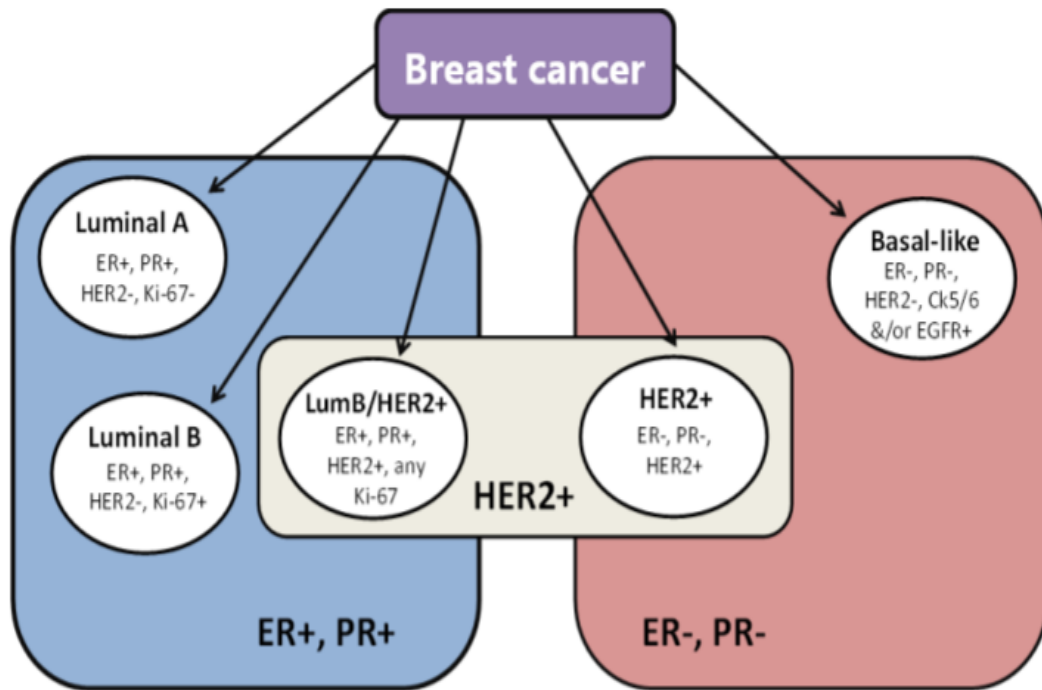


**Figure 1-5. Schematic diagram of a breast cancer classification system.**

A clinically relevant breast cancer classification system based on the immunohistochemical detection of the estrogen receptor, progesterone receptor, human epidermal growth factor receptor 2, and Ki-67, a cell proliferation marker. This classification system divides breast cancer into five broad, yet clinically relevant categories: Luminal A, Luminal B, Luminal B/Her2+ and triple-negative.

## **RET and Breast Cancer**

RET has been implicated in breast cancer [71-73, 114-116]. Studies initially showed RET and GFR $\alpha$ 1 over-expression in subsets of ER-positive breast cancer, but more recently, elevated levels of RET have been reported in other subtypes as well [71-73, 114]. RET activating mutations have not been found in breast cancer [116]. RET rearrangements were reported in 13% of invasive ductal breast cancer cases, and 18% of mice expressing the constitutively active RET/PTC1 gene fusion formed tumors of the mammary gland [115]. RET copy number gains have also been observed, but not functionally explored [117]. While RET rearrangements and copy number gains have been reported in a few cases [115, 117], wild-type RET expression seems to be more functionally relevant in breast cancer.

RET ligands, GDNF and artemin, have also been shown to be expressed in breast cancer [118, 119]. Specifically, GDNF expression is elevated in Luminal B subtypes of breast cancer in comparison to other breast cancer subtypes, and artemin expression is associated with decreased overall survival, and with estrogen receptor status in breast cancer patients [118, 119]. Subsequent studies have suggested that RET may be implicated in tamoxifen and aromatase inhibitor resistance [73, 114]. The mechanisms, however, by which RET is involved in endocrine resistance are not well understood. GDNF-mediated RET activation increases ER phosphorylation independent of the ER ligand, estrogen, and transcriptional activation of ER-dependent genes, suggesting potential mechanisms of RET-mediated anti-estrogen resistance [73]. Conversely, recent work has found two estrogen response elements on the RET promoter, and accordingly, estrogen stimulation increases RET expression in ER+ breast cancer cells [120]. Further,

tamoxifen treatment has been shown to decrease RET expression in luminal breast cancer cells [73]. Together, these data suggest the complexity of the relationship between RET and the estrogen receptor, and the need to fully delineate the molecular mechanisms of RET-mediated endocrine resistance. RET inhibition in combination with antiestrogen therapy was shown to be more efficacious than antiestrogens alone [82, 121], suggesting that such a combination treatment regimen may be advantageous for RET positive luminal breast cancers.

Although many groups have explored RET expression in luminal breast cancers, and its association and functional relationship with the estrogen receptor, recent data have shown that RET is also expressed in ER-negative, and triple-negative breast cancers [72]. The transcription factor AP-2 gamma (TFAP2C) promotes ER-independent *RET* expression, suggesting functional relevance of RET in subtypes other than luminal forms of breast cancer [82]. GDNF-mediated activation of RET promotes migration of breast cancer cell lines, and interestingly, blocking RET reduces tumor growth and metastasis in an ER+ mouse model, suggesting RET has a broader role in breast tumor growth and metastasis [72]. Further, high RET expression levels are positively associated with both decreased metastasis-free survival and overall survival, demonstrating the clinical relevance of RET in breast cancer [72].

### **1.3 Cell Migration**

Cell migration has several important normal functions in humans, including embryonic development, organogenesis, and wound repair. Dysregulation of cell migration, however, may result in various consequences, such as tumor metastasis [122]. The process of cell migration is multifactorial and involves several cyclical steps including cell polarization, protrusion, adhesion, and finally cell body translocation and retraction of the rear [122]. The initial step of cell migration involves cell polarization and extension of protrusions towards the path of movement in response to a migration-promoting factor [122]. These protrusions of the front, leading edge of the cell are dependent upon actin polymerization, and can be composed of lamellipodia and filopodia [122]. Lamellipodia-based protrusions are sheet-like, and composed of a branched network of actin, whereas, filopodia are finger-like, and comprised of bundles of filamentous actin. The protrusive structures subsequently adhere to the extracellular matrix or neighbouring cells, and these resulting adhesions function as a traction site, allowing for the cell body to move forward via actinomyosin-dependent contraction forces [122]. The adhesions then disassemble at the rear end of the cell, leading to retraction of the rear, trailing edge of the cell [122].

### **1.4 Integrins**

Integrins link the extracellular matrix to the actin cytoskeleton, and as cell adhesion molecules have important roles in several cellular processes including cell adhesion to the extracellular matrix, growth, migration and invasion (Reviewed in [123]).

Consequently, integrins are implicated in tumor proliferation and metastasis (Reviewed in [124]). The integrin family is composed of eighteen alpha-subunits and eight beta-subunits that form heterodimers that mediate cell-to-cell and cell-to-extracellular matrix interactions (Reviewed in [123]). These  $\alpha$  and  $\beta$  subunits arrange into 24 different heterodimers with varying tissue distributions. Integrin heterodimers have particular extracellular matrix-binding specificities (Reviewed in [123]). High expression or activity of integrins is regarded as a poor prognostic indicator in breast cancer [125].

There are two characterized mechanisms by which integrins are regulated – outside-in signaling that involves environmental cues, and inside-out signaling that is associated with intracellular signals (Reviewed in [126]). Specifically, the mechanism of outside-in integrin activation is triggered following the association with the extracellular matrix (Reviewed in [126]). On the other hand, inside-out signaling of integrins is initiated via downstream signaling of RTKs (Reviewed in [126]). Integrin activation allows for the recruitment of intracellular proteins that leads to the formation of focal adhesions, leading to cell adhesion and downstream signaling (Reviewed in [126]).

#### **1.4.1 Focal Adhesions**

The assembly and disassembly of focal adhesions play important roles in cell migration [127]. Focal adhesions are integrin-based cell-matrix adhesions that involve a complex of many different signaling and structural proteins in association with the actin cytoskeleton (Reviewed in [128]). There are over 100 proteins that can incorporate into focal adhesions complexes, and these complexes possess both structural and signaling

roles (Reviewed in [128]). Focal adhesion-related components comprise integral membrane proteins, such as syndecans and integrins, proteins that interact with actin [talin, actinin], and signaling and adaptor proteins [Src, focal adhesion kinase (FAK), paxillin, vinculin, zyxin and integrin-linked kinase (ILK)] (Reviewed in [128]). Paxillin is normally ubiquitously expressed in tissues and has also been associated with various malignant tumors, including prostate, breast and lung [129]. Further, levels of paxillin expression have been positively correlated with HER2 levels in breast cancer cell models and patient samples [130]. Zyxin is a zinc-binding protein that incorporates into focal adhesions at later stages of formation, and is regarded as a late focal adhesion marker [131].

#### **1.4.2 RET and Integrins**

Activation of RET results in the phosphorylation of focal adhesion-related proteins, including paxillin, FAK and p130Cas, and the formation of focal adhesions [132, 133]. RET has been shown to interact with FAK [134, 135]. In pancreatic cells, GDNF-mediated RET activation increases the expression of certain integrin subunits, and promotes cell adhesion and invasion [136]. Cross-talk between RET and integrin signaling plays a role in dendrite development and adhesion [137]. Further,  $\beta 1$  &  $\beta 3$  integrin subunits are involved in cell adhesion and migration downstream of RET in neuroblastoma and PTC models [133]. Together, this suggests that cross-talk between RET and integrin signaling may play a broader role in tumor invasion and progression.

## 1.5 BCAR3

Breast Cancer Anti-estrogen Resistance 3 (BCAR3) was first identified in a broad screen for genes implicated in tamoxifen resistance, and was subsequently found to also promote fulvestrant resistance in hormone-dependent breast cancer cell lines [138]. The mouse homolog of BCAR3, AND-34, was initially discovered in a study of molecular mechanisms underlying thymic negative selection, and is homologous to the human form [139]. BCAR3 is part of the Novel SH2-containing Protein (NSP) family which consists of three related proteins: NSP-1, NSP-2/AND-34/BCAR3, and NSP3/SHEP1/CHAT [140]. Although the NSP family members share structural similarity, there are striking differences in their tissue distribution and functions. Initial sequence characterization revealed that BCAR3 codes for an 825 amino acid protein containing a region showing strong homology to the SH2 domains found in other proteins [138]. SH2 domains consist of around 100 amino acids, and are found in various cytoplasmic signalling proteins. Adaptor proteins with SH2 domains can bind to specific tyrosine-phosphorylated peptide motifs on receptor tyrosine kinases that have roles in normal signalling and cell transformation, and these interactions can lead to activation of downstream signaling pathways. In addition to an N-terminal SH2 domain, BCAR3 also includes a C-terminal region that is homologous to a guanine nucleotide exchange factor (GEF) domain, and a proline/serine-rich linker region connecting these two regions (Figure 1-6). While the C-terminal end of BCAR3 shares modest (ie. 28-33%) homology with the GEF-domains of other proteins (ie. Ras/RaI/Rap subfamily members), this region does not seem to possess functional GEF activity due to its closed conformation

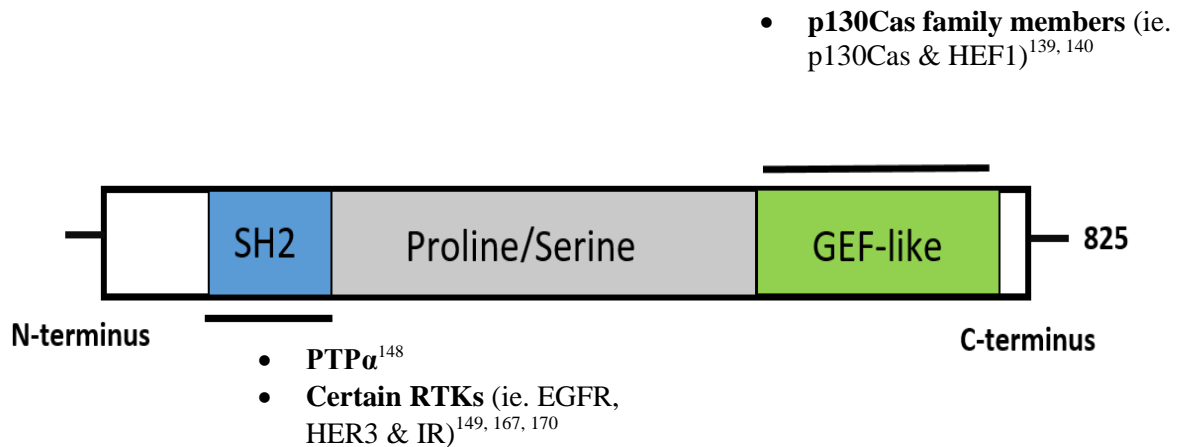


**Figure 1-6. Diagrammatic structure of BCAR3.**

Breast Cancer Anti-estrogen Resistance 3 (BCAR3) is a 95 kDa protein member of the novel SH2 domain-containing protein family. BCAR3 has an amino-terminal SH2 domain and a carboxy-terminal GEF-like domain which are linked through a proline-serine rich region. Known interacting partners of BCAR3 are outlined. BCAR3 SH2-domain binding partners include PTP $\alpha$ , and members of the human epidermal growth factor receptor (HER) family of receptor tyrosine kinases, including EGFR, and HER3. The GEF-like domain of BCAR3 interacts with p130Cas family members, p130Cas and HEF1

that essentially hides the GTPase-binding site [141, 142]. There are four known splice variants of BCAR3, three of which encode the same isoform, and the remaining one codes for a shorter isoform [143]. BCAR3 knockout in mice has no major developmental effects on fertility or lifespan, but results in a defect in the adult ocular lens due to abnormal focal adhesion complex signalling in lens epithelial cells [144]. One of BCAR3's well-characterized C-terminal binding partners is p130Cas, which has also been implicated in anti-estrogen resistance [145, 146]. Another p130Cas family member, Human enhancer of filamentation 1, (HEF1), is also known to interact with the C-terminal end of BCAR3 [147]. The crystallized structure of the complex of BCAR3-related protein, NSP3, and p130Cas provides important insight into the BCAR3-p130Cas interaction. NSP3's C-terminal end has a closed conformation, resulting in a non-functional GEF domain, but this phenomenon is crucial for its ability to associate with p130Cas [142]. Known BCAR3 SH2-domain binding partners include the Protein tyrosine phosphatase alpha (PTP $\alpha$ ), and members of the human epidermal growth factor receptor (HER) family of RTKs, including EGFR, and HER3 [148-150]. While proteins that interact with BCAR3's proline-rich region have yet to be identified, the SH3 domain of CrkII is hypothesized to associate with this domain [151].

### **1.5.1 BCAR3 & Breast Cancer**

BCAR3 has been implicated in breast cancer, but its role is ambiguous. BCAR3 over-expression promotes resistance to anti-estrogens, including tamoxifen and fulvestrant [138]. Further, BCAR3 is expressed in mesenchymal, aggressive breast cancer cell models, and plays a role in mediating various oncogenic-related processes, such as

cell proliferation, adhesion to extracellular matrix components, and cell migration [152, 153]. To date, most of the *in vitro* work has implicated BCAR3 in mediating an aggressive, migratory breast cancer phenotype, but one recent study shows that BCAR3's role even within breast cancer may be more broad, and context-dependent than initially thought [154]. Specifically, in breast cancer cells, BCAR3 is able to not only block Smad activation, but Smad-induced gene transcription, cell migration and matrix digestions, essentially acting to inhibit the TGF $\beta$ /Smad signaling pathway [154].

Two separate studies exploring the clinical relevance of BCAR3 in breast cancer highlight the complexity of the role of BCAR3 in breast cancer [154, 155]. T van Agthoven and colleagues found that *BCAR3* transcript expression is associated with a positive outcome for progression-free survival in tamoxifen-treated ER-positive breast cancer patients [155]. Consistent with this finding, high BCAR3 expression was associated with high disease-free survival (DFS), distant metastasis-free survival (DMFS), and relapse-free survival (RFS) [154]. Further, the observed association between BCAR3 and disease outcome was only seen within the ER-positive subset of breast cancer patients, and not in the ER-negative subset. Interestingly, there was a strong association between low BCAR3 levels and relapse of disease in ER-positive breast cancer patients [154].

In stark contrast to the majority of the *in vitro* studies, limited clinical studies have correlated sole high BCAR3 expression with better outcome in breast cancer patients, suggesting BCAR3's role in this disease is not clear-cut [154, 155]. As p130Cas is a well-characterized binding partner of BCAR3 and has similar functional roles, it is

plausible that co-expression of BCAR3 and p130Cas, or the activation of signalling downstream BCAR3-p130Cas is more functionally relevant to the anti-estrogen, and migratory phenotype [156]. In fact, co-expression of BCAR3 with p130Cas has been recently observed in different subtypes of breast cancers, including ER-positive, Her2-positive and triple-negative [156]. Although initial work identified that the BCAR3-p130Cas complex was not necessary for many of BCAR3's functions [157], more recent work has shown the BCAR3-p130Cas interaction is crucial to the many roles of BCAR3 in breast cancer [156].

### **1.5.2 BCAR3 and Breast Cancer Endocrine Resistance**

Studies have shown both the SH2 domain, and GEF-like domain of BCAR3 are required for its role in resistance to anti-estrogens [158]. Over-expression of BCAR3 results in enhanced PI3K signalling, which in turn induces Rac1 activation leading to endocrine resistance in breast cancer cells [141, 158]. Evidence suggests that BCAR3 regulated anti-estrogen resistance occurs via an ER $\alpha$ -independent mechanism [159]. BCAR3 over-expression leads to induction of CCND1, which has a role in regulating estrogen-dependent proliferation, and this enhancement is lost through blocking Rac1 and PAK1 [158]. Moreover, BCAR3's role in breast cancer anti-estrogen resistance is highly dependent upon interactions with its C-terminal binding partner, p130Cas [160]. The BCAR3-p130Cas interaction increases levels of both serine and tyrosine p130Cas phosphorylation, leading to p130Cas-dependent endocrine resistance [160]. Additionally, enhanced ERK1/2 activity was associated with endocrine resistance in cells over-

expressing BCAR3-p130Cas, demonstrating BCAR3-p130Cas-mediated endocrine resistance is dependent upon ERK1/2 [160]. To date, the clinical relevance of BCAR3 in human breast cancer endocrine resistance has not been well-characterized.

### **1.5.3 Additional BCAR3 Functions in Breast Cancer**

The BCAR3-p130Cas interaction has functions in addition to conferring anti-estrogen resistance in breast cancer cell lines, including several roles associated with a mesenchymal phenotype, such as cell migration and invasion [156]. The linkage of BCAR3 and p130Cas stabilizes both proteins, and promotes p130Cas-Src interactions, Src kinase activity, and Src-mediated p130Cas tyrosine-phosphorylation [161]. In aggressive breast cancer cell lines, the majority of BCAR3 interacts with p130Cas, and this interaction is crucial for BCAR3-induced adhesion disassembly, cell migration, invasion and Rac1 activity [156]. PTP $\alpha$  interacts with the SH2 domain of BCAR3, and BCAR3 serves as the molecular link between PTP $\alpha$ , and p130Cas-Src, and PTP $\alpha$ 's subsequent functions, including p130Cas localization to focal adhesions, and p130Cas signalling leading to cell migration [148].

### **1.5.4 BCAR3 Implicated in Other Models**

BCAR3 has been well characterized in various breast cancer model systems, but there have also been a limited number of recent studies assessing the broader functions of BCAR3 in other disease models, and normal development. As BCAR3 is widely expressed, and has been implicated in processes including cell proliferation and

migration, and integrin signalling, it is logical that it would play roles in other models. BCAR3, through association with CrkII, plays a role downstream of Endothelin (ET-1) signaling, which has roles in proliferation and attachment to the extracellular matrix, in kidney cells [151]. Further, the calcium-regulated non-receptor, proline-rich tyrosine kinase 2 (Pyk2), a regulator of ET-1 signaling in Glomerular Mesangial (GM) cells, plays a role in mediating the BCAR3-CrkII interaction in kidney cells [162]. BCAR3 interacts with HEF1, and recently has been shown to be necessary for HEF1-induced migration in a colon cancer cell model [163]. BCAR3 is a downstream target of Gata2 in ectoderm, and BCAR3 and p130Cas are expressed together in ectodermal cells during gastrulation of *Xenopus* [164]. As integrin function is crucial for the process of gastrulation, BCAR3-p130Cas may be necessary to mediate downstream integrin signalling in ectodermal cells [164]. Additionally, BCAR3 expression has been detected in both sertoli and germ cells of mouse testis during early development, highlighting BCAR3 may also play a role in the formation of gonads [165]. Interestingly, a spontaneous truncation mutation in the *BCAR3* gene has been implicated in lens extrusion cataracts in a murine model [166].

### **1.5.5 BCAR3 and RTKs**

As outlined earlier, BCAR3 contains a SH2 domain on its N-terminal end, suggesting that it is an adaptor molecule that can interact with phosphorylated tyrosine residues on various proteins, including RTKs, and contribute to downstream intracellular signalling pathways. Accordingly, recent analyses using high-throughput protein domain microarrays that predict possible interactions between almost all SH2 domains, and

phosphorylated tyrosine residues on RTKs revealed that the BCAR3 SH2 domain may interact with many RTKs, including EGFR, PDGFRB, ERBB2, FGFR3, KIT, MET and RET [167].

Studies have confirmed that the SH2 domain of BCAR3 functionally associates with multiple RTKs, such as EGFR, and Her3 [150, 168]. A direct, transient interaction has been reported between EGFR and BCAR3 via its SH2 domain following stimulation with EGF, and this association was important for EGF-mediated mitogenesis [168, 169]. Additionally, BCAR3 has been implicated in both migration and invasion of breast cancer cells towards EGF, yet, an endogenous EGFR-BCAR3 interaction in BT549 breast cancer cells after EGF stimulation could not be seen [169]. The BCAR3 SH2 domain plays a functional role in insulin-mediated DNA synthesis, and ERK activation, but not with IGF-1 stimulation, suggesting a functional relationship between BCAR3 and IR, but not IGFR-1 [170]. Additionally, BCAR3 has been implicated in insulin-mediated membrane ruffling, but not in GLUT4 translocation [170]. More recently, BCAR3 has been shown to interact with Her3, and this interaction connects this RTK to the Hippo-YAP pathway that promotes breast cancer metastasis to the bone [150]. While BCAR3 has been shown to functionally interact with a few RTKs, the aforementioned high-throughput study suggests BCAR3 may have a broader involvement with RTKs.

## **1.6 Rationale/Objective**

While RET has been implicated in breast cancer, its functional relevance in the disease has not been fully explored. Here, we identify suitable cell models to study the

role of RET in breast cancer, and investigate the role of RET in breast cancer cell proliferation and adhesion. Further, as the RET receptor and BCAR3 have been individually associated with cell migration, we hypothesize that BCAR3 lies downstream of RET and that this interaction may be one mechanism by which RET contributes to cancer cell migration. In our studies, we were not able to identify a suitable breast cancer cell model that co-expresses RET and BCAR3. SH-SY5Y neuroblastoma cells have been well-characterized in our lab to express RET, and its co-receptor, GFR $\alpha$ 1. As we found detectable levels of BCAR3 in these neuroblastoma cells, we used this cell line as our model for exploring the functional implications of the RET-BCAR3 interaction. As metastasis accounts for the majority of deaths from cancer, elucidation of the role that BCAR3 plays in RET-mediated cell migration may help uncover novel therapeutic options for cancers associated with RET. Here, we identify a novel interaction between RET and BCAR3, and investigate the functional implications of this interaction in a neuroblastoma model.

## **Chapter 2**

### **Elucidation of the Role of RET in Breast Cancer**

## 2.1 Abstract

RET is a receptor tyrosine kinase that is crucial for normal kidney development and spermatogenesis. RET has two main isoforms – RET9 and RET51, which are named for the number of unique amino acids after the last common residue. RET has been implicated in various diseases, including several cancer types. Activating mutations of RET are associated with the cancer syndrome MEN2, PTC and lung adenocarcinoma, whereas, expression of wild-type RET is linked to pancreatic, prostate and breast cancer. Studies suggest that 30-70% of invasive breast cancer cases express RET. While initial work suggested that RET expression was implicated specifically in luminal subtypes of breast cancer, recent studies have shown that RET is more broadly expressed in breast cancer, but is associated with aggressiveness of disease. Here, we further characterized the role of RET in breast cancer utilizing *in vitro* cell models. We have identified five RET-positive breast cancer cell lines, and further characterized the suitability of these cell lines to explore the role of RET. We have shown that RET activation increases breast cancer cell proliferation, but has no effect on 2D breast cancer cell adhesion. Utilizing single isoform knockdown and total RET knockdown breast cancer cells, our data verify that RET has a role in breast cancer cell proliferation and suggest that it may be worthwhile to assess whether the two main RET isoforms contribute differentially to this process.

## 2.2 Introduction

RET is a RTK found on the cell surface that plays an important role in the normal development of many tissues, including ones that are neuroendocrine-derived, and the kidney [171]. RET is generally activated by the formation of a tri-molecular complex involving RET, its ligand, and its co-receptor (Reviewed in [172] & [35]). Activation of RET leads to induction of various downstream signalling pathways that lead to the initiation of many cellular processes, including cell survival, cell proliferation, and cell differentiation (Reviewed in [172] & [35]). Mice that are null for RET and/or its co-receptors are embryonic lethal, highlighting the importance of normal RET signalling during development [24]. While RET is expressed in several tissues at the development stage, there is generally low or no expression in most adult tissues, including normal breast [14] & (Reviewed in [173]). There are three isoforms of RET that are referred to as RET9, RET51 and RET43 after the number of unique amino acid residues after the last common residue 1062 [7]. As RET43 is barely detected in most tissue types, RET9 and RET51 are the main isoforms of RET [8, 38]. Although RET9 and RET51 have a similar sequence, major functional differences have been reported between the two main RET isoforms [41-46]. In particular, RET9 has been shown to be crucial in the development of the kidney and the enteric nervous system, whereas, RET51 is essential for maturation of sympathetic neurons and has a greater transforming ability than RET9 [41, 47]. Additionally, RET51 contributes more to cell migration and invasion than RET9 in both MTC and PTC models [48].

RET has been associated with several human diseases, including cancer (Reviewed in [35]). Germline point mutations in RET that result in the constitutive

activation of the RET protein can cause MEN2, a cancer syndrome that affects neuroendocrine tissues (Reviewed in [35]). Somatic RET mutations can lead to sporadic MTC (Reviewed in [35]). Gene fusions of RET can cause PTC, the most common form of thyroid cancer, and lung adenocarcinoma [62, 66]. Wild-type RET expression has been implicated in tumors of the pancreas, prostate and breast [69-71, 114].

Amongst women worldwide, breast cancer remains the leading cause of cancer death [174]. One clinically relevant classification system based on immunohistochemical staining of hormone receptors subdivides breast cancer into five different subtypes – luminal A, luminal B, HER2-enriched, triple-negative, and normal-like (Reviewed in [175]). Many separate studies have shown that RET plays a role in the pathogenesis of breast cancer [71, 73, 114]. In initial studies, RET and its coreceptor, GFR $\alpha$ 1, were found to be overexpressed in 30-70% breast tumors, and correlated to the ER+ subtype of breast cancer [71, 73]. In recent studies, RET expression was reported to be also relevant in ER-negative and triple negative breast cancer cases, and correlated with decreased metastasis-free survival [72]. While estrogen has been shown to increase RET expression in an ER-dependent mechanism, TFAP2C has been shown to contribute to RET expression independent of ER [82], further emphasizing the biological relevance of RET in multiple subtypes of breast cancer.

Integrins form heterodimers that mediate the interaction of cells with components of the extracellular matrix, including fibronectin, laminin or collagen (Reviewed in [176]). Integrins play a role in processes such as cell proliferation, adhesion and migration, and are thus, implicated in tumor proliferation and metastasis (Reviewed

in [176]). In breast cancer, high expression or activity of integrins is regarded as a poor prognostic indicator [177]. There are 8 integrin beta subunits.  $\beta 2$  and  $\beta 7$  are regarded as leukocyte-specific, and thus only integrin beta subunits 1, 3-6 and 8 were investigated.

While RET has been implicated in breast cancer, the mechanism and processes by which the RET protein contributes to breast cancer pathogenesis is not well characterized. Further, studies have not yet assessed whether the RET isoforms differentially contribute to breast cancer. Here, we further investigate the role of RET in breast cancer using *in vitro* cell models, and explore whether the two main isoforms of RET contribute differently to breast cancer. We have found five RET-positive breast cancer cell lines belonging to different breast cancer subtypes, and evaluated the suitability of these cell lines to explore the role of RET in breast cancer by assessing expression of RET's co-receptors, and whether RET activation induces RET target gene expression. We showed that RET activation leads to increases in cell proliferation in four of the five breast cancer cell lines, but does not affect MCF7 adhesion to collagen. We used shRNA to generate single isoform and total RET knockdown (KD) to assess the contributions of the RET isoforms to breast cancer cell proliferation, and found that the RET isoforms differentially contribute to cell proliferation in MCF7 breast cancer cells. These data support that RET has a broad role in breast cancer pathogenesis, and that RET9 and RET51 may contribute to breast cancer proliferation to different extents.

## **2.3 Materials & Methods**

### **2.3.1 Cell Culture**

MCF7, T47D, BT20, BT-474 and MDA-MB-453 breast cancer cell lines, SH-SY5Y neuroblastoma cells, MIA PaCa-2 pancreatic cells, and HEK293T cells were obtained from American Type Culture Collection (ATCC, Manassas, VI). MCF7 and T47D cells were grown in Roswell Park Memorial Institute 1640 Medium (RPMI-1640, Sigma-Aldrich, Oakville, ON) and all other cells were cultured in Dulbecco's Modified Eagle's Medium (DMEM, Sigma-Aldrich, Oakville, ON). DMEM and RPMI-1640 growth media was supplemented with 10% Fetal Bovine Serum (FBS, Sigma-Aldrich, Oakville, ON), and 1% Ciprofloxacin (GenHunter, Nashville, TN). Cells were incubated at 37 °C with 5% CO<sub>2</sub>. TrypLE (Life Technologies, Burlington, ON) was used as a dissociation reagent to sub-culture cells.

### **2.3.2 Protein Isolation**

Cells were cultured to approximately 70-90% confluence. Prior to protein harvest, cells were placed on ice, and rinsed twice with cold 1 X phosphate buffered saline (PBS). Total protein was isolated using a cell scraper and lysis buffer composed of 1% Igepal (Sigma-Aldrich, Oakville, ON), 20 mM Tris-HCl (pH 7.8), 150 mM NaCl, 2 mM EDTA with protease inhibitors (1 mM phenylmethylsulfonyl fluoride, 10 µg/mL aprotinin, 1 mM sodium orthovanadate, and 10 µg/mL leupeptin). Whole cell lysates were rotated at 4°C for 30 minutes, and then centrifuged at 12,000 g, 4°C for 15 minutes to remove

cellular debris. The BCA protein assay (Thermo Scientific, Rockford, IL) was utilized to determine total protein concentrations of whole cell lysates according to manufacturer's instructions.

### **2.3.3 Western Blotting**

RET protein expression was assessed through western analysis. Prior to separation of whole cell lysates on a 7% SDS-polyacrylamide gel, samples were combined with Laemmli buffer (250 mM Tris pH 6.8, 4% SDS, 10% glycerol, 0.006% bromophenol blue, 2% 2-mercaptoethanol) and denatured at 95°C for 5 minutes. Following separation by SDS-PAGE, proteins were transferred electrophoretically to nitrocellulose membranes (Bio-Rad Laboratories, Mississauga, ON). Membranes were blocked for 30 minutes with 5% milk in Tris-buffered saline with 0.1% Tween-20 (TBS-T), and then incubated with primary antibody at a 1:1000 dilution (with the exception of tubulin which was added at a 1:5000 dilution) at 4°C overnight. Primary antibodies utilized included C19 RET9 (Santa Cruz Biotechnology, Santa Cruz, CA), and EIN8X Total RET (Cell Signaling Technology, Beverly, MA). Antibodies for either  $\beta$ -actin or tubulin (Sigma-Aldrich, Oakville, ON) served as the internal loading controls. Prior to the addition of the secondary antibody, TBS-T was used to rinse membranes three times at 15 minutes per wash. Secondary antibodies were added at a 1:3000 dilution for 1-2 hours at room temperature. Membranes were rinsed with TBS-T three times for 15 minutes. The Western Lightning Chemiluminescence Reagent Plus (PerkinElmer, Waltham, MA) and CURIX Ultra UV-G Plus film (AFGA Healthcare, Toronto, ON)

were used to detect protein expression levels. Films were scanned with an Epson Perfection 4990 photo scanner (Epson, Long Beach, CA) to create digital images. These images were used to calculate pixel density values with ImageJ software.

#### **2.3.4 RNA Isolation and Quantitative Real-Time PCR (qRT-PCR)**

Cells were grown to approximately 70-90% confluence. RNA was extracted utilizing Trizol reagent (Invitrogen, Burlington, ON) as per the manufacturer's instructions. RNA concentration was quantified spectrometrically (Nanodrop 2000 Spectrophotometer, Thermo Fischer Scientific, Rockford, IL). The one-step QuantiTect SYBR green quantitative real-time PCR kit (Qiagen, Mississauga, ON), and a SmartCycler II (Cepheid, Sunnyvale, CA) were used to reverse transcribe RNA into cDNA, and amplify resulting cDNA according to the manufacturer's instructions. Primer sequences are given in Table 2-1. PCR cycling conditions are provided in Table 2-2. Melt curve analysis was performed to ensure primer pairs resulted in a single product, with no primer dimers. The cycle threshold (Ct) value, which is defined as the number of cycles required for a statistically significant increase in fluorescence (ie. exceeds beyond background level) (Reviewed in [178]), was used to provide a relative measure of the amount of the target gene of interest in PCR reactions. *Beta-glucuronidase (GusB)* was used as a housekeeping gene to normalize transcript levels between different samples [49]. The relative amounts of *RET* transcript were determined for each sample of 200 ng RNA using a standard curve previously generated by Eric Lian [48].

**Table 2-1. Primer sequences used for qRT-PCR experiments.**

<b><u>Gene Target</u></b>	<b><u>Forward Primer</u> (5' – 3')</b>	<b><u>Reverse Primer</u> (5' – 3')</b>	<b><u>Product Size</u></b> (bp)
<i>GusB</i>	GAAAATACGTGGTTGGAGAGC	AAGGAACGCTGCACTTTTTG	131
<i>RET</i>	AATTTGGAAAAGTGGTCAAGGC	CTGCAGGCCCCATAACAAT	186
<i>ITGB1</i>	AACTGCACCAGCCCATTTAG	TCTGTGGAAAACACCAGCAG	203
<i>ITGB3</i>	CTCGAAAACCCCTGCTATGA	TCATTCCTCCAGCCAATCTT	206
<i>ITGB4</i>	CCATAGAGTCCCAGGATGGA	TCACAAACTCCTGGGTCACA	207
<i>ITGB5</i>	TTGTCAAAAATGGCTGTGGA	TTCATGGACAGGGAGAGGTC	244
<i>ITGB6</i>	GAAGAAATTGCCAACCCCTTG	AGGAGGTGGAGGGAGTCATT	227
<i>ITGB8</i>	GCCTGGGTGTTTTCACTTGT	ATCAACTGAGCAGCCTTTGC	204
<i>EGR1</i>	AGATGATGCTGCTGAGCAACG	ATGTCAGGAAAAGACTCTGCGGT	214
<i>ARC</i>	GAATCAGAGCTCAGCTCATGACT	GACTTTGTGGGAACCTTGAGAC	139
<i>CCND1</i>	CGAGAAGCTGTGCATCTACA	AATGAAATCGTGCGGGGTCA	123

**Table 2-2. PCR cycling conditions for one-step qRT-PCR.**

<b><u>Step</u></b>	<b><u>Temperature</u></b>	<b><u>Time</u></b>
Reverse Transcription	50 °C	1800 s
Initial Denaturation	95 °C	900 s
Denaturation (40X cycles)	95 °C	15 s
Annealing (40X cycles)	55 °C	25 s
Extension (40X cycles)	72 °C	15 s
Melt Curve	Ramp from 60 °C to 95 °C	---
Storage	4 °C	Hold

RET target gene expression was quantified using the comparative Ct method. Relative levels of *GFRα1*, *GFRα3*, and *ITGB1*, *ITGB3-6* & *ITGB8* gene expression was reported by subtracting the Ct values from the baseline value of 40 cycles to generate an Inverted Ct value. The qRT-PCR assays were performed at least in triplicate with a minimum of three biological replicates.

### **2.3.5 Cell Adhesion Assays**

Cells were grown to approximately 70-90% confluence, and dissociated with 1X citric saline (10X solution: 1.35M KCl and 0.15M sodium citrate) prior to seeding for adhesion assays. Wells of a 96-well plate were coated with 200 ng/μl collagen, 20 ng/μl fibronectin (BD Biosciences, Bedford, MA) or BSA, and blocked with 3% BSA in PBS. Breast cancer cells were seeded at a density of  $5 \times 10^4$  cells per well in 100 μl of 0.3% BSA in DMEM or RPMI, and placed at 37°C for one hr. Cells were washed with PBS, fixed in 3.7% paraformaldehyde, and stained in 0.5% Toluidine Blue-O for 3 hours. Cells were rinsed with ddH<sub>2</sub>O, and solubilized with 0.2% Triton-X100 for 20 minutes. Relative level of cell adhesion was measured by assessing absorbance at 570 nm (ELx 800UV plate reader, Bio-Tex Instruments, Houston, TX) and normalizing to BSA controls.

### **2.3.6 Cell Proliferation Assays**

Cell viability assays were performed using 3-(4, 5-Dimethylthiazol-2-yl)-2, 5-diphenyltetrazolium bromide (MTT, Life Technologies, Burlington, ON) as previously described [37]. In a 96-well plate,  $1 \times 10^4$  cells per well were seeded in 100 μl of DMEM

or RPMI growth media containing 0.1% FBS in the presence or absence of 50 ng/ml GDNF (PeproTech, Rocky Hill, NJ). After 3 days of cell proliferation, a final concentration of 45 µg/mL MTT in PBS was added for 24 hours at 37°C. Formazan crystals were dissolved with a 4 hour incubation with 100 µL of 20% SDS acidified with 0.04 M HCl at room temperature with shaking. Reduced MTT was quantified by absorbance at 570 nm (ELx 800UV plate reader, Bio-Tex Instruments, Houston, TX).

### **2.3.7 Short Hairpin RNA Production**

Three different short hairpin RNAs (shRNA) for each of the two forms of RET, RET9, RET51 and total RET in pLKO.1 vectors, were obtained from Open Biosystems (Huntsville, AL), and validated by BLAST by Eric Lian [48]. RET9, RET51 and total RET shRNA constructs or an empty pLKO.1 vector (Mock KD) control were grown in HEK293T packaging cells by transfecting a three plasmid packaging system including the psPAX2 and pMD2.G packaging and envelop vectors (Addgene, Cambridge, MA) using Lipofectamine 2000 (Life Technologies, Burlington, ON). The growth media of the HEK293T cells was changed to serum-free OptiMEM (Life Technologies, Burlington, ON) before transfection. After transfection, cells recovered overnight prior to the addition of 10% FBS to the media. Lentivirus was harvested every 12 hours for a 2 day period after transfection, and replaced with growth media supplemented with 30% FBS following each collection. Harvested medium was centrifuged to remove cell debris, filtered with a 0.45 µm filter (EMD Millipore, Billerica, MA) and then pooled, aliquoted and stored at -80°C.

### **2.3.8 Generation of Stable RET-KD MCF7 Cell Lines**

MCF7 cells expressing wild-type RET were grown to 70% confluence, and transduced with aforementioned described lentiviral constructs to generate polyclonal stable RET-KD cell lines. Specifically, MCF7 cells were infected with 750  $\mu$ l of lentiviral particles of an empty vector, or RET9, RET51 or total RET shRNA, and incubated for 24 hours. The media was then changed to RPMI media supplemented with 10% FBS and 1  $\mu$ g/mL puromycin to select for transduced cells. As described above, RET KD was validated using western blotting, and quantified using densitometry with ImageJ software.

### **2.3.9 Statistical Analysis**

Data are represented as mean  $\pm$  standard error of the mean (SEM) of a minimum of three experimental replicates. A two-tailed, unpaired student's t-test or one-way ANOVA was used to perform statistical analysis, and a p-value of less than 0.05 was considered to be significant.

## **2.4 Results**

### **2.4.1 Endogenous RET Expression in Breast Cancer Cell Lines**

To identify suitable cell models to study the role of RET in breast cancer, we initially screened for RET protein expression in a panel of 13 breast cancer cell lines

utilizing western blotting. We identified five RET-positive cell lines, BT474, MCF7, T47D, MDA-MB-453 and BT20, belonging to different breast cancer subtypes (Figure 2-1A). The characteristics, including receptor status, of these breast cancer cell lines are outlined in Table 2-3. Briefly, MCF7 and T47D cells are luminal A breast cancer cell lines, the BT474 cell line is a luminal B subtype of breast cancer, and MDA-MB-453 and BT20 cells are triple negative breast cancer cells [179]. As observed in other cell lines, RET is expressed in these breast cancer cell lines as a doublet consisting of bands of 155 kDa corresponding to the immature form and 175 kDa corresponding to the mature form. We observed a range of RET protein expression levels in the five RET-positive breast cancer cells. MCF7 cells expressed the highest level of RET protein, BT474 breast cancer cells expressed moderate levels of RET protein, and T47D, MDA-MB-453 and BT20 cells expressed lower levels of RET protein (Figure 2-1A). Interestingly, we found that the mature form of RET in BT474s is larger than that is observed in other cells. As glycosylation accounts for the difference observed between the immature and mature forms of RET, the differential size of the mature form of RET in BT474 cells may be due to a differing glycosylation pattern.

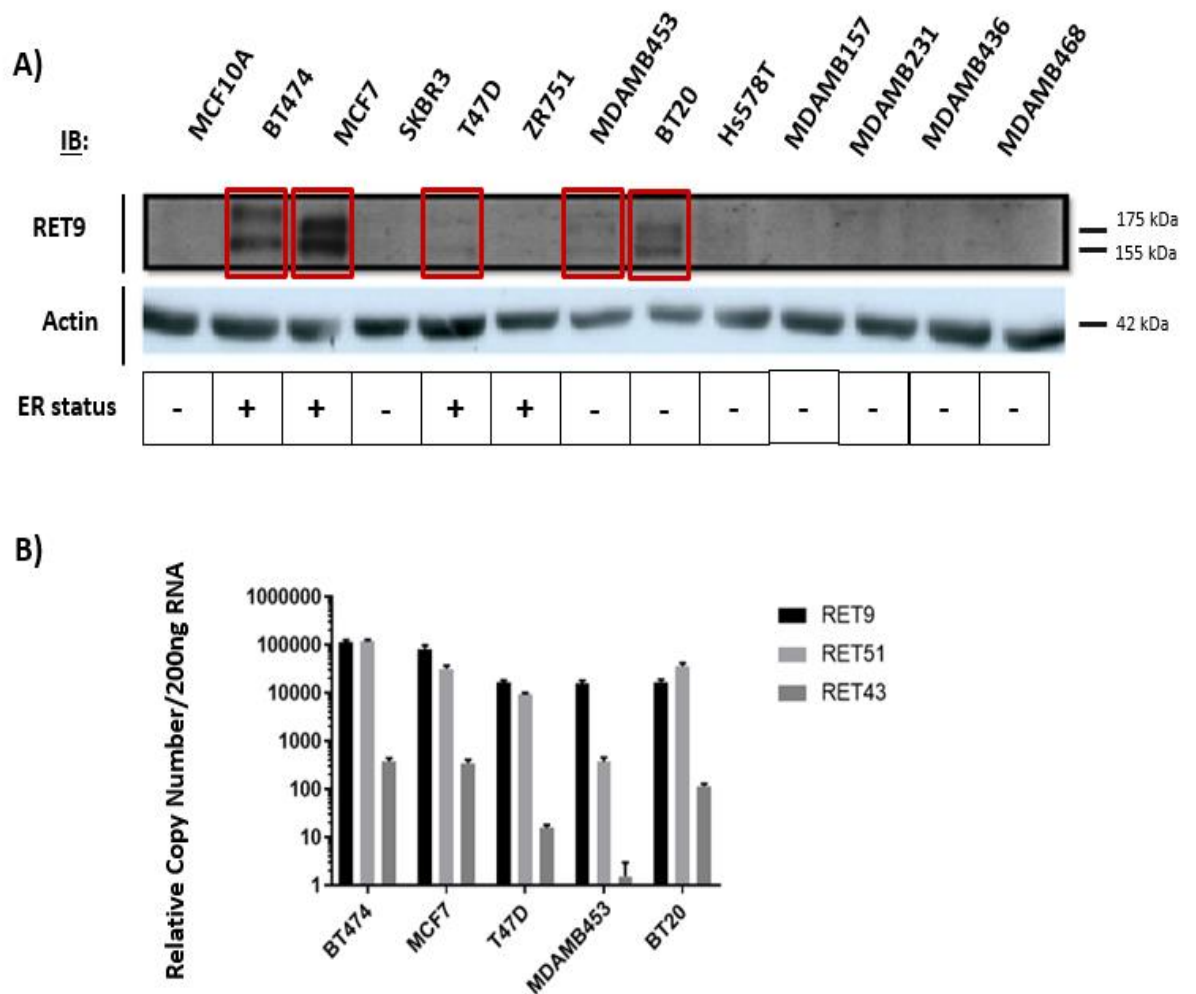


**Figure 2-1. RET expression in breast cancer cell lines.**

**A)** Western blot analyses of RET9 expression in a panel of breast cancer cell lines. The RET protein is expressed as a doublet – there is an immature, partially glycosylated form of RET that is 155 kDa, and a mature, glycosylated form that is 175 kDa. BT474, MCF7, T47D, MDA-MB-453 and BT20 cells are RET protein-expressing breast cancer cell lines. There is relatively high RET protein expression in BT474, MCF7 and BT20. The mature form of RET in BT474 is larger than what is normally observed. Whole cell lysates of each cell line were separated by SDS-PAGE, and probed for RET9. Actin was used as the loading control. Red boxes indicate RET-positive breast cancer cell lines. The table below the blots indicates the estrogen receptor status of each cell line. **B)** RET transcript expression in 5 RET protein-expressing breast cancer cell lines. We used quantitative real-time PCR (qRT-PCR) to assess transcript expression of *RET* isoforms, *RET9*, *RET51* and *RET43*. Data are represented as relative copy number of transcripts per 200 ng RNA on a logarithmic scale. Error bars represent standard error across three experimental replicates.

**Table 2-3. Receptor status of ER, PR, and HER2 in RET-expressing breast cancer cell lines.**

<b>Cell Line</b>	<b>ER<sup>1</sup></b>	<b>PR<sup>1</sup></b>	<b>HER2<sup>1</sup></b>
<b>BT474</b>	-	+	+
<b>MCF7</b>	+	+	-
<b>T47D</b>	+	+	-
<b>MD-MB-453</b>	-	-	-
<b>BT20</b>	-	-	-

<sup>1</sup> [179]

We wanted to verify *RET* transcript expression in the five RET-protein positive breast cancer cell lines. Total RNA was harvested from these cells, and used to assess transcript levels corresponding to individual RET isoforms using qRT-PCR. SH-SY5Y neuroblastoma cells, which have been previously well-characterized in our lab as a RET-expressing cell line, were used as a positive control in these qRT-PCR experiments. Sterile water was used as a negative control. As observed in other tissue and cell types, *RET9* and *RET51* were co-expressed in breast cancer cells, whereas, *RET43* is barely detected (Figure 2-1B). Like SH-SY5Y cells, in MCF7, MDA-MB-453 and T47D breast cancer cell lines, *RET9* was more highly expressed than *RET51* (Figure 2-1B). In BT474 cells, *RET9* and *RET51* were expressed at similar levels, and in BT20 cells, there was more *RET9* present than *RET51* transcripts. In general, the levels of RET protein and transcript expression in these cells seem concordant.

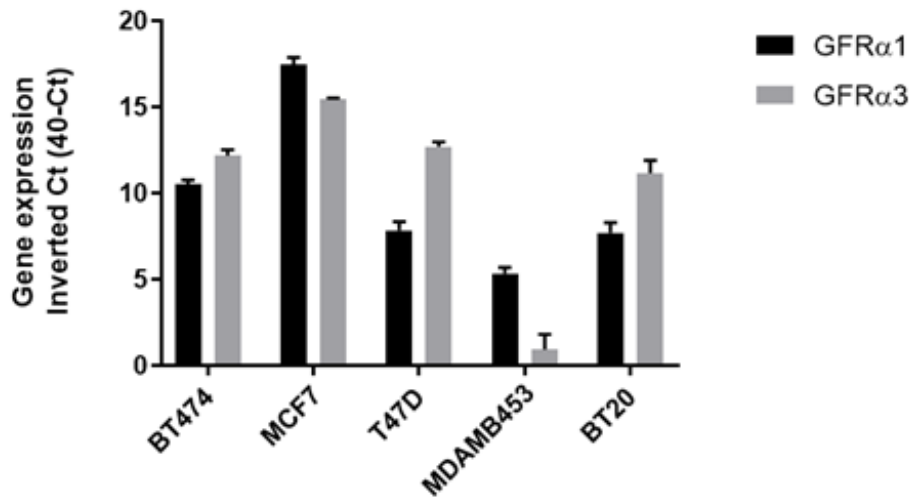
#### **2.4.2 Endogenous RET Co-Receptor Expression in Breast Cancer Cell Lines**

To further confirm the suitability of the five RET-protein positive breast cancer cell lines to study the role of RET, we assessed the expression of two of RET's co-receptors. As there are, to date, no suitable commercially available antibodies to assess expression of any of the RET co-receptors, we evaluated expression of *GFR $\alpha$ 1* and *GFR $\alpha$ 3* transcripts. SH-SY5Y cells were utilized as a positive control, and sterile water was used as a negative control in these qRT-PCR experiments. We found detectable levels of *GFR $\alpha$ 1* transcript expression in all five breast cancer cell lines assessed (Figure

2-2A). With the exception of MDA-MB-453 cells, *GFR $\alpha$ 3* was also detected (Figure 2-2A). In MDA-MB-453 cells, while *GFR $\alpha$ 1* was expressed, *GFR $\alpha$ 3* was barely expressed (Figure 2-2A). We detected high expression levels of *GFR $\alpha$ 1* and *GFR $\alpha$ 3* in MCF7, suggesting that both GDNF, the preferred ligand for GFR $\alpha$ 1, and artemin, the ligand of preference for GFR $\alpha$ 3, may activate RET in these cells [180].

Previous gene expression analyses have identified genes modulated downstream of RET [36, 181, 182]. Induction of RET target genes following activation of the RET tri-molecular complex would indicate a cell line biologically relevant to investigate the role of the RET protein. As MCF7 cells express detectable levels of RET and its co-receptors, we assessed the modulation of known target genes following RET activation in this cell line. We evaluated transcript expression of RET target genes, *CCND1*, *EGR1* and *ARC*, after RET activation with either GDNF or artemin treatment in MCF7 breast cancer cells (Figure 2-2B) using qRT-PCR. Sterile water was utilized as a negative control. Previous studies have shown *CCND1* and *EGR1* expression are increased following RET activation in HEK293 cells transiently expressing wild-type RET [36, 37]. RET activation led to induction of these three target genes in MCF7 breast cancer cells (Figure 2-2B). We found increases in *EGR1* following 1 hour and 6 hours of both GDNF and artemin treatment relative to untreated cells. *CCND1* was more highly expressed after 6 hours of ligand treatment in comparison to untreated cells. *ARC* expression was increased following 1 hour of GDNF treatment, and 6 hours of artemin treatment compared to no treatment. These gene expression data suggest that these cells would be a good *in vitro* model to study the role of RET in breast cancer. Additionally, as these results

A)



B)

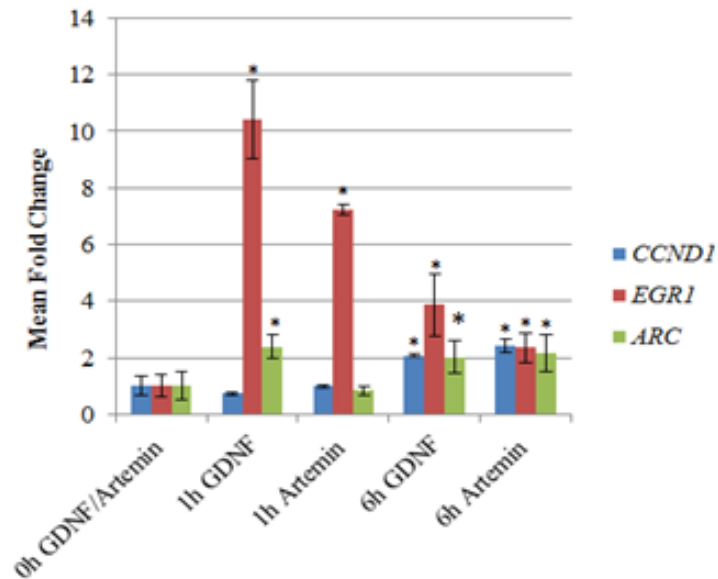


**Figure 2-2. Transcript expression of RET co-receptors *GFR $\alpha$ 1* and *GFR $\alpha$ 3*, and RET target genes, *CCND1*, *EGR1* and *ARC*, after induction with RET ligands, GDNF & Artemin.**

**A)** We used qRT-PCR to assess transcript expression of *GFR $\alpha$ 1* and *GFR $\alpha$ 3* in a panel of breast cancer cell line RNA, including BT474, MCF7, T47D, MDAMB453 and BT20. Data are represented as inverted Ct-values (the Ct value was subtracted from the baseline value of 40 cycles), and show that there are detectable levels of *GFR $\alpha$ 1* and *GFR $\alpha$ 3* expression in these breast cancer cell lines. **B)** Activation of RET via GDNF and artemin leads to increases in *CCND1*, *EGR1* and *ARC* expression in MCF7 cells. Data are represented as mean fold change relative to expression in untreated cells. A minimum of three biological replicates with three technical repeats were used for the analysis, and error bars represent standard error. (\* $p < 0.05$ ).

demonstrate that both artemin and GDNF treatment lead to normal RET activation, both ligands would be ideal to use to assess the role of RET in breast cancer.

### **2.4.3 RET Activation has an Effect on Breast Cancer Cell Proliferation, but not Adhesion**

Our lab has previously shown that integrin  $\beta 1$  and integrin  $\beta 3$  play roles in cell adhesion and migration downstream of RET in neuroblastoma and PTC models [133]. Thus, we chose to investigate a potential functional interaction between integrin subunits and RET in breast cancer. We found detectable levels of six integrin beta subunits in our five selected breast cancer cells using qRT-PCR (Figure 2-3). Across the five breast cancer cells lines evaluated, there was high expression levels of *ITGB4*. Additionally, with the exception of BT20 cells, there was low expression of *ITGB3*, and *ITGB8*. We assessed the optimal extracellular matrix conditions for the attachment of RET-positive cell lines for use in our subsequent cell adhesion experiments, and identified that the cells preferentially adhere to 200 ng/ul collagen (Figure 2-4). Using collagen as extracellular matrix, we performed adhesion assays with MCF7 breast cancer cells pre-treated with GDNF for various times, including 0 hours, 1 hours, 3 hours, 6 hours and 12 hours. Our data suggest that RET activation does not affect cell adhesion in MCF7 cells (Figure 2-5).

In order to determine whether RET activation had an effect on breast cancer cell proliferation, we performed MTT cell viability assays with our five cell lines of interest over a period of three days in the absence and presence of GDNF treatment. Levels of cell proliferation of our breast cancer cells in the absence of GDNF treatment were used

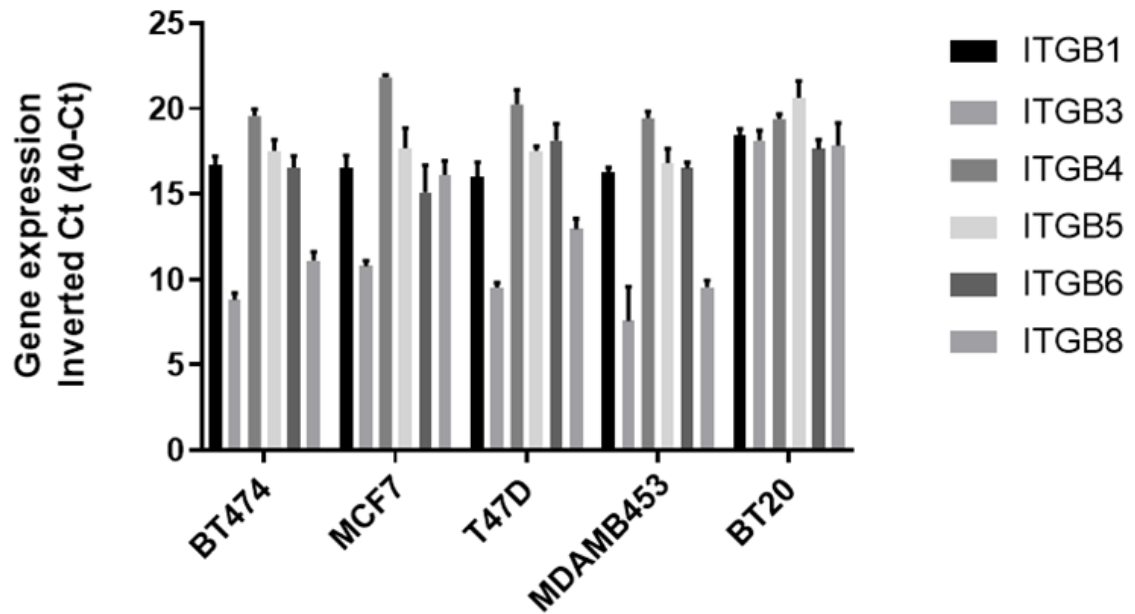


**Figure 2-3. Expression of integrin beta subunits in breast cancer cell lines.**

We used qRT-PCR to measure integrin beta subunit transcript expression in the five RET-protein positive breast cancer cell lines, MCF7, BT474, T47D, MDA-MB-453 and BT20. All six integrin beta subunits assessed are expressed at detectable levels in the breast cancer cells in our panel. Data are represented as inverted Ct [40-Ct] normalized to *GusB* housekeeping gene expression. At least three biological replicates and three technical replicates were used in the analysis. Error bars correspond to standard error.

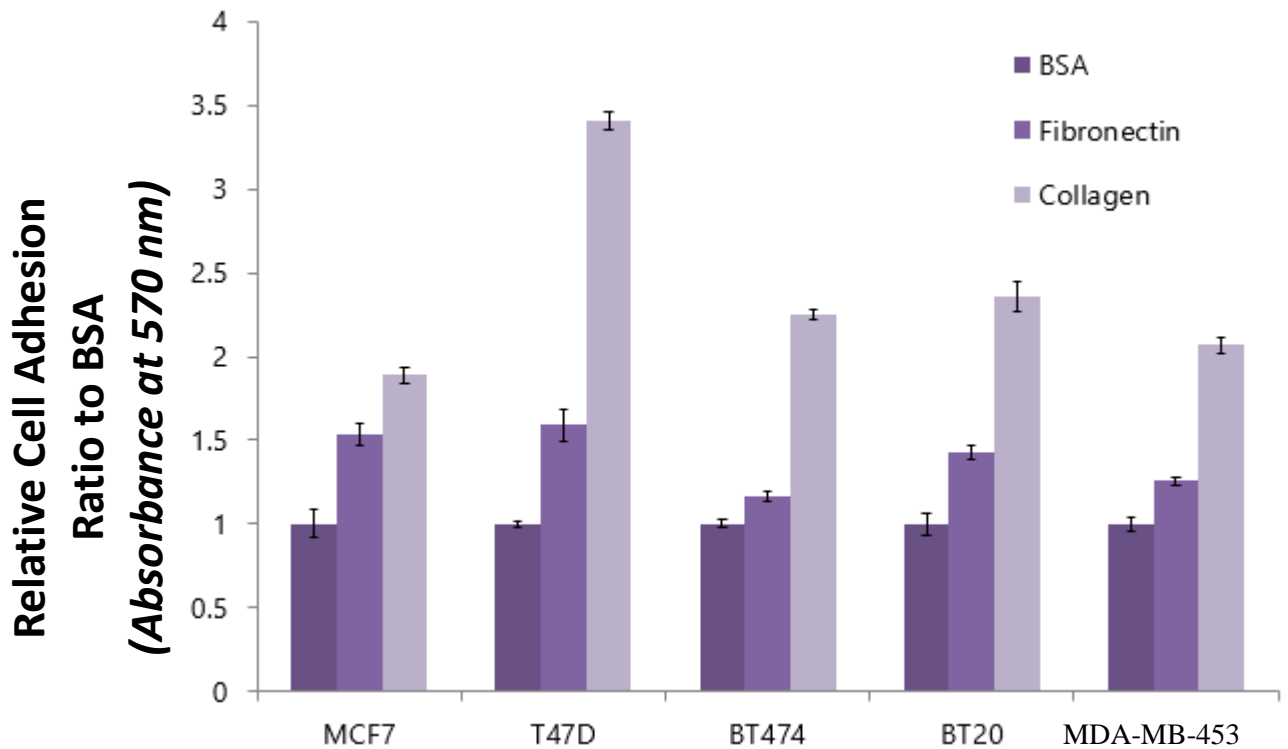


**Figure 2-4. Collagen is the preferred extracellular matrix for assessed RET-positive breast cancer cell lines.**

Adhesion assays were performed for breast cancer cells as previously described [133] with few modifications as indicated in the Methods. Binding preferences of the five breast cancer cell lines to either fibronectin or collagen was assessed. There is greater cell adhesion with all cell lines using collagen in comparison to fibronectin and BSA negative control. Cell adhesion was quantified at 570 nm absorbance, and data are represented here normalized to BSA controls. Error bars correspond to standard error across at least three technical replicates.

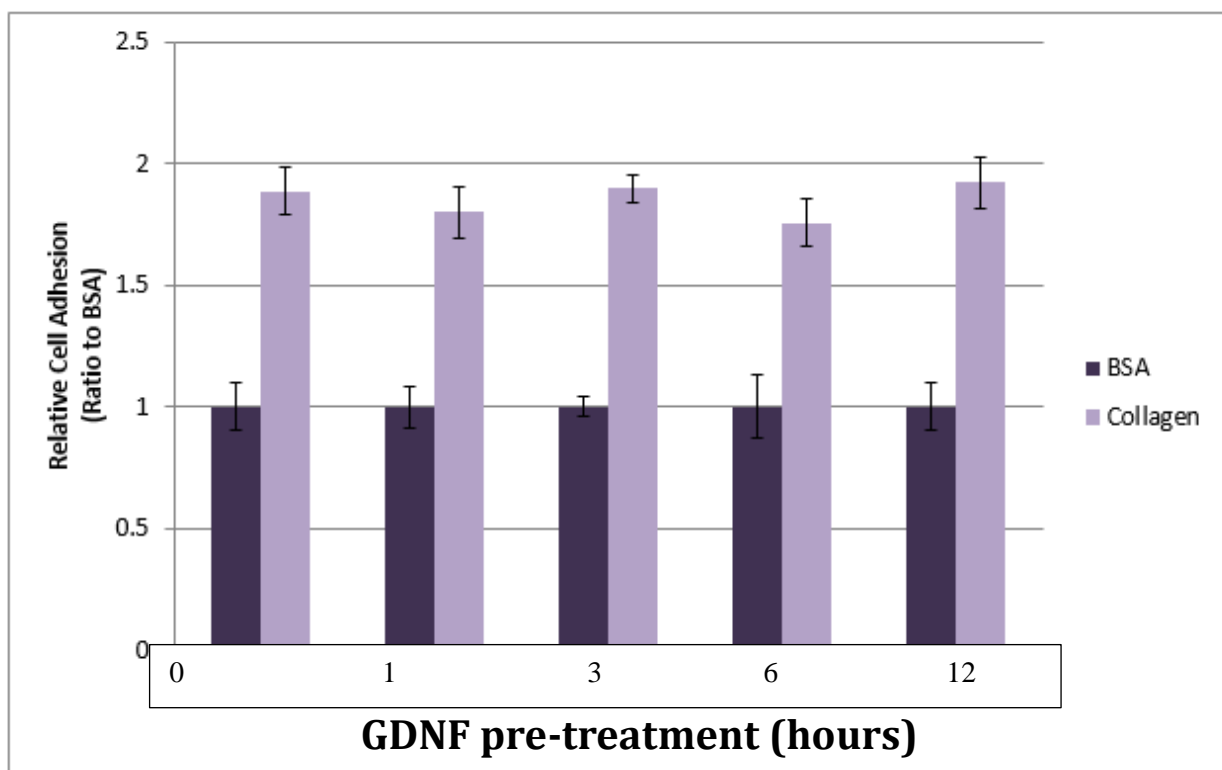


**Figure 2-5. RET activation via GDNF treatment does not affect MCF7 cell adhesion.**

Adhesion assays were performed with MCF7 breast cancer cells as previously described [133]. Prior to adhesion, cells were pre-treated with GDNF for indicated times. Adhesion was quantified at 570 nm absorbance, and data are represented normalized to BSA controls to identify relative cell adhesion. Error bars represent standard error across a minimum of three replicates.

as the baseline to assess the effects of breast cancer cell proliferation following RET activation. Interestingly, RET activation results in a small, but significant increase in cell proliferation in MCF7, BT20, MDA-MB-453 and T47D breast cancer cells (Figure 2-6).

#### **2.4.4 Quantification of RET Isoform-Specific Knockdown in MCF7 Breast Cancer Cells**

To assess the relative contributions of the RET isoforms to breast cancer cell proliferation, we used lentiviral delivery of shRNA specifically targeting sequences unique to RET9 or RET51 or to all RET forms (panRET) [48], to generate polyclonal MCF7 cell lines expressing single RET isoforms or no RET. Successful knockdown of RET in the three MCF7 cell lines was verified by Western blotting using an antibody to total RET, and quantified by densitometry (Figure 2-7A & B). Additionally, retinoic acid (RA) treatment increased RET expression levels in MCF7 cells (Figure 2-7A).

#### **2.4.5 Effects of RET KD on Cell Proliferation**

MTT cell viability assays were used to assess the effects of RET KD on cell proliferation. Total RET KD decreased basal cell proliferation levels, and abolished the GDNF-mediated increase in cell proliferation observed in the control Mock KD cells (Figure 2-7C). In isoform-specific RET9 KD cells, GDNF still results in an increase in cell proliferation, albeit much more modest than in Mock KD cells (Figure 2-7C).

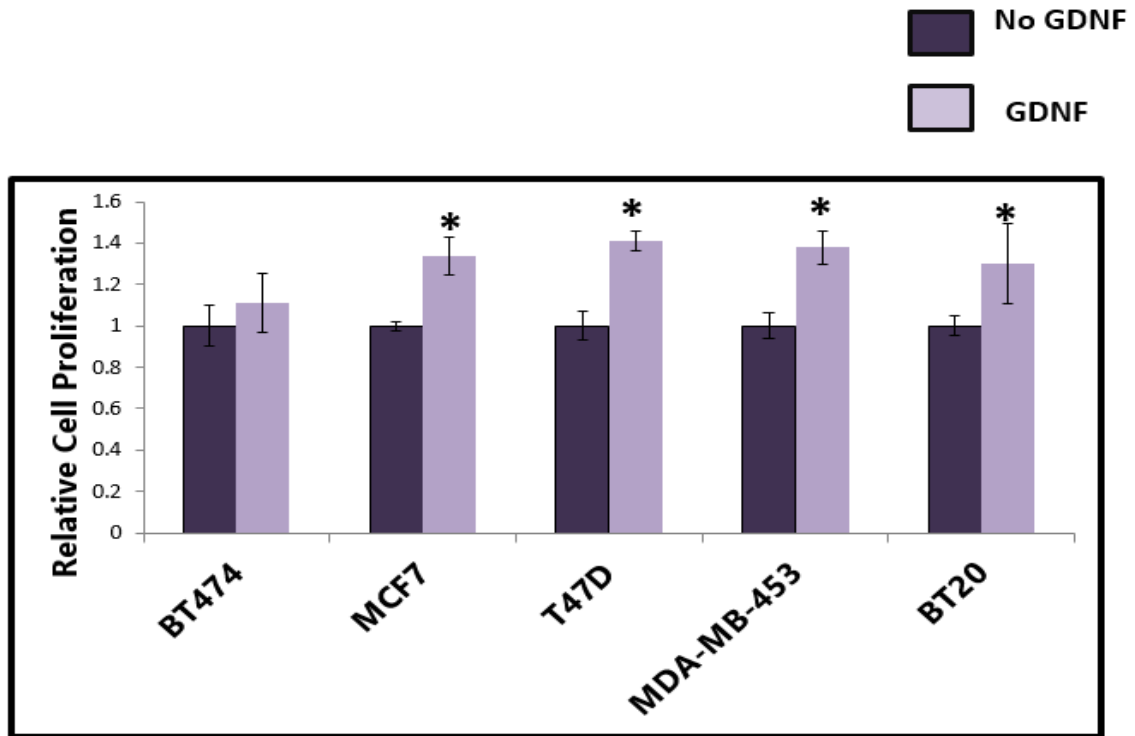


**Figure 2-6. GDNF-mediated RET activation increases cell proliferation in MCF7, T47D, MDA-MB-453 and BT20 breast cancer cells.**

Cell proliferation of indicated breast cancer cell lines was determined by MTT assays, with or without GDNF (50 ng/ $\mu$ l). After 3 days of proliferation in the presence or absence of GDNF, a final concentration of 45  $\mu$ g/mL MTT in PBS was added for 24 hours at 37°C. Data are represented here as relative cell proliferation to no GDNF treatment, to assess effects of RET activation. [\* indicates statistical significance; p-value <0.05]. Error bars correspond to standard error across at least three technical replicates.

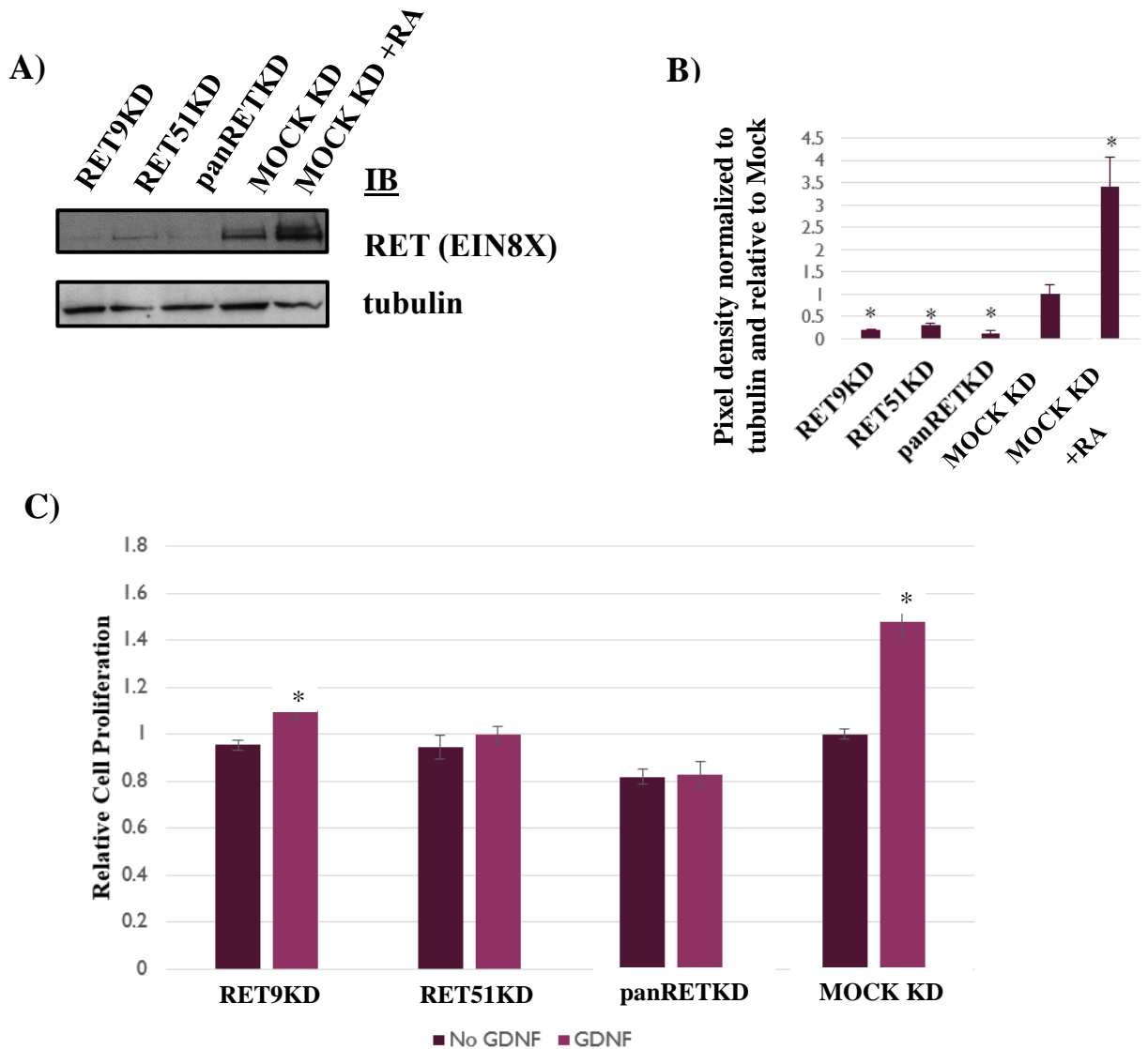


**Figure 2-7. Validation of RET KD in MCF7 cells, and effect of RET KD on MCF7 breast cancer cell proliferation.**

**A)** Western blotting with a total RET antibody (EIN8X) was used to verify RET knockdown in RET9, RET51 and total RET KD cell lines compared to control Mock KD cells. Retinoic acid was added for an overnight period to indicated condition. Tubulin was used as the loading control. **B)** RET KD was quantified by densitometry, and represented as pixel density normalized to tubulin and relative to Mock KD. **C)** MTT assays were used to measure cell proliferation in RET isoform-specific knockdown MCF7 cells. Data are represented as cell proliferation relative to Mock KD MCF7 that had no GDNF treatment. Error bars correspond to standard error across a minimum of three experimental replicates. [\* indicates statistical significance; p-value <0.05].

more to GDNF-mediated cell proliferation than RET9. Together, this suggests that the GDNF-mediated increase in cell proliferation is RET-dependent, and that the isoforms of RET differentially contribute to GDNF-mediated MCF7 breast cancer cell proliferation.

## 2.5 Discussion

The RET receptor tyrosine kinase has been implicated in various cancer types, including of the thyroid, prostate and breast. 30-70% of invasive breast cancer cases have been reported to have expression of wild-type RET [71, 72, 114]. In this present study, we have identified suitable models to explore the role of RET in breast cancer, and utilized them to assess the role of RET in breast cancer cell proliferation and adhesion. Our qRT-PCR results suggest that the shorter RET9 isoform is more abundant than the longer RET51 isoform in three of the breast cancer cell lines, MCF7, T47D and MDA-MB-453. Further, our data show that BT-474 cells have similar amounts of the two main RET isoforms, and that in BT-20 cells, RET51 is more highly expressed than RET9. Griseri and colleagues also assessed RET isoform transcript expression using qRT-PCR in MCF7 and T47D [183], and consistent with our results also found that RET9 is more highly expressed than RET51 in these two cell lines. Boulay *et al.* assessed RET isoform transcript and protein expression in a panel of breast cancer cell lines, including MCF7, T47D, MDA-MB-453 and BT-474, and found that both isoforms were co-expressed, but did not make quantitative comparisons of the expression levels of the two RET isoforms [114]. This group reported that RET9 and RET51 protein were both expressed in a

similar pattern in the assessed breast cancer panel, but only showed the RET9 protein expression data [114]. Generally, in various tissue types, RET9 is more highly expressed than RET51 [39, 184]. Our data suggest that in breast cancer cell lines there may be more variability in the relationship between RET9 and RET51 transcript levels than in other tissue types. However, it is worth mentioning that expression level differences of the isoforms may be different at the protein level compared to transcript levels.

As mentioned previously, our western blotting data suggest that the mature form of the RET doublet is larger in BT-474 cells than what is normally observed, and this is consistent with other RET protein expression data [114]. The difference between the immature band of RET at 155 kDa, and the mature band of RET at 175 kDa is the degree of glycosylation, suggesting that the RET present in BT-474 cells may have a different glycosylation pattern than usually observed.

GFR $\alpha$ 1 is the most commonly associated co-receptor of RET, but as GFR $\alpha$ 3 has been independently shown to be important for breast cancer cell growth, and effect the survival of breast cancer patients, we assessed the transcript expression levels of both these co-receptors in our 5 RET-positive breast cancer cell lines. Our data show that there are detectable levels of both co-receptors in the assessed cell models, providing support that GDNF, the main ligand associated with GFR $\alpha$ 1, and artemin, the main ligand associated with GFR $\alpha$ 3, would be useful for RET activation. While we did not quantitatively compare the levels of the co-receptors, it may be useful to do so in the future as it may help identify the ideal ligand to use in functional assays. Although other groups have utilized various GFR $\alpha$ 1 antibodies, we have yet to identify a suitable GFR $\alpha$ 1

antibody to evaluate protein expression by western blotting. With a well-characterized and specific GFR $\alpha$ 1 antibody, it would be interesting to explore whether our transcript co-receptor expression data is concordant with the protein level.

Groups have shown that RET activation by GDNF treatment increases phosphorylation of RET, AKT and ERK in the ER positive breast cancer cell lines, MCF7 and T47D [71, 72]. We wanted to further characterize the suitability of our breast cancer cell lines to explore the role of RET, and to do so, we evaluated the effect of the RET ligand, GDNF, on the expression levels of known RET target genes, *EGR1*, *CCND1* and *ARC* in the MCF7 breast cancer cell line. Our data suggest that GDNF treatment increases expression of these RET target genes. As our data along with data from other groups show GFR $\alpha$ 3 is expressed in breast cancer cell lines [119], we also assessed the effect of the RET ligand, artemin, treatment on expression of the three RET target genes. Similar to GDNF, artemin activates RET in MCF7 breast cancer cells, providing further evidence that this breast cancer cell line is suitable to explore the role of RET.

Esseghir et al demonstrated that GDNF treatment increases MCF7 cell proliferation utilizing BrdUrd assays [71]. Similar to the work of Esseghir and colleagues, our MTT assay data suggest that RET activation increases cell proliferation of the breast cancer cell lines assessed including, MCF7, T47D, MDA-MB-453 and BT-20. Interestingly, our data show that RET activation via GDNF treatment does not have an effect on proliferation of BT-474 cells. As mentioned earlier, we noticed that the immature form of RET in BT-474 cells is larger than normal likely due to a differing glycosylation pattern, which may be interfering with its ability to properly bind its ligand.

This hypothesized impaired binding in BT-474 cells would be one possible explanation for why RET activation does not affect cell proliferation in these cells. It would be interesting to perform glycoproteomic assays to explore whether BT-474 cells do in fact have a different glycosylation pattern that may interfere with normal RET activation.

Our lab has previously shown that RET activation increases cell adhesion in SH-SY5Y neuroblastoma cells [133], but we do not see an effect on cell adhesion following GDNF treatment in the MCF7 breast cancer cells. Further, as artemin treatment increases the expression of RET target genes, it may be worthwhile to explore whether RET activation via artemin has an effect on breast cancer cell adhesion.

Initial clinical evidence suggested that RET expression was associated specifically with the ER-positive subtype of breast cancer [71], but a subsequent study showed that RET was more broadly expressed in human breast cancer and associated with decreased overall survival [72]. Consistent with more recent studies, our data suggest that there may be functional relevance of RET more broadly in breast cancer. For example, our data suggest that RET activation increases proliferation of MDA-MB-453 breast cancer cells, a triple negative breast cancer cell model. Spanheimer and colleagues identified that TFAP2C regulates RET expression, and that this regulation is independent of the ER expression in breast cancer [82]. Specifically, in addition to MCF7 and T47D ER positive breast cancer cell lines, this group also used MDA-MB-453 breast cancer cells, and showed that in the all three cell models, KD of TFAP2C decreased RET expression [82], providing further support that RET may play a broader role in breast cancer.

Further research utilizing different, more comprehensive cohorts of breast cancer patients, and a wide range of breast cancer cell models is required to more comprehensively understand the contribution of RET to breast cancer. Our data suggest that the RET isoforms contribute differentially to breast cancer cell proliferation. This warrants further exploration of the contribution of RET9 and RET51 to other breast cancer processes in *in vitro* models, such as migration and invasion, and to human breast cancer using RET isoform-specific antibodies and tissue microarrays.

Moreover, expression of wild-type RET has been associated with breast cancer, however, very recently, a group has identified RET Y791F, a common population variant in RET which has also been found in patients with MEN2A syndrome or thyroid cancer, as a potential variant correlated with increased risk of breast cancer [185]. This suggests additional research is required to not only understand how wild-type RET expression may be mechanistically contributing to breast cancer, but also to verify if RET variants are associated with breast cancer.

In summary, we have identified suitable breast cancer cell models to evaluate the role of RET in this cancer type. Our data suggest that RET activation has a broad role in breast cancer cell proliferation irrespective of ER status. Further, we showed that RET9 and RET51 contribute differentially to the process of MCF7 breast cancer cell proliferation. These data support a role for RET in breast cancer, and warrant further investigation of the RET isoforms in other breast cancer functions and tumors to obtain a more comprehensive understanding of RET's contribution to the disease. Clinically, there are various receptor tyrosine kinase inhibitors that target RET [83], including

Vandetanib, which is currently used as a treatment for aggressive MTC (Reviewed in [35]). It may be useful to assess the benefit of combination therapy comprised of Vandetanib and the standard adjuvant treatment depending on the subtype (ie. tamoxifen/fulvestrant for ER positive breast cancer patients, and Herceptin for HER2 positive breast cancer patients) for certain subsets of breast cancer patients.

## **Chapter 3**

### **Characterization of the novel RET-BCAR3 interaction, and its functional implications**

### **3.1 Abstract**

RET is a receptor tyrosine kinase that is crucial for normal development of neuroendocrine tissues and the kidney, and has been implicated in various diseases, including cancer. Activation of RET results in the induction of various pathways that lead to the promotion of cellular processes including cell survival, differentiation and proliferation. BCAR3 has been shown to play a role in cell proliferation, motility and invasion. Various receptor tyrosine kinases, including EGFR and HER3, have been shown to interact with BCAR3. As both RET and BCAR3 contribute to similar cellular processes, such as proliferation, adhesion and migration, we hypothesized that the two proteins interact, and that this interaction may have functional implications for RET-mediated processes. Here, we identified a novel interaction between the RET receptor and the adaptor protein BCAR3, utilizing co-immunoprecipitation and Far Western blotting techniques. Using SH-SY5Y neuroblastoma cells, we explored whether BCAR3 KD affects RET-mediated processes, including cell proliferation, adhesion and migration. We found that BCAR3 KD has a general effect, independent of RET activation, on many of the cellular processes investigated, including cell proliferation, and adhesion in neuroblastoma cells. Disruption of BCAR3 may be a potential therapeutic option for certain subgroups of cancer patients.

### 3.2 Introduction

The RET receptor is a tyrosine kinase that is involved in the development of neuroendocrine tissues, and the kidney, and the process of spermatogenesis (Reviewed in [35]). Activation of RET occurs through the formation of a tri-molecular complex consisting of RET, its ligand, GDNF, and its co-receptor, GFR $\alpha$ 1 (Reviewed in [35]). RET activation leads to the recruitment of adaptor proteins that activate certain downstream signalling pathways that promote cell survival, proliferation and differentiation (Reviewed in [35]).

RET has also been implicated in various human diseases, including cancer (Reviewed in [35]). Expression of wild-type RET has been associated with aggressiveness in breast and prostate tumours [71, 73, 114, 186], whereas constitutive activation of RET, either through germ-line point mutations or gene fusions, has been implicated in thyroid and lung cancer, respectively [66, 187]. Understanding the underlying molecular mechanisms by which RET may be contributing to various tumor types will assist in uncovering novel treatment approaches for certain cancer patients. An initial step in elucidating the mechanistic contribution of RET to cancer would be identifying adaptor proteins that interact with RET to promote tumorigenesis. Koytiger and colleagues quantitatively assessed potential interactions between phosphorylated tyrosine residues on RTKs, and SH2 or PTB domains from adaptor proteins with a large protein-domain microarray, and identified a potential interaction between RET and the adaptor protein, Breast Cancer Anti-estrogen 3 (BCAR3) [167].

BCAR3 is an adaptor protein that has been shown to interact with various RTKs and contribute to cellular processes including cell migration and invasion [149, 156, 188,

189]. Li and colleagues have recently shown that BCAR3 molecularly connects ROR1-HER3 with the Hippo-YAP pathway to mediate breast cancer bone metastasis [150]. Further, using GST-pull downs, BCAR3 has been shown to associate with the EGFR [149]. Additionally, BCAR3 plays a role in many EGF-induced processes, including membrane ruffling, p130Cas localization to the ruffles, increase in p130Cas/CrkII interactions and cell migration [190]. Mice that are null for BCAR3 develop a defect in the adult ocular lens, and have reduced p130Cas expression [144]. Interestingly, RET is known to contribute to many of the same cellular processes as BCAR3, and also has a role in retinal development [191]. As there is overlap between the known roles and functions of RET and BCAR3, we hypothesized that there may be a functional significance of this interaction.

We have previously shown that SH-SY5Y neuroblastoma cells express endogenous RET, and that RET activation increases SH-SY5Y cell migration and adhesion [133]. While BCAR3 has been extensively studied in breast cancer models [156, 189], it has not been well-characterized in other cancers, including neuroendocrine tumors. Here, we investigated whether RET and BCAR3 interact, and then assessed the functional implications of the interaction. Our data suggest that RET and BCAR3 can interact, and that this novel association is direct, and requires RET phosphorylation. We used the SH-SY5Y neuroblastoma model to generate both a BCAR3 and a Mock KD cell line to evaluate RET-BCAR3 relationships. Our data suggest that BCAR3 has a broad effect on investigated cellular processes, including cell proliferation, and cell adhesion. With Reverse Phase Protein Array (RPPA) assays, verified with follow-up Western

blotting, we saw that BCAR3 KD decreases phosphorylation of various components of downstream signalling pathways, including Protein Kinase B (AKT) and Extracellular Signal-Regulated Kinase (ERK) in the neuroblastoma cell model. Together, our data suggest a novel interaction between the RET receptor and the BCAR3 adaptor protein, and that BCAR3 may play a broad role in various cellular processes irrespective of RET, providing support that the adaptor protein may have functions in tumor types other than breast cancer.

### **3.3 Materials and Methods**

#### **3.3.1 Cell Culture**

The SH-SY5Y neuroblastoma cell line, HEK293 human embryonic kidney cell line, HEK293T and HeLa cervical cancer cell line were obtained from the American Type Culture Collection (ATCC; Manassas, VA). Cells were cultured in Dulbecco's Modified Eagles Medium (DMEM; Invitrogen, Burlington, ON) with the addition of 10% fetal bovine serum (FBS; Sigma-Aldrich, St. Louis, MO). SH-SY5Y cells were treated with 10  $\mu$ M retinoic acid overnight to increase RET expression. Stable, polyclonal BCAR3 and Mock shRNA KD cell lines were generated in SH-SY5Y and HeLa cells using puromycin at 1.5  $\mu$ g/mL. Cells were treated with GDNF (Peprotech, Rocky Hill, NJ) for specified times in order to activate RET.

### **3.3.2 Expression Constructs, DNA Isolation, Quantification and Transfection**

His-tagged constructs for BCAR3-SH2, Src Homology 2 domain containing – phosphotyrosine binding (SHC-PTB), and Disabled-2 phosphotyrosine binding (DAB2-PTB) were obtained from Dr. Gavin MacBeath (Harvard Medical School, Boston, MA) [167]. pXJ40-FLAG-tagged BCAR3 wild-type (WT) was a gift from Dr. Catherine Pallen (University of British Columbia, Vancouver, BC) [148]. Paxillin-pEGFP was a gift from Dr. Rick Horwitz (Addgene plasmid #15233) [192], and RFP-zyxin was a gift from Dr. Anna Huttenlocher (Addgene plasmid #26720) [193]. GFP-tagged vinculin was obtained from Dr. Daniel Rosel [194]. GST-tagged RET9 (amino acid residues 664-1072), or RET51 (amino acid residues 664-1114), used as the bait in our Far Western assays, were previously described [195]. GFR $\alpha$ 1 and full-length RET9 and RET51 wild-type, kinase dead (K758M), point mutant (Y1096F), and EGFP-tagged and mCherry-tagged RET isoform constructs were previously described [53, 196]. Lentiviral shRNAs targeting BCAR3 and an empty vector (Mock KD) were obtained from Open Biosystems (Huntsville, AL). Small- scale and medium-scale plasmid DNA isolations were prepared utilizing the Macherey-Nagel kits (Duren, Germany). DNA concentration and purity (260/280 ratio) was assessed using a NanoDrop 2000 Spectrophotometer (Thermo Fisher Scientific, Waltham, MA). Constructs were transfected into HEK293 cells and HeLa cells using Lipofectamine 2000 (Invitrogen, Burlington, ON) according to the manufacturer's instructions.

### **3.3.3 BCAR3 shRNA KD**

HEK293T cells were transfected with psPAX2 packaging, pMD2.G envelope, and pLKO.1 Mock or BCAR3 lentiviral shRNA constructs with the Lipofectamine 2000 (Invitrogen, Burlington, ON) transfection reagent as per supplier's instructions. Virus was harvested every 12 hours for 48 hours, pooled and filtered with a 0.45  $\mu$ m filter. BCAR3 and pLKO.1 Mock lentivirus were added to SH-SY5Y neuroblastoma and HeLa cells, and subjected to selection with 1.5  $\mu$ g/mL puromycin to generate KD cell lines. Western blotting was utilized to verify KD of the BCAR3 protein.

### **3.3.4 Purification of His and GST-tagged Recombinant Proteins**

His-tagged BCAR3-SH2, SHC-PTB and DAB2-PTB bacterial expression constructs were introduced into *E. coli* BL21-CodonPlus-RP cells, and grown overnight. Cells were harvested by centrifugation and resuspended in PBS. Following disruption of the cells using 20 mL Binding Buffer (25 mM Tris pH 8.0, 250 mM NaCl, 8 M urea), the lysate was clarified by centrifugation, and subjected to purification with a Ni<sup>2+</sup>-chelating Sepharose bead column (GE Healthcare Life Sciences, Pittsburgh, PA) equilibrated with Binding Buffer. The column was rinsed with Binding Buffer with 10 mM imidazole (pH 7.4) and bound protein eluted in Binding Buffer with 300 mM imidazole. Eluted fractions were combined, and dialyzed overnight in PBS.

GST-tagged RET intracellular domain proteins, and GST were expressed in *E. coli* BL21-CodonPlus-RP, harvested and resuspended, as described above. Cells expressing GST were disrupted by sonication on ice, whereas GST-RET proteins were disrupted using a French Pressure Cell at 10 000 psi. Debris was pelleted and lysates

were incubated for 2-4 hours with Glutathione Sepharose beads (GE Healthcare Life Sciences, Pittsburgh, PA) that were pre-washed in a 1X PBS with 1% Triton X-100, 1 mM PMSF, 10 µg/mL aprotinin and 10 µg/mL leupeptin. 50 mM Tris-HCl pH 8.8, 150 mM NaCl, 20 mM Glutathione was used to elute the GST proteins, and the pooled fractions were dialyzed overnight in PBS.

### **3.3.5 Far Western Blotting**

His-tagged BCAR3, SHC-PTB, and DAB2-PTB were separated on 12% sodium dodecyl sulfate polyacrylamide gel electrophoresis (SDS-PAGE). Proteins were transferred to nitrocellulose membranes, which were blocked overnight with 5% milk in Tris-buffered saline with Tween 20 (TBS-T) at 4°C. Membranes were incubated with either GST-tagged intracellular RET or GST alone, in 5% milk in TBS-T for 8 hours at 4°C. Blots were rinsed ten times for 5 minutes/wash in TBS-T prior to incubation with either an anti-GST or anti-His antibody (Santa Cruz Biotechnologies, Santa Cruz, CA) at a 1:1000 dilution for 2 hours at room temperature. Probing the purified His-tagged proteins with the anti-His antibody served as loading control. Blots were washed three times for 15 minutes/wash in TBS-T to remove any non-specific binding. Membranes were incubated with the appropriate secondary antibody at a 1:3000 dilution for 1 hour at room temperature, rinsed with TBS-T and exposed to film with chemiluminescence.

### 3.3.6 Protein Harvest, Co-Immunoprecipitation and Western Blotting

HEK293 cells were grown to 70% confluence prior to transient transfection. The medium was changed six hours after transfection to DMEM supplemented with 10% FBS. After 24 hours, cells were serum-starved as the media was replaced with DMEM without FBS. Whole cell lysates were prepared 48 hours following transfection. Cells were treated with GDNF (PeproTech, Rocky Hill, NJ) at a final concentration of 50 ng/mL for 20 minutes prior to protein harvest. Cells were washed twice with cold PBS, and collected utilizing lysis buffer (20 mM Tris-HCl – pH 7.8, 0.15 M NaCl, 1% Igepal, 2 mM Na<sub>2</sub>EDTA 1 mM phenylmethylsulfonyl fluoride, 10 µg/mL aprotinin, 1 mM sodium orthovanadate, 10 µg/mL aprotinin) with a cell scraper. The whole cell lysates were solubilized by rotating for 30 minutes at 4 °C, and debris pelleted by centrifugation for 15 minutes at 4 °C at 11,000 RPM. Protein concentrations were calculated utilizing the BCA Protein Assay (Thermo Scientific, Rockford, IL) as per the supplier's instructions. Lysates (700 – 1000 µg protein) were pre-cleared with 25 µL A/G Sepharose (Santa Cruz Biotechnologies, Santa Cruz, CA) on a rotator at 4 °C for 1 hour. Beads were centrifuged at 5000 RPM for 4 minutes and supernatant collected. The supernatant was incubated with 1 µg mouse anti-Flag antibody (Sigma-Aldrich, Oakville, ON) at 4 °C for 2 hours, 40 µL of A/G Sepharose beads were added at 4 °C overnight. The beads were pelleted at 5000 RPM for 4 minutes, supernatant removed, and the pellet washed with 1X lysis buffer. Laemmli buffer (250 mM Tris pH 6.8, 4% SDS, 10% glycerol, 0.006% bromophenol blue, and 2% 2-mercaptoethanol) was added to beads. Co-immunoprecipitation samples and whole cell lysates were separated by SDS-PAGE.

Gels were transferred to a nitrocellulose membrane (Bio-Rad Laboratories, Hercules, CA), and blocked with 5 % milk in TBS-T for at least 30 minutes at room temperature. Membranes were incubated with a primary antibody at a dilution of 1:1000 in either 5 % milk in TBS-T or 5% Bovine Serum Albumin (BSA) in TBS-T overnight at 4 °C. Phospho-antibodies were added to membranes with BSA in TBS-T rather than milk to reduce background. Membranes were rinsed three times with TBS-T for 15 minutes/rinse. Secondary antibodies were added at a dilution of 1:3000 with 5% milk in TBS-T for 1-2 hours at room temperature. Following three washes with TBS-T for 15 minutes / wash, membranes were exposed using enhanced chemiluminescence with the Pierce ECL Western Blotting Substrate as per manufacturer's conditions (VWR, Mississauga, ON). Antibodies used for immunoprecipitation and western blotting are described in Table 3.1.

### **3.3.7 RNA Isolation and Quantitative Real-time PCR (qRT-PCR)**

Total RNA was isolated from SH-SY5Y wild-type, Mock KD and BCAR3 KD neuroblastoma cells using Trizol (Life Technologies, Burlington, ON) according to the manufacturer's instructions. The total RNA yield and purity (A260/A280) was verified utilizing NanoDrop 2000 Spectrophotometer (Thermo Fisher Scientific, Waltham, MA). Sequences of primers used are listed in Table 3.2. The Applied Biosystems 7500 Real-Time PCR System (Applied Biosystems, San Diego, CA) was used with the one-step QuantiTect SYBR green qRT-PCR kit (Qiagen, Mississauga, ON), and qRT-PCR cycling conditions are outlined in Table 3.3. Verification that PCR product obtained contained no

primer-dimers was performed through melt curve analysis. Delta cycle threshold (Ct) values were calculated (Reviewed in [197]) for all conditions using the housekeeping gene *GUSB* as the reference to correct for differences between samples. Fold change of expression was determined utilizing the delta delta Ct method, by subtracting the Ct value of the control condition from the Ct value of the condition of interest (Reviewed in [197]). A minimum of three biological replicates with at least three technical replicates were used for each condition.

### **3.3.8 Cell Proliferation Assay**

3-(4,5-Dimethylthiazol-2-YI)-2,5-Diphenyltetrazolium Bromide (MTT, Life Technologies, Burlington, ON) was used to assess cell proliferation, as previously described [37]. Briefly, SH-SY5Y Mock KD and BCAR3 KD cells were seeded into 96-well plates in DMEM with 0.1% FBS and retinoic acid. Wells were untreated or treated with 50 ng/mL of GDNF (Peprotech, Rocky Hill, NJ) every 24 hours. Following three days of cell growth, MTT solubilized in PBS was added at a final concentration of 45  $\mu\text{g/mL}$  at 37 °C for 24 hours. The resulting purple precipitate was solubilized by shaking in the dark at room temperature with 100  $\mu\text{L}$  of 20% SDS in 0.04 M HCl, and absorbance measured at 570 nm using a plate reader (ELx 800UV plate reader, Bio-Tex Instruments, Houston, TX). Each condition was performed at least in triplicate with a minimum of three biological replicates.

### **3.3.9 Cell Adhesion Assay**

SH-SY5Y cells with either Mock or BCAR3 KD were grown to approximately 70-90 % confluency. Cells were detached with citric saline (10X solution: 1.35M KCl and 0.15M sodium citrate) . Before plating cells, the wells were either coated with 200 ng/ $\mu$ l type I collagen (BD Biosciences, Bedford, MA), or BSA as a control. After coating for 1 hour at 37 °C, wells were rinsed and blocked with 3% BSA in PBS to reduce non-specific binding.  $5 \times 10^4$  cells/well were plated with 100  $\mu$ L of 0.3% BSA in DMEM, and allowed to adhere for 1 hour at 37 °C. Cells were subjected to a few rinses with PBS, and fixed in 3.7% paraformaldehyde. 0.5% Toluidine Blue – O was used to stain fixed cells for 3 hours. Cells were washed with water, and solubilized for 20 minutes with 0.2% Triton-X100. A plate reader (ELx 800UV plate reader, Bio-Tex Instruments, Houston, TX) was used to measure adhesion at 570 nm absorbance, and values were then normalized to the Mock KD in the absence of GDNF condition.

### **3.3.10 Single-Cell Migration Assay**

Cells were seeded sparsely ( $1 \times 10^4$ ) onto 24-well plates in DMEM with 0.1% FBS, and retinoic acid in the presence or absence of GDNF. Cells were left to settle for 4 hours prior to imaging with the IncuCyte ZOOM system (Essen BioScience Inc., Ann Arbor, Michigan) every 45 minutes for up to 13 hours. At least four representative images were taken per well. Images were aligned using MetaMorph software (Universal Imaging Corporation, Downingtown, PA). To evaluate the area that cells of interest move over time, mean square displacements (MSDs) of individual cells were calculated and

spider plots generated using the DiPer program run on Microsoft Excel [198]. A minimum of 50 cells per condition/experiment, and at least 3 replicates were analyzed.

### **3.3.11 Cell Morphology Assessment**

Wells of a 24-well plate were coated with 500  $\mu$ L acidified collagen (type 1) at a final concentration of 50  $\mu$ g/mL per well for 1 hour at 37 °C. Wells were washed once with serum-free DMEM medium. SH-SY5Y cells were resuspended in 0% DMEM with retinoic acid, with or without GDNF prior to plating triplicates of each condition into wells. Cells were imaged four hours after plating with the IncuCyte Zoom system (Essen Bioscience Inc., Ann Arbor, MI), and 2-4 representative images were taken per well.

### **3.3.12 Imaging of Focal Adhesion Proteins**

HeLa cells were transiently transfected with GFR $\alpha$ 1, either a mCherry-tagged RET isoform or a GFP-tagged RET isoform, and one of the following fluorescently-tagged focal adhesion markers, GFP-paxillin [192], GFP-vinculin [194] or RFP-zyxin [193]. Cells were serum-starved the following day for 3 hours prior to the addition of GDNF for 1 hour. Live cells were imaged by total internal fluorescence microscopy (TIRF) using a 63X oil objective on an inverted Olympus BX-80 confocal microscope (Olympus, Tokyo, Japan) equipped with a multi-colour TIRF module and a Hamamatsu EM-CCD digital camera (Spectral Applied Research, Richmond Hill, ON). Metamorph software (Universal Imaging Corporation, Downingtown, PA) was utilized to align the acquired images, and quantify the number of focal adhesions.

### **3.3.13 Reverse Phase Protein Array (RPPA) Assays**

SH-SY5Y Mock KD and BCAR3 KD cells were treated with GDNF for the indicated times (0, 5, 15 or 30 minutes), washed twice with cold 1 X PBS, and frozen at -80 °C. The RPPA assays were performed by Dr. Taran Gujral (Harvard University, Boston, MA). Briefly, cells were lysed in 50 mM Tris-HCl, 2% SDS, 5 % glycerol, 5 mM EDTA, 1 mM NaF with 10 mM  $\beta$ -GP, 1 mM PMSF, 1 mM  $\text{Na}_3\text{VO}_4$ , 1 mM DTT, immediately before use, and samples were prepared, probed, and scanned as previously described [199]. A series of phospho-antibodies were used to probe samples on the RPPA assays, including p-AKT, p-ERK, p-S6 and p-Protein Kinase C (PKC). The  $\beta$ -actin antibody was used to normalize the RPPA data.

### **3.3.14 Statistical Analyses**

Experiments were performed at least in triplicate, and the standard error of the mean (SEM) was calculated. A student's two-tailed, unpaired T-test was utilized to assess differences between Mock and BCAR3 KD cell lines, and a p-value < 0.05 was considered to be significant.

**Table 3-1. Antibodies Utilized for Immunoblotting and Immunoprecipitation.**

<b>Antibody target</b>	<b>Supplier</b>
<b>Primary Antibodies</b>	
RET (C-20) goat	Santa Cruz Biotechnology, Santa Cruz, CA
RET (E1N8X) rabbit	Cell Signaling Technology, Boston, MA
$\gamma$ -Tubulin mouse	Sigma-Aldrich, Oakville, ON
GST	Santa Cruz Biotechnology, Santa Cruz, CA
His	Santa Cruz Biotechnology, Santa Cruz, CA
FLAG mouse	Sigma-Aldrich, Oakville, ON
Total ERK	Santa Cruz Biotechnology, Santa Cruz, CA
pERK	Santa Cruz Biotechnology, Santa Cruz, CA
Total AKT	Santa Cruz Biotechnology, Santa Cruz, CA
pAKT	Cell Signaling Technology, Boston, MA
pRET Y905	Cell Signaling Technology, Boston, MA
<b>Secondary Antibodies</b>	
Anti-Mouse IgG (HRP-linked)	Cell Signaling Technology, Boston, MA
Anti-Rabbit IgG (HRP-linked)	Cell Signaling Technology, Boston, MA
Anti-Goat IgG (HRP-linked)	Santa Cruz Biotechnology, Santa Cruz, CA

**Table 3-2. Sequences for Primer Pairs Used for qRT-PCR.**

<b><u>Gene Target</u></b>	<b><u>Forward Primer</u> (5' – 3')</b>	<b><u>Reverse Primer</u> (5' – 3')</b>
<i>GUSB</i>	GAAAATACGTGGTTGGAGAGC	AAGGAACGCTGCACTTTTTG
<i>SNAI1</i>	TTCTCTAGGCCCTGGCTGC	TACTTCTTGACATCTGAGTGGGTCTG
<i>SNAI2</i>	CTGGGCTGGCCAAACATAAG	CTTGTCACAGTATTTACAGCTGAAAG
<i>TWIST1</i>	GGCTCAGCTACGCCTTCTC	TCCTTCTCTGGAAACAATGACA
<i>ZEB1</i>	GCACCTGAAGAGGACCAGAG	TGCATCTGGTGTCCAATTTT
<i>VIM</i>	TGTCCAAATCGATGTGGATGTTTC	TTGTACCATTCTTCTGCCTCCTG
<i>MMP2</i>	CAGGCTCTTCTCCTTTCACAAC	AAGCCACGGCTTGGTTTTTCCTC
<i>MMP9</i>	TGGGCTACGTGACCTATGACAT	GCCCAGCCCACCTCCACTCCTC
<i>OCN</i>	AAGGGAAGAGCAGGAAGGTC	CTCCAACCATCTTCTTGATGTG
<i>HUGL2</i>	TTGAGCGCTTCTCTCTCTCC	GACGCTCAGCCACTCACTCT
<i>CDH2</i>	AGCGCAGTCTTACCGAAGG	TCGCTGCTTTCATACTGAACTTT
<i>CCND1</i>	CGAGAAGCTGTGCATCTACA	AATGAAATCGTGCGGGGTCA

**Table 3-3. One-Step Quantitative Real-time PCR Cycling Conditions.**

<u>Step</u>	<u>Temperature</u>	<u>Time</u>
Reverse Transcription	50 °C	1800 s
Initial Denaturation	95 °C	900 s
Denaturation (40X cycles)	95 °C	15 s
Annealing (40X cycles)	55 °C	25 s
Extension (40X cycles)	72 °C	15 s
Melt Curve	Ramp from 60 °C to 95 °C	---
Storage	4 °C	Hold

## 3.4 Results

### 3.4.1 The RET tyrosine kinase receptor interacts with the BCAR3 SH2 domain

High-throughput studies suggest that the BCAR3 adaptor protein may interact with several RTKs, including RET [167]. To verify whether the RET receptor and the BCAR3 adaptor protein interact, we initially performed a Far Western assay. Using a His-tagged BCAR3 protein, and GST-tagged RET isoform proteins, our Far Western data suggest that RET and BCAR3 interact *in vitro*, and that this is a direct interaction (Figure 3-1A). Of note, the His-tagged BCAR3 protein used is comprised of only the SH2 domain [167], suggesting that this region of BCAR3 is required for binding RET. The SHC protein is known to directly interact with RET isoforms [51], whereas, the DAB2 protein does not associate with the RET isoforms. Thus, His-tagged SHC and His-tagged DAB2 were used as our positive and negative control, respectively. Our data confirm that SHC and RET directly interact, but that DAB2 and RET do not associate, suggesting the specificity of the RET-BCAR3 interaction (Figure 3-1A). The Far Western blot was probed with an anti-His antibody as a loading control. We have previously shown that the GST-tagged RET proteins are phosphorylated [196], suggesting that it may be worthwhile to assess whether the RET-BCAR3 association is phospho-dependent.

We used co-immunoprecipitations (co-IP) of whole cell lysates of HEK293 cells transiently expressing GFR $\alpha$ 1, with WT RET or a RET kinase dead mutant, and FLAG-tagged BCAR3 to confirm the RET-BCAR3 association. Consistent with our Far Western data, our co-IP experiments suggest that RET and BCAR3 interact in these cells,

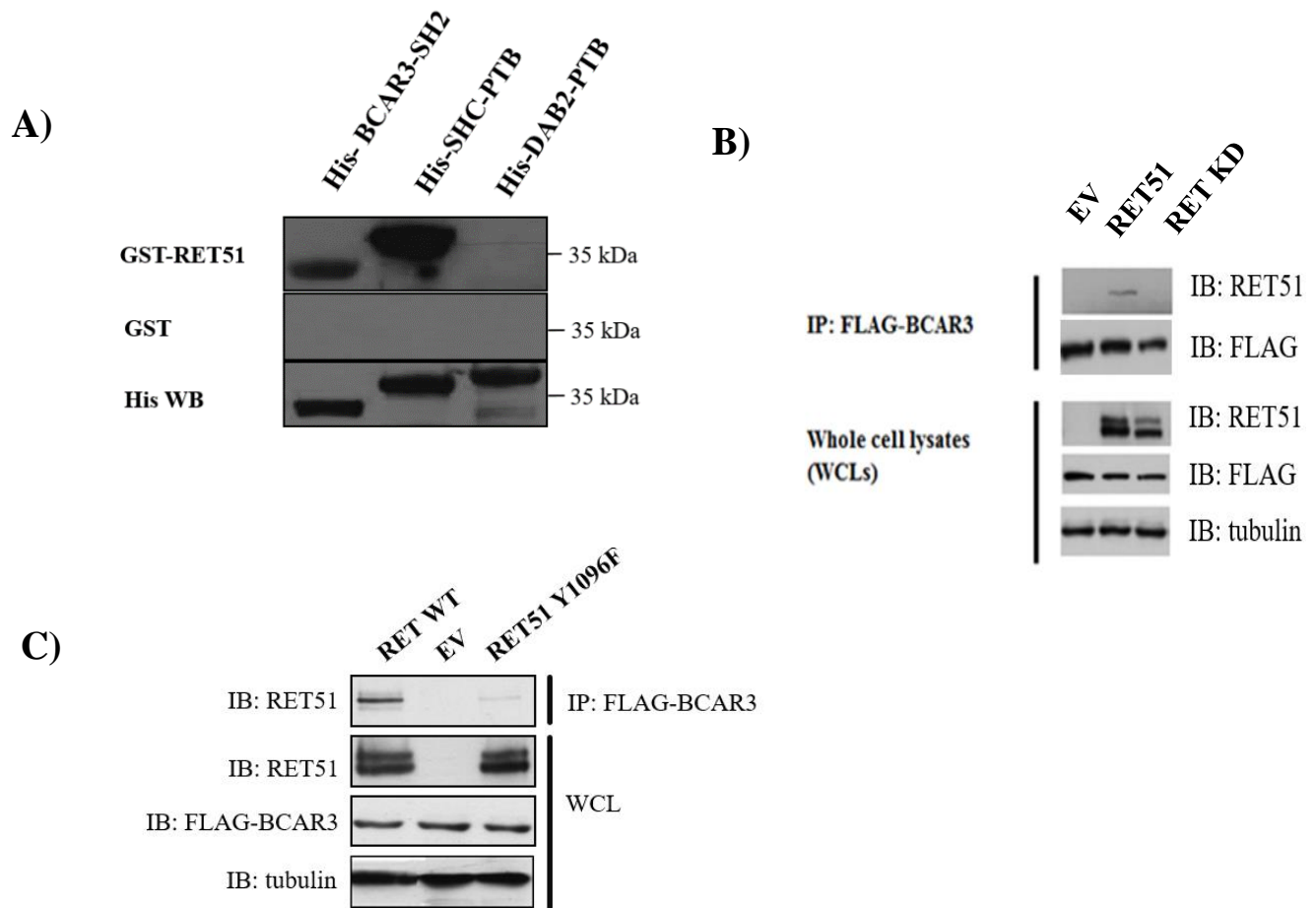


**Figure 3-1. RET receptor interacts with the BCAR3 adaptor protein.**

**A. RET directly interacts with the BCAR3 SH2 domain.** Far Western assay showing an interaction between RET and BCAR3. His-tagged BCAR3-SH2, SHC-PTB, and DAB2-PTB were separated on a 12% SDS-PAGE gel, transferred to a nitrocellulose membrane, and initially probed with GST-tagged RET51, then the GST antibody, followed by anti-mouse secondary. His-tagged constructs were probed with the His antibody as a loading control, and blotted with the GST alone as a negative control. **B. RET interacts with BCAR3, and this association is kinase-dependent.** Whole cell lysates (WCL) from HEK293 cells transiently transfected with GFR $\alpha$ 1, one of the following: RET51 wild-type or RET51 kinase-dead or pcDNA, and FLAG-tagged BCAR3 were immunoprecipitated with the anti-FLAG antibody, and then separated, transferred and probed with indicated antibodies. Tubulin was utilized as loading controls. **C. RET tyrosine 1096 is important for the RET-BCAR3 protein interaction.** The RET Y1096F mutation construct was transiently transfected in combination with RET's co-receptor and FLAG-tagged BCAR3, and then immunoprecipitated and analyzed by western blotting as described above to assess whether the Y1096 residue on RET51 is important for the RET-BCAR3 association. Tubulin served as the loading control. WT = wild-type; IP = immunoprecipitate; EV = empty vector; IB = immunoblot; WB = western blot

and this interaction is kinase-dependent (Figure 3-1B). Residue Y1096 is an important signalling hub site on RET (Reviewed in [35]), and is the site previously predicted by the high throughput protein domain microarray for BCAR3 binding [167]. We utilized a RET construct in which the tyrosine 1096 has been mutated to a phenylalanine (Y1096F) to assess whether this residue is crucial in the binding of RET to BCAR3. Our co-IP data show that the RET-BCAR3 interaction is diminished for the Y1096F RET, suggesting that Y1096 is an important site for the RET-BCAR3 association (Figure 3-1C).

#### **3.4.2 BCAR3 contributes to SH-SY5Y neuroblastoma cell proliferation**

Our lab has previously shown that SH-SY5Y cells express robust levels of endogenous RET and the co-receptor, GFR $\alpha$ 1 [133, 200]. Our Western blotting analyses using SH-SY5Y neuroblastoma cells demonstrate that BCAR3 protein is also endogenously expressed (Figure 3-2A). Using this cell model, we generated both BCAR3 and Mock KD cells utilizing shRNA. BCAR3 KD in SH-SY5Y cells was verified through western blotting, and quantified by densitometry (Figure 3-2A).

We used MTT cell viability assays to assess the effects of RET activation on SH-SY5Y cell proliferation over 3 days. Our data show that GDNF treatment increased cell proliferation of SH-SY5Y cells compared to the untreated condition (Figure 3-2B). We then explored the effect of BCAR3 kds on RET-mediated SH-SY5Y cell proliferation. Interestingly, our data showed a significant decrease in the proliferation of SH-SY5Y BCAR3 KD cells in comparison to SH-SY5Y Mock KD cells in the absence of RET activation, suggesting that BCAR3 generally plays a role in proliferation of these cells

(Figure 3-2B). Further, with the addition of GDNF, there was no increase in proliferation SH-SY5Y BCAR3 KD cells compared to GDNF-treated SH- SY5Y cells, suggesting that BCAR3's role in SH-SY5Y cell proliferation is irrespective of RET activation (Figure 3-2B).

### **3.4.3 RET-mediated migration is BCAR3-dependent**

Our lab has previously shown that in the presence of GDNF, SH-SY5Y cells become more migratory using wound healing assays [133]. As BCAR3 has been shown contribute to breast cancer cell migration [169], we evaluated whether BCAR3 plays a role in RET-mediated SH-SY5Y cell migration. We utilized the IncuCyte Zoom System to assess real-time single cell migration in BCAR3 KD SH-SY5Y cells. There is no statistically significant difference between the BCAR3 KD condition in comparison to the BCAR3 KD treated with GDNF condition. Unlike the SH-SY5Y MOCK KD cells, with the BCAR3 KD cells, GDNF does not have an effect on migration, suggesting that RET-mediated migration is BCAR3 dependent. Consistent with previous wound healing migration assays, our data suggest that RET activation increases SH-SY5Y Mock KD migration as measured by mean square displacement analysis (Figure 3-3B).

### **3.4.4 RET51-mediated focal adhesion formation**

Hela cells were transiently transfected with GFR $\alpha$ 1, a fluorescently-tagged RET isoform, and a fluorescently-tagged focal adhesion marker [ie. paxillin (early stage focal adhesion marker), vinculin (mid-stage focal adhesion marker), or zyxin (late stage focal

adhesion marker)] to assess whether the RET isoforms differentially contribute to focal adhesion formation. We imaged live cells using TIRF microscopy.

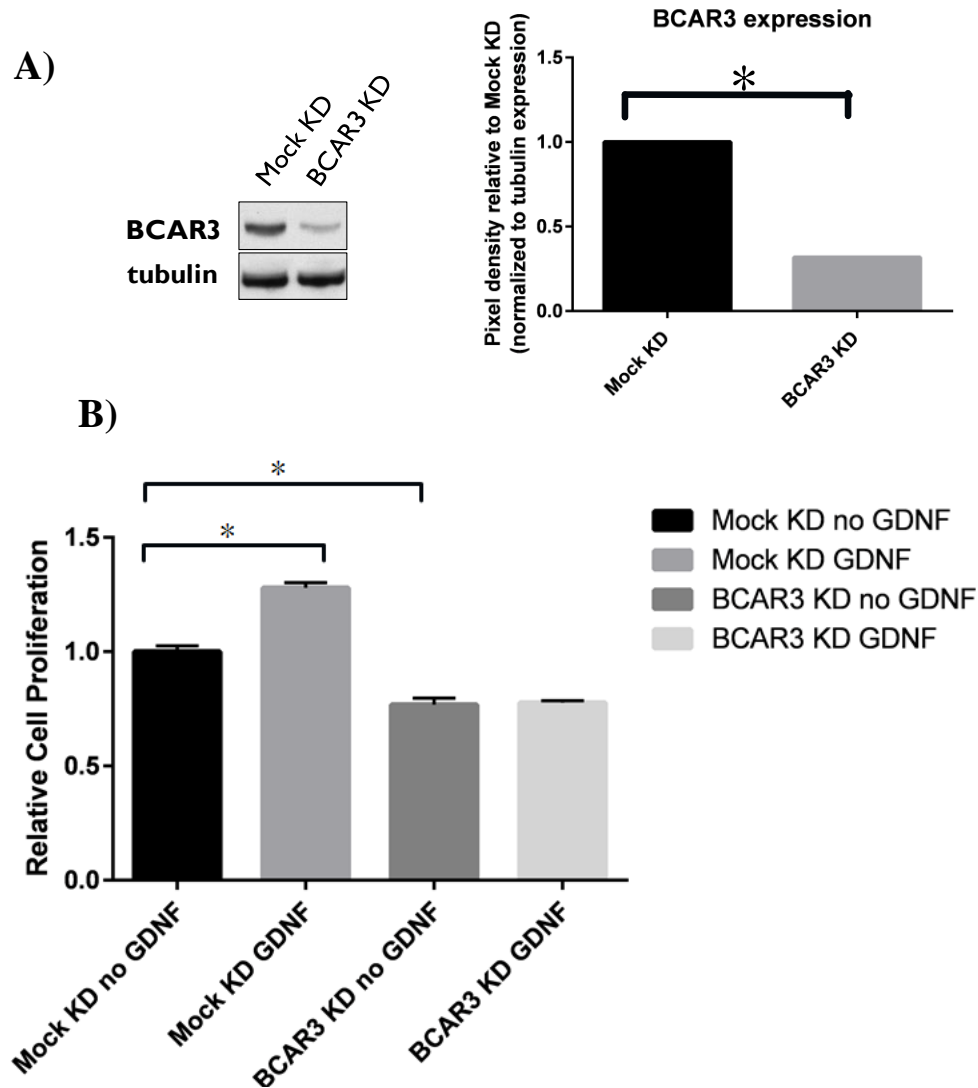


**Figure 3-2. BCAR3 plays a role in SH-SY5Y neuroblastoma cell proliferation.**

**A.** BCAR3 shRNA knockdown was evaluated in in stable polyclonal SH-SY5Y cells by western blotting. BCAR3 protein levels were significantly diminished in the BCAR3 KD cells compared to the Mock KD cell line. Tubulin served as the loading control. **B.** MTT cell viability assays were used to assess cell proliferation of SH-SY5Y Mock KD and BCAR3 KD in the presence or absence of GDNF (50 ng/ $\mu$ L) with the addition of retinoic acid over 72 hours. Data are represented as cell proliferation levels relative to SH-SY5Y Mock KD without GDNF treatment to evaluate the effects of RET activation, and BCAR3 KD. Error bars represent the standard error across a minimum of three technical replicates. \* signifies statistical significance, and p-value is less than 0.05

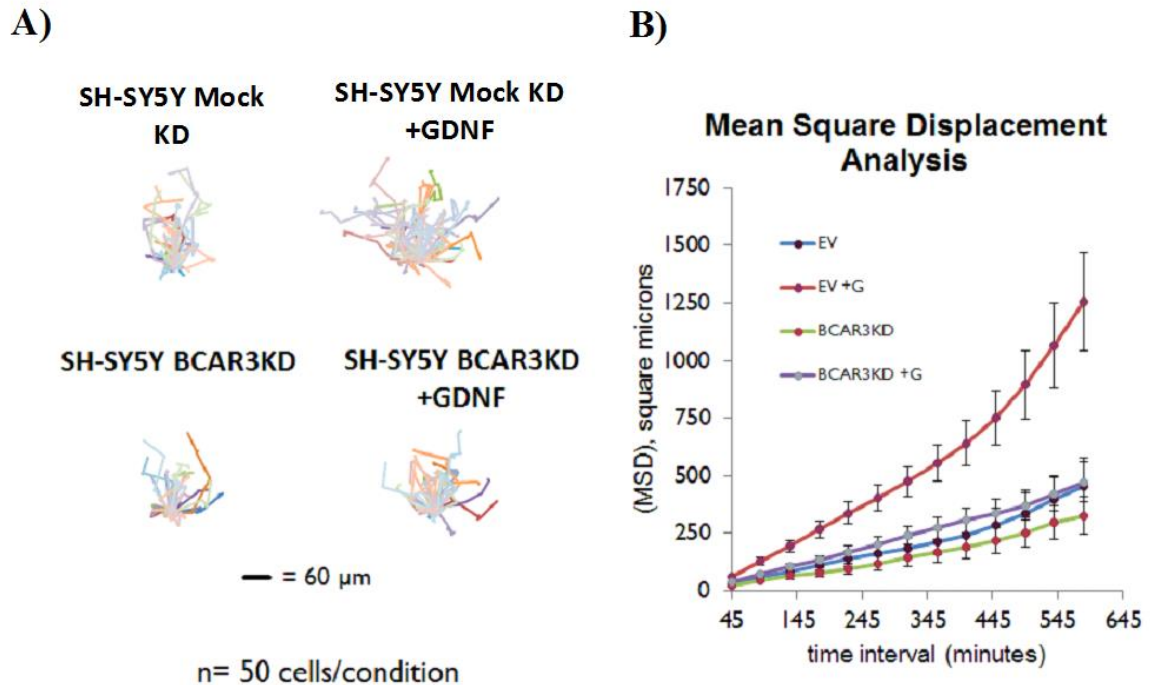


**Figure 3-3. BCAR3 plays a role in SH-SY5Y neuroblastoma cell migration.**

**A.** Spider plots graphically depict single cell migration of SH-SY5Y Mock KD and BCAR3 KD in the presence or absence of GDNF. Cells were sparsely seeded with retinoic acid into a 24-well plate, and imaged with the IncuCyte real-time imaging system every 45 minutes for 13 hours. MetaMorph software was used to align images, and DiPer software was used to generate spider plots. A minimum of 50 cells were assessed per condition. **B.** Mean Square Displacement analysis of single cell migration of SH-SY5Y Mock and BCAR3 KD with or without GDNF (50 ng/ $\mu$ L) over 13 hours. Error bars represent the standard error across a minimum of three technical replicates. There is no statistically significant difference between the SH-SY5Y BCAR3 KD compared to the SH-SY5Y BCAR3 KD +GDNF conditions. MSD = Mean square displacement

We saw approximately 60-80 paxillin-positive spots/cell in the presence of RET51 compared to 20-30 paxillin-positive spots with RET9. These general trends for the RET isoforms were also observed when assessing vinculin and zyxin positive spots, but absolute numbers of focal adhesions were lower than observed with paxillin. Our data suggest that there is an increase in the number of focal adhesions (as measured by GFP-paxillin, GFP-vinculin, and RFP-zyxin) in the presence of RET51 compared to RET9 (Figure 3-4). This suggests that either RET51 may contribute more effectively to focal adhesion formation, or RET9 may be suppressing focal adhesion formation. However, in the absence of RET condition, we saw similar numbers of focal adhesion to the RET9 condition, suggesting that RET51 may be contributing to focal adhesion formation to a larger degree than RET9 (Figure 3-5). Interestingly, there is no increase in the amount of focal adhesions with the RET51 kinase dead mutant compared to the wild-type RET51 (Figure 3-5), suggesting that RET kinase activity is important for RET51-induced focal adhesion formation. Moreover, with the RET51 Y1096F mutant, we also do not observe an increase in the number of focal adhesions as with the RET51 wild-type (Figure 3-5), indicating that interactions at this site are important for focal adhesion formation. As we wanted to evaluate whether BCAR3 KD had an effect on RET-mediated focal adhesion formation, we generated a stable polyclonal BCAR3 KD HeLa cell line. We transiently transfected the HeLa Mock and BCAR3 KD cells with GFR $\alpha$ 1, EGFP- paxillin, and mCherry-tagged RET51. After 24 hours post-transfection, cells were subjected to 3 hours serum starvation, and treated with 1 hour GDNF.

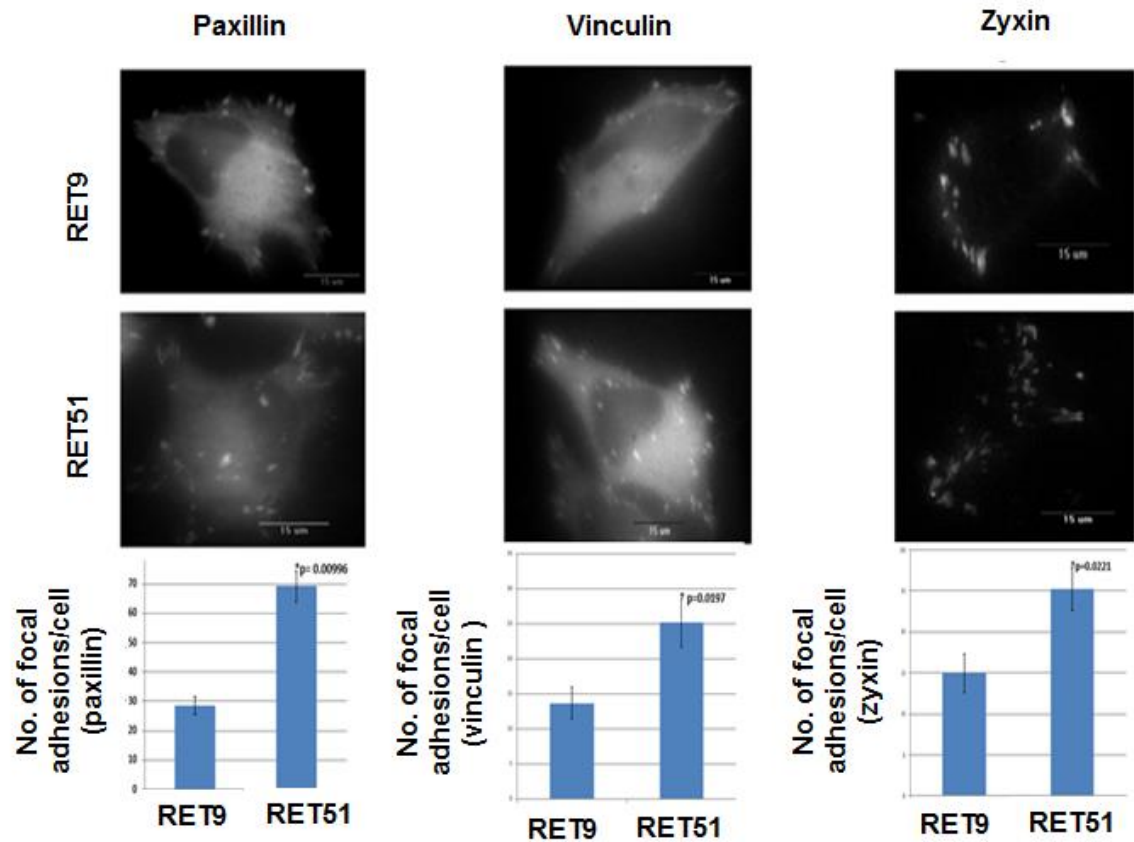


**Figure 3-4. RET isoforms differentially contribute to focal adhesion formation.**

HeLa cells were transiently transfected with GFR $\alpha$ 1, either a mCherry or GFP-tagged RET isoform, and one of GFP-tagged paxillin, GFP-tagged vinculin, RFP-tagged zyxin. 24 hours post-transfection, cells were serum-starved for 3 hours, and GDNF added for 1 hour prior to imaging by total internal fluorescence microscopy. Upper panel Representative images of cells expressing focal adhesion markers (ie. paxillin, vinculin and zyxin) and either RET9 or RET51. Scale bar = 15  $\mu$ m. Graphical data are represented as average of number of focal adhesions per cell. Error bars represent the standard error across at least three technical replicates. \*signifies statistical significance, and p-value < 0.05

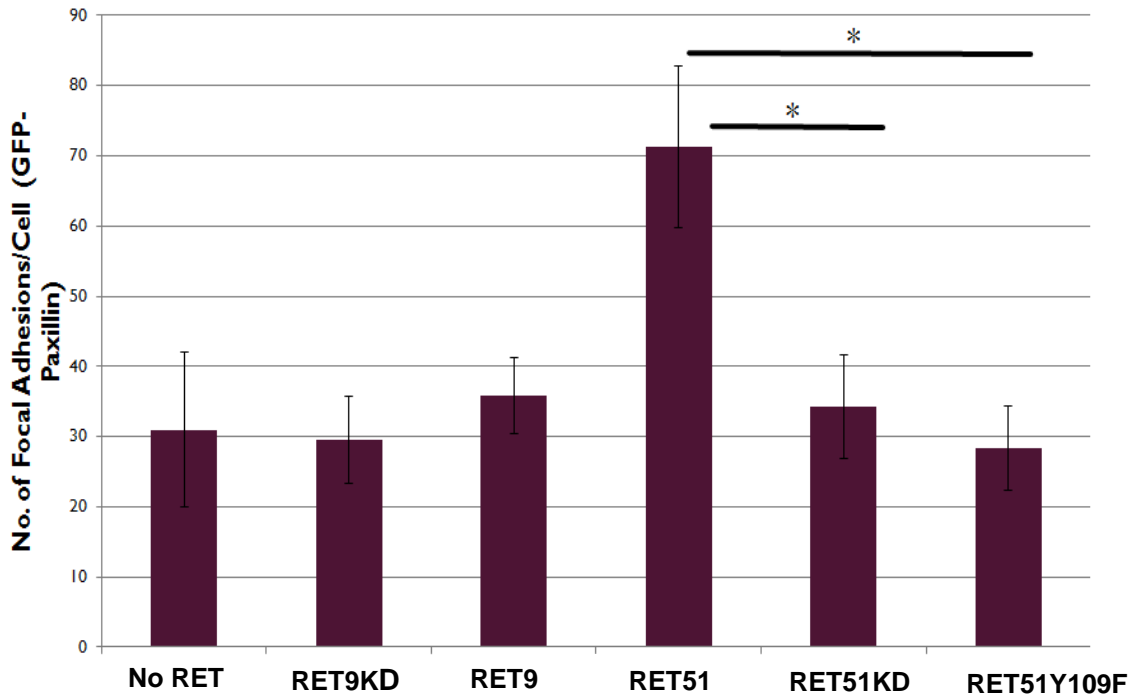


**Figure 3-5. RET51 focal adhesion formation is dependent on Y1096F and is kinase-dependent.**

**A.** HeLa cells were transiently transfected with GFR $\alpha$ 1, GFP-tagged paxillin, and either pcDNA (no RET) or one of the following m-Cherry tagged constructs: RET9 kinase dead (RET9KD), RET9 wild-type, RET51 wild-type, RET51 kinase dead (RET51 KD), or RET51 Y1096F. Cells were serum-starved for 3 hours the following day, treated with GDNF for 1 hour and imaged by TIRF microscopy. Data are represented as the number of focal adhesion as quantified by the number of GFP-paxillin positive spots per cell. Standard error was calculated across a minimum of three technical replicates, and represented by the error bars. \* signifies statistical significance, and p-value < 0.05

There was a decrease in paxillin-positive focal adhesions in RET51-expressing HeLa BCAR3 KD cells compared to HeLa Mock KD cells (Figure 3-6), suggesting that RET51-mediated focal adhesion formation is BCAR3-dependent. While the number of focal adhesions in the absence of RET in HeLa Mock KD is comparable to the number observed in the HeLa BCAR3 KD cells expressing RET51 condition, it would be useful to include a HeLa BCAR3 KD without RET expression as a control.

We also assessed the effects of BCAR3 KD on neuroblastoma cell adhesion on collagen coated wells in the presence or absence of GDNF treatment. Wells coated with BSA was used as our negative control, and in this condition we did not see much adherence of cells as measured by absorbance at 570nm. Our data suggest that there is an increase in SH-SY5Y cell adhesion following GDNF treatment compared to the untreated control, and that there is a relative reduction in cell adhesion in the BCAR3 KD cells (Figure 3-7A). In passaging of the cells, we noticed that the BCAR3 KD cells are more adherent, but think that in a one hr time span of the cell adhesion assay, we are not able to adequately assess BCAR3 KD cell adhesion levels. To more adequately assess cell adherence, we assessed the morphology of cells seeded onto collagen-coated wells. Our data suggest that BCAR3 KD cells have a flatter, more spread out morphology than wild-type SH-SY5Y cells (Figure 3-7B).

#### **3.4.5 RET activation increases gene expression of Vimentin and MMP9 migratory markers**

As RET activation results in an increase in SH-SY5Y neuroblastoma cell migration [133], we evaluated whether various migratory-related markers, including

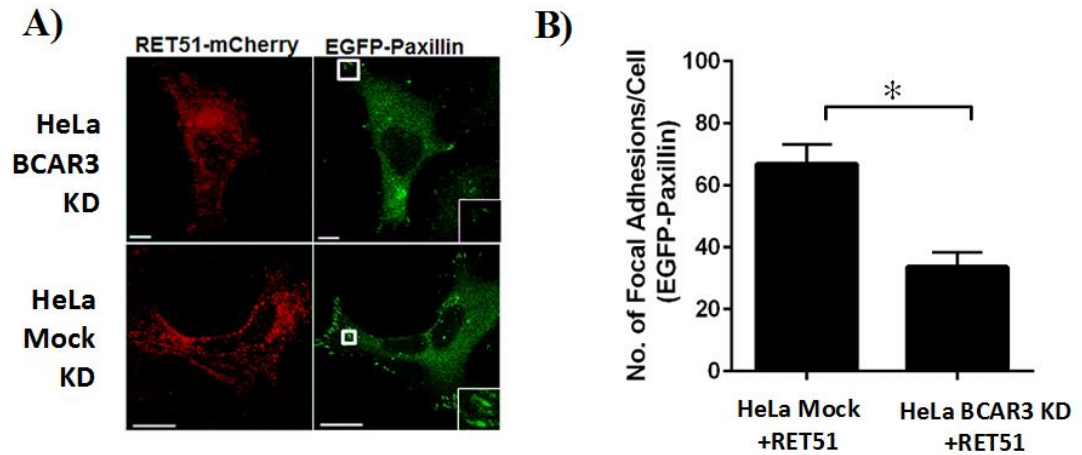
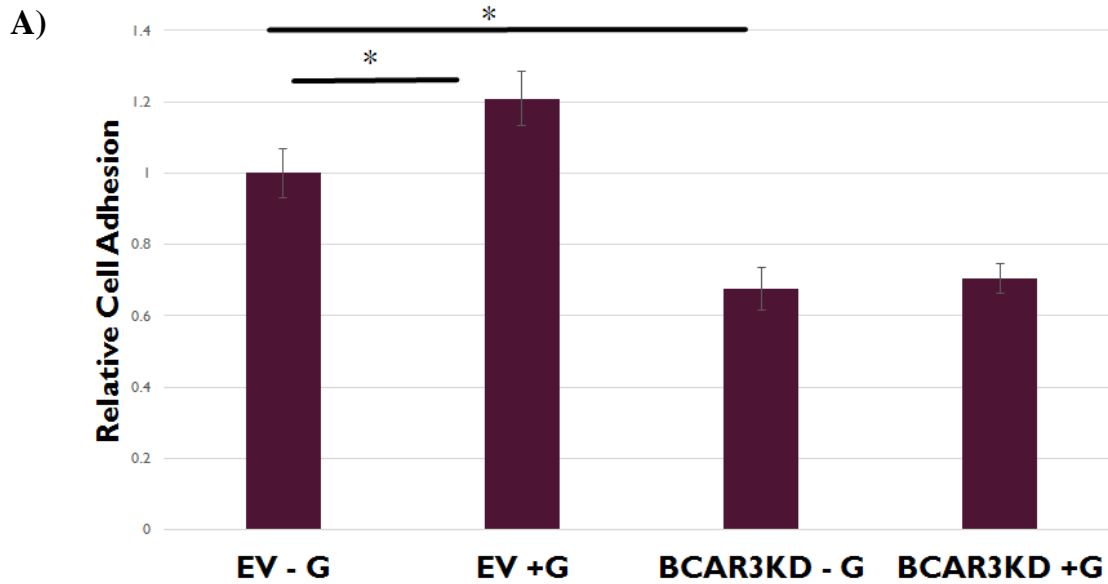


**Figure 3-6. BCAR3 contributes to RET51-mediated focal adhesion formation.**

**A.** HeLa Mock KD and BCAR3 KD cells were transiently transfected with GFR $\alpha$ 1, EGFP-paxillin, and mCherry-tagged RET51. After 24 hours post-transfection, cells were subjected to a 3 hour serum starvation process, and treated with 1 hour GDNF. Representative fluorescent images of mCherry-RET51, and EGFP-paxillin in HeLa Mock KD and BCAR3 KD cells. Mention the box in lower right. Scales bars = 15  $\mu$ m. **B.** Graphical representation of quantification of focal adhesion number in Mock KD compared to BCAR3 KD cells. Data are represented here as number of focal adhesions per cell as determined by the assessment of GFP-paxillin. A minimum of five cells per condition were analyzed. Error bars represent the standard error. \* signifies statistical significance, and p-value is less than 0.05



**B)**

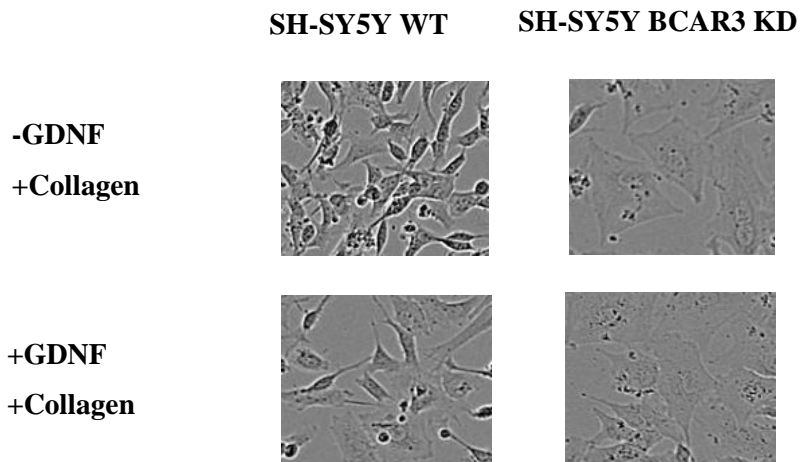


**Figure 3-7. BCAR3 plays a role in cell adhesion and flattened cell morphology.**

**A.** Cell adhesion assays were performed as indicated in the methods section. Levels of cell adhesion are represented as relative to SH-SY5Y wild-type in the absence of GDNF treatment. Standard error was calculated across a minimum of three technical replicates, and represented by the error bars. \* signifies statistical significance, and  $p$ -value  $< 0.05$  **B.** Cell morphology was assessed as described in the methods. Representative images of wild-type and BCAR3 KD SH-SY5Y cell morphology are shown.

*Snail*, *Slug*, *Twist1*, *Vimentin*, *MMP2*, *MMP9*, *Zeb1*, *OCLN*, *HUGL2*, and *Cdh2*, were differentially expressed following GDNF treatment. Isolated RNA from SH-SY5Y wild-type cells treated with various times of GDNF to activate RET were subjected to qRT-PCR. We confirmed that the products generated were of the predicted size on agarose gels. Genes expressed at least 2-fold times more relative to the untreated condition were considered to be differentially expressed following RET activation. Our data suggest that RET activation results in increases in *vimentin*, and *MMP9* transcript expression in SH-SY5Y cells (Figure 3-8A & B). While we saw increases in transcript expression, it would be worthwhile to assess if protein expression levels are also differentially regulated following RET activation with GDNF.

#### **3.4.6 Effect of BCAR3 KD on RET-mediated *Cyclin D1*, *Vimentin*, and *MMP9* transcript expression**

We evaluated two migratory genes, *Vimentin* and *MMP9*, that are differentially regulated by RET activation, in BCAR3 KD cells in order to further characterize the role of BCAR3 in RET-mediated migration. *MMP9* and *Vimentin* gene expression was less in untreated SH-SY5Y BCAR3 KD cells in comparison to SH-SY5Y Mock KD with no GDNF treatment (Figure 3-9). *GusB* transcript expression levels were comparable across all conditions. There was an increase in *Vimentin* and *MMP9* transcript levels in SH-SY5Y BCAR3 KD cell lines compared to the untreated BCAR3 KD cells (Figure 3-9), suggesting that while BCAR3 may have an effect generally on the expression of these

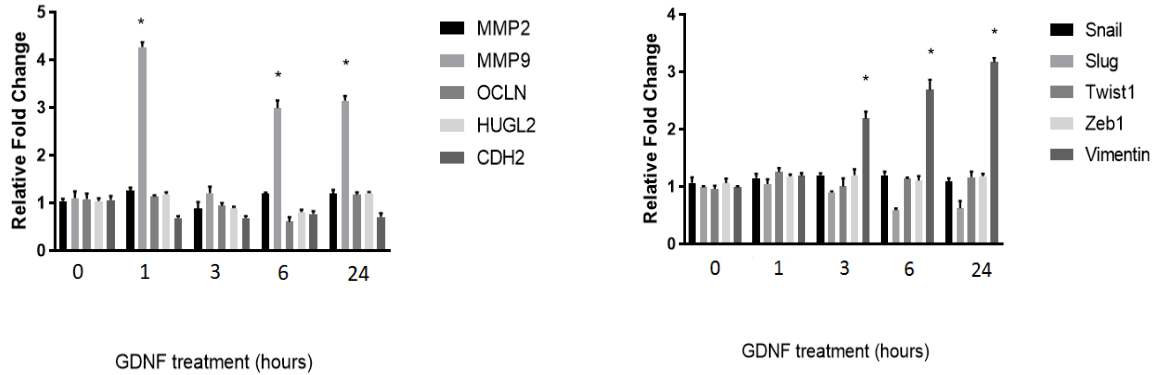


**Figure 3-8. *Vimentin* and *MMP9* expression increases following RET activation in SH-SY5Y cells.**

Gene expression of various migratory markers, A) *Snail*, *Slug*, *Twist1*, *Zeb1*, *Vimentin*, & B) *MMP2*, *MMP9*, *OCN*, *HUGL2*, *Cdh2*, were evaluated after RET activation in SH-SY5Y neuroblastoma cells. SH-SY5Y wild-type cells were treated with GDNF for the indicated times. Isolated RNA was subjected to one-step quantitative real-time PCR. Gene expression was normalized to the housekeeping gene, *GusB*, and reported relative to the untreated condition. Red boxes indicate genes that are expressed at greater levels following RET activation. A minimum of three replicates were assessed per condition.

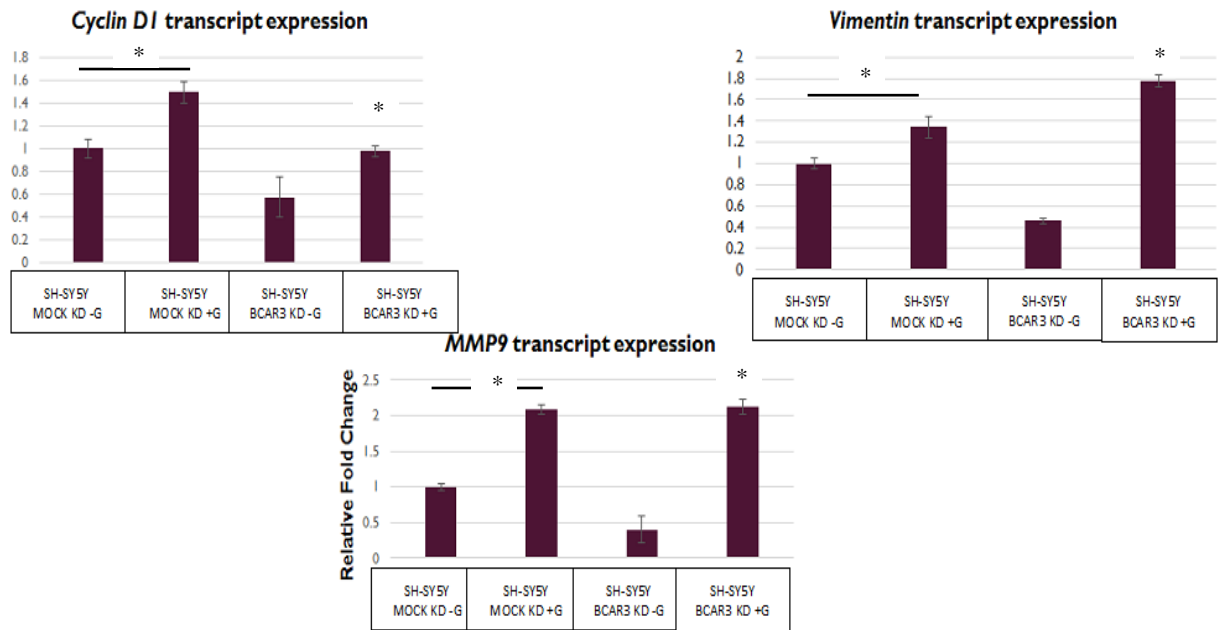


**Figure 3-9. *Cyclin D1*, *Vimentin* & *MMP9* expression in BCAR3 KD cells.**

Gene expression of three genes known to be increased following RET activation, **A) *Cyclin D1***, **B) *Vimentin*** & **C) *MMP9***, was assessed in SH-SY5Y BCAR3 KD cells compared to SH-SY5Y Mock KD cells. GDNF was added to cells for 24 hours prior to RNA isolation. RNA was harvested from SH-SY5Y Mock and BCAR3 KD cells, and one -step qRT-PCR was performed. Data that have been normalized to *GusB*, the housekeeping gene, are reported as relative fold change to the untreated Mock KD condition.

genes, it does not seem to affect the RET-mediated increases of the two migratory markers.

Cyclin D1 has been previously shown to be upregulated following RET activation [37]. As *CCND1* is activated in the presence of BCAR3 [141], we also explored the effect of BCAR3 KD on RET-mediated *CCND1* expression. Our data suggest that *CCND1* gene expression is decreased in the untreated and GDNF treated SH-SY5Y BCAR3 KD cell lines in comparison to the untreated and GDNF-induced SH-SY5Y Mock KD cell lines (Figure 3-9). *CCND1* expression is still increased following RET activation in BCAR3 KD cells (Figure 3-9), suggesting that RET-mediated increases in *CCND1* expression is not BCAR3-dependent. We initially evaluated the effects of BCAR3 KD on the phosphorylation levels of various signalling proteins, including AKT, ERK and ribosomal S6, in SH-SY5Y cells treated with GDNF for various times using a RPPA assay. We saw a gradual increase in levels of phosphorylated AKT, ERK and S6 following increasing durations of GDNF treatment in SH-SY5Y Mock control cells (Figure 3-10A). Interestingly, in our BCAR3 KD cell lines, there was a reduction in the phosphorylation of the AKT, ERK and ribosomal S6 compared to the Mock control (Figure 3-10A). RET activation, and BCAR3 KD had no effect on phosphorylation levels of PKC, serving as a negative control (Figure 3-10B). To verify our RPPA results, we performed western blotting. Our data demonstrate that there were reduced phosphorylation levels of our proteins of interest in the BCAR3 KD compared to the Mock control cells (Figure 3-10B). Together, these data suggest that BCAR3 may be important for AKT, ERK and ribosomal S6 phosphorylation in SH-SY5Y cells.

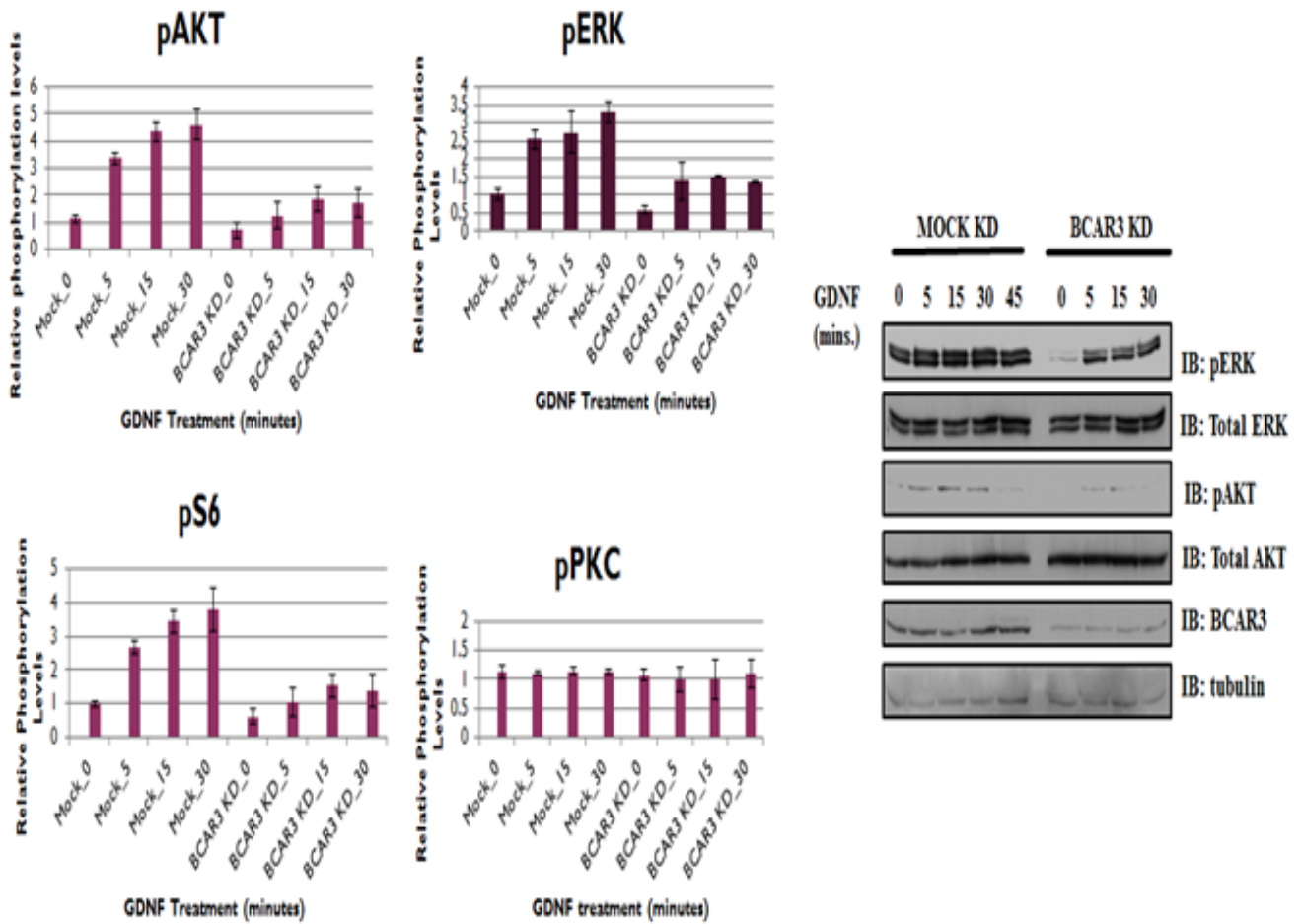


**Figure 3-10. Levels of phosphorylated signalling proteins in SH-SY5Y BCAR3 KD cells.**

**A.** SH-SY5Y cells were serum-starved in the presence of retinoic acid overnight, and treated with GDNF for the indicated times prior to lysis. Samples were prepared, processed, printed on microarrays, and probed by Dr. Taran Gujral as previously described [199]. Expression of phosphorylated proteins, ERK, AKT, S6 and PKC, were normalized to  $\beta$ -actin and data are represented relative to the Mock untreated control. **B.** Whole cell lysates from SH-SY5Y cells treated with GDNF for indicated times were separated by SDS-PAGE, probed with the indicated antibodies. Tubulin served as the loading control.

### 3.5 Discussion

We confirmed a previously predicted novel interaction between the RET receptor tyrosine kinase and the BCAR3 adaptor protein, and assessed the functional consequences of this association. In the protein domain microarray dataset in which Koytiger and colleagues identified BCAR3 as a potential binding partner to RET [167], several other receptor tyrosine kinases were predicted to also associate with BCAR3. BCAR3 includes a SH2 domain, a domain known to interact with phosphorylated tyrosine residues, suggesting that it may be worthwhile to validate BCAR3's functional relationship with other receptor tyrosine kinases in *in vitro* cell models.

We demonstrated an interaction between RET and BCAR3 through *in vitro* Far Western blotting analyses, and co-immunoprecipitations in lysates from cells in which our two proteins of interest were transiently expressed. However, we did not detect an endogenous RET-BCAR3 interaction in SH-SY5Y neuroblastoma cells (data not shown). Interestingly, while GST-pulldowns have shown that EGFR and BCAR3 associate [149], another group could not detect an endogenous EGFR-BCAR3 interaction in BT549 cells after EGF stimulation [169]. According to RNA expression from a panel of cell lines obtained from the Human Protein Atlas (<http://www.proteinatlas.org/>), SH-SY5Y cells express detectable levels of BCAR3 transcript, but much lower levels than other cell lines assessed. This relatively low BCAR3 expression in SH-SY5Y cells may explain why we were unable to detect an endogenous RET-BCAR3 interaction. Limitations with currently available BCAR3 antibodies for co-immunoprecipitation may be another possibility for the inability to detect RET and BCAR3 interacting endogenously. It is also possible that

RET-BCAR3 may not interact robustly endogenously in these cells, and that Grb2, another adaptor protein known to interact with RET at the same site as BCAR3 [55], may be more relevant in this particular cell type.

Our data suggest that BCAR3 has a broad role in many functions in SH-SY5Y neuroblastoma cells irrespective of RET activation. This is likely the result of BCAR3's ability to interact with several other proteins, including other RTKs and PTP $\alpha$  [148]. Interestingly, it is worth mentioning that while our data demonstrate that BCAR3 has multiple roles in the SH-SY5Y cell line, the only significant phenotype observed in the BCAR3 knockout mice is a defect in the adult ocular lens [144]. BCAR3 is member of the novel SH2 domain containing protein (NSP) family, which is comprised of two other members NSP1 and NSP3, which are known to have complementary roles to BCAR3 (also referred to NSP2) (Reviewed in [201]). While there are differences in tissue distribution and roles of the NSP family members, it is likely that in the animal model NSP1 and NSP3 may compensate for BCAR3, resulting in a minimal phenotype. In the case of the SH-SY5Y cell line, it may be possible that NSP1 and NSP3 are not expressed, or not expressed as highly as BCAR3, and as a result, BCAR3 KD may lead to a more pronounced effect than that observed in the mouse knockout. It may be worthwhile to investigate the expression levels of NSP1 and NSP3 in SH-SY5Y cells, and subsequently assess the functional implications of knocking down these two proteins individually to determine if a similar phenotype to BCAR3 KD is observed.

Cross and colleagues demonstrated that BCAR3 and its well-known C-terminal binding partner, p130Cas, are co-expressed in many subtypes of human breast cancer

[156]. It may be interesting to more comprehensively assess BCAR3 protein expression in human tumors, and evaluate whether expression is correlated with various clinical parameters, including stage, grade, and sub-type of disease. RET is expressed in approximately 70% of breast cancer patients, and associated with metastatic parameters [72]. Further, it would be worthwhile to assess the co-expression of RET and BCAR3 in human cancer patient samples, and explore whether expression of both these proteins is associated with clinical patient parameters. As an initial step, *in silico* analysis of RET and BCAR3 co-expression in human tumors could be evaluated utilizing various bioinformatic tools, including synTARGET and Gene expression-based Outcome for Breast cancer Online. These data can be independently verified using well-characterized antibodies, and human tissue microarrays with comprehensive patient data. Validation and analysis of RET and BCAR3 co-expression may ultimately help stratify cancer patients who might benefit from certain types of treatment.

Together, we have demonstrated a novel direct interaction between the RET receptor tyrosine kinase and the SH2 domain of the BCAR3 adaptor protein. This interaction is kinase-dependent. While multiple groups have investigated the contributions of BCAR3 in breast cancer, the role of BCAR3 has not been well-explored in other human tumor models. To our knowledge, our study is the first to explore the functions of BCAR3 in a neuroblastoma model. We have shown that BCAR3 plays a role in SH-SY5Y neuroblastoma cell proliferation, adhesion and phosphorylation of various signaling proteins, including AKT, ERK and S6, suggesting the importance of the BCAR3 protein in these cells. RET activation leads to phosphorylation of paxillin, focal

adhesion kinase and p130Cas [132]. Our data suggest that the RET isoforms may play differential roles in focal adhesion formation, and that BCAR3 may be implicated in RET-mediated focal adhesion formation in addition to migration. Overall, our data provide enticing support that the BCAR3 adaptor protein should be more broadly studied in cancer types in addition to breast cancer. Designing disrupting peptides that block BCAR3's interaction with its binding partners may be useful to explore in a pre-clinical setting in the future.

## **Chapter 4**

### **Discussion**

RET is an important RTK that has key roles in normal development and disease (Reviewed in [35]). RET has been implicated in several human diseases, including Hirschsprung disease and a broad range of human tumors (Reviewed in [35]). Although many RET-related tumors are the result of constitutive activation of the RTK due to either oncogenic gene fusions or point mutations, expression of wild-type RET also has been associated with certain cancer types, such as tumors of the breast (Reviewed in [35]). While the initial report of RET-associated breast cancer suggested wild-type expression of the RTK was associated specifically with the hormone receptor positive subtype of breast cancer [71], subsequent work has suggested a much broader role of RET in this disease [72, 82, 185]. Our data provide evidence to support the literature that RET's contribution to breast cancer is likely not restricted to the hormone receptor positive subtype, and suggest that further work is required to fully appreciate the role of RET to the progression of this tumor type.

The phosphorylation of tyrosine residues is an initial step of the signalling of RTKs, including RET (Reviewed in [202]). Phosphopeptide motifs, comprising a phosphotyrosine residue amongst a specific consensus sequence, act as binding sites on RTKs, such as RET, for recruitment of cytoplasmic adaptor proteins that contain either a SH2 domain or PTB domain (Reviewed in [202]). Recruitment of adaptor proteins to these specific binding sites on RET regulates downstream signalling, and subsequent

cellular functions (Reviewed in [35]). Characterization of wild-type RET's interactions with adaptor proteins will help us mechanistically understand how the RTK may contribute to the progression of certain human cancers, and ultimately aid in the development of novel therapeutic strategies. We have shown a novel interaction between RET, and the adaptor protein BCAR3, and begun to investigate the functional consequence of this association. While our data suggest that BCAR3 may play a role in certain RET-mediated functions, including migration and focal adhesion formation, it seems that this adaptor protein has a general role in other cellular processes, such as adhesion and proliferation, and phosphorylation levels of ERK and AKT. BCAR3 is known or hypothesized to interact with RTKs other than RET [149, 150], as predicted by a previous high throughput protein domain microarray study [167]. Additionally, BCAR3 has been shown to interact with the phosphatase PTP $\alpha$  [148]. Accordingly, the broad role of BCAR3 in cellular processes observed in our studies may be due to its interactions with other RTKs or PTP $\alpha$  (Figure 4-1). Further, a more comprehensive understanding of the molecular contribution of adaptor proteins, such as BCAR3, to cancer will also assist in the identification of tailored approaches to treat the disease.

#### **4.1 RET's Contribution to Breast Cancer**

We have identified suitable cell models to study the role of RET in breast cancer, and showed that RET activation has an effect on breast cancer cell proliferation, but not adhesion. The literature exploring RET in breast cancer has predominantly focused on ER-positive tumors or cell lines as the initial report implicating RET expression in breast

cancer observed a positive correlation between RET mRNA and protein expression and hormone receptor positive breast cancer [71]. A subsequent study showed that RET was implicated in tamoxifen resistance in endocrine breast cancers [73]. As the luminal breast cancers comprise approximately two-thirds of the breast cancer population (Reviewed in [203] ), most of the well-characterized breast cancer cell lines used in *in vitro*, preclinical studies are ER-positive – a potential reason why initial work on RET may have been conducted mostly on luminal breast cancer cell lines.

Our data show that RET activation not only affects proliferation of hormone receptor positive breast cancer cell lines MCF7 and T47D, but also non-estrogen receptor positive BT-20 and MDA-MB-453 cell lines, providing support that RET may have a role in breast cancer irrespective of subtype. Our data are consistent with more recent studies showing that RET expression may have a broader role in breast cancer [72, 204]. Specifically, Gattelli and colleagues observed RET protein expression at high rates in all subtypes of breast cancer assessed, including HER2-positive, triple-negative and ER-positive, and found that expression was correlated with both metastasis-free, and overall survival in a cohort of 108 patients [73]. More recently, a group utilized reverse transcriptase PCR to assess RET expression in a cohort of 446 breast cancer patients, and 57 patient-derived xenografts, and found that expression was observed broadly among breast cancer subtypes [204]. Interestingly, although most of RET's association with breast cancer is the presence of wild-type expression of RET, a very recent study shows that a RET polymorphism, Y791F, normally associated with MTC, is associated with breast cancer predisposition [185]. Although it was initially believed that RET Y791F

was a pathogenic, clinically actionable variant, more recent literature suggest that it is a benign polymorphism [205]. Comprehensive analyses of populations suggest the RET Y791F variant alone is not associated with MTC [205]. Overall, this suggests that the role of RET in breast cancer is complex and multi-factorial, and warrants further investigation to fully characterize the multiple roles which the receptor plays in breast cancer.

While we showed that RET activation increases breast cancer cell proliferation, it would be interesting to explore the role of RET in other breast cancer oncogenic processes, such as cell spreading, cell migration and cell invasion. Our lab has previously shown that RET activation promotes cell migration in neuroblastoma cells, and both migration and invasion in thyroid cancer models [133, 206]. Previous studies have shown that activation of RET through GDNF treatment induces breast cancer cell migration in multiple assays [72]. Further, high expression levels of RET are associated with decreased metastasis-free survival in a cohort of breast cancer patients [72], suggesting that invasion would be a suitable function to assess.

Our data showed that ligands, GDNF and artemin, are able to induce expression of RET downstream target genes in the MCF7 breast cancer cell line. Artemin is the preferred ligand for RET's GFR $\alpha$ 3 co-receptor, but can also form a complex with GFR $\alpha$ 1 (Reviewed in [11]). Previous studies have shown that artemin is expressed in multiple tumor types, and plays a role in tumor growth and metastasis [207]. In breast tumors, reports have suggested that artemin is involved in metastasis, and has been implicated in relapse and death [119]. While we only used GDNF in our functional assays, it would be interesting to assess whether artemin expression has similar effects to GDNF in the breast

cancer cellular processes described. RET activation utilizing GDNF has been shown to increase phosphorylation of signalling proteins downstream of RET, such as AKT and ERK [73, 114]. It may be worthwhile to verify if the same RET-mediated pathways are activated following artemin treatment in breast cancer cells.

We have shown that the integrin beta subunits, *ITGB1*, *ITGB3-6* & *ITGB8*, are expressed at detectable levels in our panel of RET-positive breast cancer cell lines. Our lab has previously shown that RET activation increases SH-SY5Y neuroblastoma cell adhesion, and that integrin  $\beta 1$  and integrin  $\beta 3$  both play roles in this RET-mediated adhesion [133]. While we did not observe an effect of GDNF treatment on breast cancer cell adhesion on collagen, it may be worthwhile to explore whether RET activation plays a role in other integrin-related processes, such as cell spreading, focal adhesion formation, and activation of proteins implicated downstream of integrin engagement, in breast cancer cells. Previous studies have shown that RET interacts with the integrin-related protein, FAK, and suggested that this may be a direct interaction through the FERM domain on FAK [135]. Additionally, the inhibition or silencing of FAK reduces RET phosphorylation and RET-dependent cell proliferation [135]. Interestingly, Gattelli and colleagues have shown that RET inhibition reduces FAK phosphorylation in breast cells, suggesting there is a relationship between RET and FAK in breast cancer [72]. Integrin inhibition alone, or in combination with a RET inhibitor, may be an useful treatment strategy for certain subsets of breast cancer patients.

## 4.2 Novel RET-BCAR3 interaction

We have shown a novel association between the RET receptor and the BCAR3 adaptor protein, and that knockdown of BCAR3 has an effect on oncogenic-related processes, such as adhesion and proliferation in neuroblastoma cells. While most of the previous studies on BCAR3 have explored its role in the context of breast cancer, our data suggest that this adaptor protein may have functional relevance in other tumor types. Recently, one group has shown that BCAR3 interacts with HEF1, a member of the p130Cas family, to promote colorectal cancer cell migration [208], providing further evidence that this adaptor protein likely has functions beyond breast cancer. It would be worthwhile to initially perform bioinformatic analyses to assess expression levels and clinical significance of BCAR3 in a broad range of tumor types in order to identify cancers in which it would be relevant to perform further *in vitro* investigation of the functions of BCAR3.

While we identified an interaction between RET and the BCAR3 adaptor protein using far western blotting, and co-immunoprecipitations with transiently expressed proteins, we were not able to detect an endogenous interaction in SH-SY5Y neuroblastoma cells. SH-SY5Y cells express detectable levels of BCAR3, but expression data from the Protein Atlas suggest that there are many other cell lines that express much higher levels of BCAR3, indicating one potential explanation for the inability to detect an endogenous RET-BCAR3 interaction. Additionally, while we assessed various times of RET activation via GDNF treatment (ie. 5, 10, 15, 20 & 30 minutes), it may be that the RET-BCAR3 association is transient, and highly time-dependent. There are not many BCAR3 antibodies commercially available, so we may also have been limited in the

reagents used to detect an endogenous interaction. Additionally, while we have identified a robust, *in vitro* RET-BCAR3 interaction, it is possible that the RET-BCAR3 interaction may not occur in SH-SY5Y neuroblastoma cells. It is worth mentioning that while *in vitro* experiments have shown an interaction between EGFR-BCAR3 [168], another group has been unable to detect an endogenous association between BCAR3 and EGFR in breast cancer cells [169].

Recently, Li and colleagues showed that BCAR3 connects ROR-HER3 to the Hippo-Yap pathway to promote breast cancer bone metastasis [150]. Additionally, there are several other RTKs that are predicted to interact with BCAR3 [167]. Together, this suggests that it would be valuable to initially characterize the potential interactions of the BCAR3 SH2 domain with other RTKs, and then further functionally evaluate any verified associations.

A group has suggested that BCAR3 expression may have prognostic value in breast cancer [154]. As our data provide novel evidence that BCAR3 may have a role in neuroblastoma, it may be worthwhile to investigate whether BCAR3 expression levels have any prognostic or predictive value in other tumor types. A more comprehensive molecular characterization of BCAR3 in cancer may help elucidate whether there is benefit in this adaptor protein being utilized in a prognostic and/or therapeutic setting.

Receptor tyrosine kinase

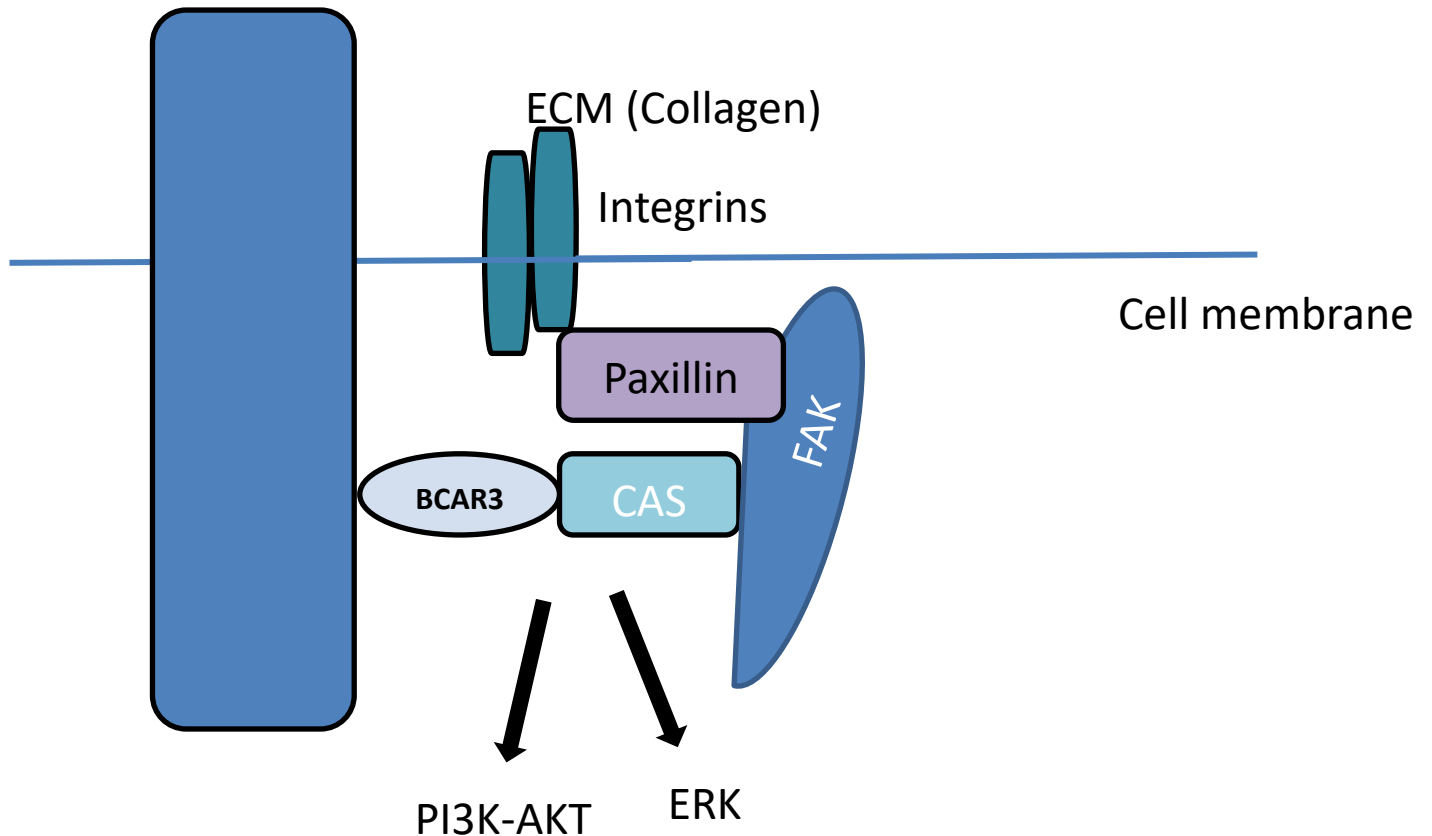


**Figure 4-1. Model of downstream effects of RTK-BCAR3 interaction.**

We hypothesize that BCAR3 serves as a molecular connector of certain RTKs to p130Cas, situating p130Cas in focal adhesions and promoting integrin activation. These interactions are likely important for the downstream activation of PI3K-AKT and ERK signaling pathways. Our data support roles for BCAR3 in phosphorylation of AKT, ERK, and cellular processes, including proliferation and adhesion of SH-SY5Y neuroblastoma cells. While many of these functions do not appear to be RET-mediated, the phenotype we observe may be due to BCAR3's interactions with other RTKs or proteins, such as PTP $\alpha$ .

### 4.3 Significance

According to the recent statistics from the Canadian Cancer Society, approximately one in two Canadians are expected to develop cancer during their lifetime, and one in four are expected to die due to the disease (Canadian Cancer Statistics, 2017). These statistics emphasize the prevalence of cancer in our society, and highlight the immense importance of further cancer research in a range of disciplines, including prevention, biology and treatment. Moreover, cancer is not a single disease – rather, it is a collection of more than a hundred diseases (Canadian Cancer Statistics, 2017), and current treatments have varying efficiencies in patients, underscoring the complexity of developing effective novel therapeutic strategies that will benefit all cancer patients. Understanding the molecular mechanisms underlying the broad range of tumor types is an important initial step in the identification of personalized, precise treatments for cancer patients that may alleviate suffering and improve the quality of life.

Breast cancer is a heterogenous disease that can be further sub-divided into clinically relevant groups (Reviewed in [209]). Endocrine therapies, including tamoxifen, fulvestrant, and aromatase inhibitors, are the standard form of adjuvant treatment for the hormone-receptor positive subtype of breast cancer [210]. Groups have shown cross-talk between the RET and ER $\alpha$  pathways [114, 211]. Previous preclinical work has investigated the efficacy of broad receptor tyrosine kinases inhibitors, including Vandetanib and sunitinib, in both luminal and non-luminal RET-positive breast cancer [82, 121, 204]. Studies have demonstrated that combinatorial treatment of tamoxifen, and either vandetanib or sunitinib is more effective than either treatment regimen individually [82, 121]. Interestingly, sunitinib had more of an effect on the induction of apoptosis than

tamoxifen on breast cancer cells, providing a functional explanation for the greater efficacy of the combination treatment compared to each treatment alone [121]. Hatem and colleagues have also demonstrated in a preclinical setting that Vandetanib may be an effective treatment strategy in non-luminal RET and EGFR positive breast cancers as well [204]. Cabozantinib is another multi-kinase inhibitor that targets RET, and also has activity against MET, VEGFR2, and AXL [212] and like Vandetanib, has been approved to treat advanced MTC associated with RET mutations (Reviewed in [213]). To date, while preclinical and clinical studies have assessed the efficacy of Cabozantinib for metastatic breast cancer [212], these studies have not utilized a breast cancer patient population that has comprehensive data on RET status. To extend these data and determine whether RET may be a suitable therapeutic target in certain subsets of breast cancer patients, it may be interesting to evaluate these broad spectrum RTK inhibitors that have activity against RET in combination with anti-estrogen therapies.

Our data suggest that RET has a role in cell proliferation of both luminal (MCF7, and T47D) and non-luminal (BT20, and MDA-MB-453) breast cancer cell lines. This supports further pre-clinical and subsequent clinical research in validating the efficacy of broad RTK inhibitors that target RET both in combination with endocrine therapy in luminal breast cancer cohorts, and also alone in non-luminal breast cancer. (Reviewed in [214]). Additionally, vandetanib has been previously clinically investigated for other indications, including non-small cell lung cancer (Reviewed in [215] ), and locally advanced/metastatic pancreatic cancer [216], both of which ultimately did not show therapeutic benefit. If additional preclinical validation of RET's contribution to breast

cancer warrants clinical investigation, data from previous clinical trials for other indications may help design studies to explore the efficacy of vandetanib in certain populations of breast cancer patients.

Interestingly, Gattelli and colleagues did not observe additive benefit with the combination of fulvestrant and the broad spectrum RET inhibitor, NVP-AST-487 in a breast cancer model, suggesting that only certain combinations of anti-estrogens and RET inhibitors have therapeutic benefit [72]. These multi-kinase inhibitors have broad effects, which clinically may not be the ideal approach as they may also down-regulate activity of other kinases, and lead to unwanted side-effects. As a result, many groups have developed and begun to characterize RET-specific inhibitors (Reviewed in [217]). It may be worthwhile to assess the combinatorial therapeutic benefit of RET-specific inhibitors with endocrine therapies in RET-expressing populations of breast cancer patients as this may be a more beneficial and effective treatment approach than a multi-kinase inhibitor.

Our data suggest that BCAR3 may have a role in many oncogenic functions in neuroblastoma. While, to date and to our knowledge, there are no therapeutic approaches to target BCAR3, it may be useful to design, and characterize therapeutic peptides that disrupt the interaction between RET and BCAR3. As BCAR3 has been shown to interact with other receptor tyrosine kinases, such as HER3 and EGFR, and our data suggest a role for BCAR3 in certain functions irrespective of RET, it may be worthwhile to develop disrupting peptides that include the SH2 domain of BCAR3. Although more research is required to fully understand the clinical relevance of BCAR3 in cancer, such

disrupting peptides, may ultimately have a broad clinical application in tumors in which BCAR3 is expressed.

#### **4.4 Conclusions**

We have shown that RET is expressed and plays a role in proliferation of both luminal and non-luminal breast cancer cells. Additionally, we have demonstrated both GDNF and artemin lead to the induction of RET target genes in MCF7 breast cancer cells. We have characterized integrin beta transcript expression levels in a panel of breast cancer cells, and shown that RET activation via GDNF does not seem to affect MCF7 cell adhesion. Together, these data suggest that further research is required to delineate the multi-faceted roles of RET in this disease. Further, we have identified a novel interaction between RET and the adaptor protein BCAR3, and were the first group to investigate the functional relevance of BCAR3 in a neuroblastoma model. Our data suggest that BCAR3 plays a role in oncogenic-related processes in this disease type, and further work is warranted to better understand this still relatively unknown adaptor protein.

## References

1. Takahashi M, & Cooper GM (1985) ret transforming gene encodes a fusion protein homologous to tyrosine kinases. *Mol Cell Biol* **7**(4): 1378-1385.
2. Pachnis V, Mankoo B, & Costantini (1993) Expression of the c-ret proto-oncogene during mouse embryogenesis. *Development* **119**(4): 1005-1017.
3. Tsuzuki T, Takahashi M, Asai N, Iwashita T, Matsuyama M & Asai J (1995) Spatial and temporal expression of the ret proto-oncogene product in embryonic, infant and adult rat tissues. *Oncogene* **10**(1): 191-198.
4. Jain S, Naughton CK, Yang M, Strickland A, Vij K, Encinas M, Golden J, Gupta A, Heuckeroth R, Johnson EM Jr & Milbrandt J (2004) Mice expressing a dominantnegative Ret mutation phenocopy human Hirschsprung disease and delineate a direct role of Ret in spermatogenesis. *Development* **131**(21): 5503-5513.
5. Ishizaka Y, Itoh F, Tahira T, Ikeda I, Sugimura T, Tucker J, Fertitta A, Carrano AV & Nagao M (1989) Human ret proto-oncogene mapped to 10q11.2. *Oncogene* **4**(12): 1519- 1521.
6. Pasini B, Hofstra RM, Yin L, Bocciardi R, Santamaria G, Grootsholten PM, Ceccherini I, Patrone G, Priolo M & Buys CH (1995) A physical map of the human RET protooncogene. *Oncogene* **11**(9): 1737-1743.
7. Myers SM, Eng C, Ponder BA & Mulligan LM (1995) Characterization of RET protooncogene 3' splicing variants and polyadenylation sites: a novel C-terminus for RET. *Oncogene* **11**(10): p. 2039-2045.
8. Carter MT, Yome JL, Marcil MN, Martin CA, Vanhorne JB & Mulligan LM (2001) Conservation of RET proto-oncogene splicing variants and implications for RET isoform function. *Cytogenet Cell Genet* **95**(3-4): 169-176.
9. Hahn M & Bishop JM (2001) Expression pattern of Drosophila ret suggests a common ancestral origin between the metamorphosis precursors in insect endoderm and the vertebrate enteric neurons. *Proc Natl Acad Sci USA* **98**(3): 1053-1058.
10. Anders J, Kjar S & Ibanez CF (2001) Molecular modeling of the extracellular domain of the RET receptor tyrosine kinase reveals multiple cadherin-like domains and a calciumbinding site. *J Biol Chem* **276**(38): 35808-35817.
11. Airaksinen MS & Saarma M (2002) The GDNF family: signalling, biological functions and therapeutic value. *Nat Rev Neurosci* **3**(5): 383-394.
12. Takahashi M, Buma Y & Taniguchi M (1991) Identification of the ret proto-oncogene products in neuroblastoma and leukemia cells. *Oncogene* **6**(2): 297-301.

13. Kjaer S, Kurokawa K, Perrinkaquet M, Abrescia C & Ibanez CF (2006) Self-association of the transmembrane domain of RET underlies oncogenic activation by MEN2A mutations. *Oncogene* **25**(53): 7086-795.
14. Takahashi M, Ritz J & Cooper GM (1985) Activation of a novel human transforming gene, ret, by DNA rearrangement. *Cell* **42**(2): 581-588.
15. Schuchardt A, D'Agati V, Larsson-Blomberg L, Costantini F & Pachnis V (1994) Defects in the kidney and enteric nervous system of mice lacking the tyrosine kinase receptor Ret. *Nature* **367**(6461): 380-383.
16. Shakya R, Watanabe T & Costantini F (2005) The Role of GDNF/Ret Signalling in Ureteric Bud Cell Fate and Branching Morphogenesis. *Developmental Cell* **8**(1): 65-74.
17. Naughton CK, Jain S, Strickland AM, Gupta A & Milbrandt J (2006) Glial cell-line derived neurotrophic factor-mediated RET signaling regulates spermatogonial stem cell fate. *Biol Reprod* **74**(2): 314-321. 114
18. Durbec P, Marcos-Gutierrez CV, Kilkenny C, Grigoriou M, Wartiovaara K, Suvanto P, Smith D, Ponder B, Costantini F, Saarma M, Sariola H & Pachnis V (1996) GDNF signalling through the Ret receptor tyrosine kinase. *Nature* **381** (6585): 789-793.
19. Wang H, Hughes I, Planer W, Parsadanian A, Grider JR, Vohra B, Keller-Peck C & Heuckeroth RO (2010) The timing and location of GDNF expression determines enteric nervous system structure and function *J Neurosci* **30**(4): 1523-1538.
20. Kordower JH, Emborg ME, Bloch J, Ma SY, Chu Y, Leventhal L, McBride J, Chen EY, Palfi S, Roitberg BZ, Brown WD, Holden JE, Pyzalski R, Taylor MD, Carvey P, Ling Z, Trono D, Hantraye P, Deglon N & Aebischer P (2000) Neurodegeneration prevented by lentiviral vector delivery of GDNF in primate models of parkinson's disease. *Science* **290**(5492): 767-773.
21. Sun M, Kong L, Wang X, Lu XG, Gao Q & Geller AI (2005) Comparison of the capability of GDNF, BDNF, or both, to protect nigrostriatal neurons in a rat model of Parkinson's disease. *Brain Research* **1052**(2): 119-129.
22. Pichel JG, Shen L, Sheng HZ, Granholm AC, Drago J, Grinberg A, Lee EJ, Huang SP, Saarma M, Hoffer BJ, Sariola H & Westphal H (1996) Defects in enteric innervation and kidney development in mice lacking GDNF. *Nature* **382**(6586): 73-76.
23. Sánchez MP, Silos-Santiago I, Frisen J, He B, Lira SA & Barbacid M (1996) Renal agenesis and the absence of enteric neurons in mice lacking GDNF. *Nature* **382**(6586): 70-73.
24. Moore MW, Klein RD, Farinas I, Sauer H, Armanini M, Phillips H, Reichardt LF, Ryan AM, Carver-Moore K & Rosenthal A (1996) Renal and neuronal abnormalities in mice lacking GDNF. *Nature* **382**(6586): 76-79.
25. Airaksinen MS, Titievsky A & Saarma M (1999) GDNF family neurotrophic factor signaling: four masters, one servant? *Mol Cell Neurosci* **13**(5): 313-325.

26. Baloh RH, Tansey MG, Lampe PA, Fahrner TJ, Enomoto H, Simburger KS, Leitner ML, Araki T, Johnson EM & Milbrandt J (1998) Artemin, a novel member of the GDNF ligand family, supports peripheral and central neurons and signals through the GFRalpha3-RET receptor complex. *Neuron* **21**(6): 1291-1302.
27. Cacalano G, Farinas I, Wang LC, Hagler K, Forgie A, Moore M, Armanini M, Phillips H, Ryan AM, Reichardt LF, Hynes M, Davies A & Rosenthal A (1998) GFRalpha1 is an essential receptor component for GDNF in the developing nervous system and kidney. *Neuron* **21**(1): 53-62.
28. Cik M, Masure S, Lesage AS, Van Der Linder I, Van Gompel P, Pangalos MN, Gordon RD & Leysen JE (2000) Binding of GDNF and neurturin to human GDNF family receptor alpha 1 and 2. Influence of cRET and cooperative interactions. *J Biol Chem* **275**(36): 27505-27512.
29. Baloh RH, Enomoto H, Johnson EM & Milbrandt J (2000) The GDNF family ligands and receptors - implications for neural development. *Curr Opin Neurobiol* **10**(1): 103-110.
30. Takahashi M (2001) The GDNF/RET signaling pathway and human diseases. *Cytokine Growth Factor Rev* **12**(4): 361-373.
31. Parkash V, Leppanen VM, Virtanen H, Jurvansuu JM, Bespalov MM, Sidorova YA, Runeberg-Roos P, Saarma M & Goldman A (2008) The structure of the glial cell linederived neurotrophic factor-coreceptor complex: insights into RET signaling and heparin binding. *J Biol Chem* **283**(50): 35164-35172.
32. Ibanez CF (2013) Structure and physiology of the RET receptor tyrosine kinase. *Cold Spring Harb Perspect Biol* **5**(2): a009134. 115
33. Tsui-Pierchala BA, Ahrens RC, Crowder RJ, Milbrandt J & Johnson EM (2002) The long and short isoforms of Ret function as independent signaling complexes. *J Biol Chem* **277**(37): 34618-25.
34. Kawamoto Y, Takeda K, Okuno Y, Yamakawa Y, Ito Y, Taguchi R, Kato M, Suzuki H, Takahashi M & Nakashima I (2004) Identification of RET autophosphorylation sites by mass spectrometry. *J Biol Chem* **279**(14): 14213-14224.
35. Mulligan LM (2014) RET revisited: expanding the oncogenic portfolio. *Nat Rev Cancer* **14**(3): 173-86.
36. Myers SM & Mulligan LM (2004) The RET receptor is linked to stress response pathways. *Cancer Research* **64**(13): 4453-4463.
37. Gujral TS, van Veelen W, Richardson DS, Myers SM, Meens JA, Acton DS, Dunach M, Elliott BE, Hoppener JW & Mulligan LM (2008) A novel RET kinase-beta-catenin signaling pathway contributes to tumorigenesis in thyroid carcinoma. *Cancer Res* **68**(5): 1338-1346.

38. Matera I, De Miguel-Rodriguez M, Fernandez-Santos JM, Santamaria G, Puliti A, Ravazzolo R, Davidson G & Ceccherini I (2000) cDNA sequence and genomic structure of the rat RET proto-oncogene. *DNA Sequence* **11**(5): 405-417.
39. Tahira T, Ishizaka Y, Itoh F, Sugimura T & Nagao M (1990) Characterization of ret proto-oncogene mRNAs encoding two isoforms of the protein product in a human neuroblastoma cell line. *Oncogene* **5**(1): 97-102.
40. Ivanchuk SM, Myers SM & Mulligan LM (1998) Expression of RET 3' splicing variants during human kidney development. *Oncogene* **16**(8): 991-996.
41. de Graaff E, Srinivas S, Kilkenny C, D'Agati V, Mankoo BS, Costantini F & Pachnis V (2001) Differential activities of the RET tyrosine kinase receptor isoforms during mammalian embryogenesis. *Genes Dev* **15**(18): 2433-2444.
42. Rossel M, Pasini A, Chappuis S, Geneste O, Fournier L, Schuffenecker I, Takahashi M, van Grunsven LA, Urdiales JL, Rudkin BB, Lenoir GM & Billaud M (1997) Distinct biological properties of two RET isoforms activated by MEN 2A/FMTC and MEN 2B mutations. *Oncogene* **14**(3): 265-275.
43. Jain S, Encinas M, Johnson EM & Milbrandt J (2006) Critical and distinct roles for key RET tyrosine docking sites in renal development. *Genes Dev* **20**(3): 321-333.
44. Iwashita T, Kato M, Murakami H, Asai N, Ishiguro Y, Ito S, Iwata Y, Kawai K, Asai M, Kurokawa K, Kajita H & Takahashi M (1999) Biological and biochemical properties of Ret with kinase domain mutations identified in multiple endocrine neoplasia type 2B and familial medullary thyroid carcinoma. *Oncogene* **18**(26): 3919-3922.
45. Pasini A, Geneste O, Legrand P, Schlumberger M, Rossel M, Fournier L, Rudkin BB, Schuffenecker I, Lenoir GM & Billaud M (1997) Oncogenic activation by two distinct FMTC mutations affecting the tyrosine kinase domain. *Oncogene* **15**(4): 393-402.
46. Le Hir H, Charlet-Berguerand N, Gimenez-Roqueplo A, Mannelli M, Plouin P, de Franciscis V & Thermes C (2000) Relative expression of the RET9 and RET51 isoforms in human pheochromocytomas. *Oncology* **58**(4): 311-318.
47. Barlow A, de Graaff E & Pachnis V (2003) Enteric nervous system progenitors are coordinately controlled by the G protein-coupled receptor EDNRB and the receptor tyrosine kinase RET. *Neuron* **40**(5): 905-16.
48. Lian EY, Maritan SM, Cockburn JG, Kasaian K, Crupi MJ, Hurlbut D, Jones SJ, Wiseman SM & Mulligan LM (2017) Differential roles of RET isoforms in medullary and papillary thyroid carcinomas. *Endocr Relat Cancer* **24**(1): 53-69. 116
49. Hickey JG, Myers SM, Tian X, Zhu SJ, Shaw JL, Andrew SD, Richardson DS, Brettschneider J & Mulligan LM (2009) RET-mediated gene expression pattern is affected by isoform but not oncogenic mutation. *Genes Chromosomes Cancer* **48**(5): 429- 440.

50. Schuetz G, Rosario M, Grimm J, Boeckers TM, Gundelfinger ED & Birchmeier W (2004) The neuronal scaffold protein Shank3 mediates signaling and biological function of the receptor tyrosine kinase Ret in epithelial cells. *J Cell Biol* **167**(5): 945-952.
51. Lorenzo MJ, Gish GD, Houghton C, Stonehouse TJ, Pawson T, Ponder BA & Smith DP (1997) RET alternative splicing influences the interaction of activated RET with the SH2 and PTB domains of Shc, and the SH2 domain of Grb2. *Oncogene* **14**(7): 763-771.
52. Scott RP, Eketjall S, Aineskog H & Ibanez CF (2005) Distinct turnover of alternatively spliced isoforms of the RET kinase receptor mediated by differential recruitment of the Cbl ubiquitin ligase. *J Biol Chem* **280**(14): 13442-13449.
53. Richardson DS, Rodrigues DM, Hyndman BD, Crupi MJF, Nicolescu AC & Mulligan LM (2012) Alternative splicing results in RET isoforms with distinct trafficking properties. *Mol Biol Cell* **23**(19): 3838-3850.
54. Alberti L, Borrello MG, Ghizzoni S, Torriti F, Rizzetti MG & Pierotti MA (1998) Grb2 binding to the different isoforms of Ret tyrosine kinase. *Oncogene* **17**(9): 1079-1087.
55. Hyndman BD, Crupi MJF, Peng S, Bone LN, Rekab AN, Lian EY, Wagner SM, Antonescu CN & Mulligan LM (2017) Differential recruitment of E3-ubiquitin ligase complexes regulates RET isoform internalization. *Journal of Cell Science* **130**: 3282 - 3296.
56. Edery P, Lyonnet S, Mulligan LM, Pelet A, Dow E, Abel L, Holder S, Nihoul-Fekete C, Ponder BA & Munnich A (1994) Mutations of the RET proto-oncogene in Hirschsprung's disease. *Nature* **367**(6461): 378-380.
57. Attié T, Pelet A, Edery P, Eng C, Mulligan LM, Amiel J, Boutrand L, Beldjord C, Nihoul-Fekete C, Munnich A, et al. (1995) Diversity of RET proto-oncogene mutations in familial and sporadic Hirschsprung disease. *Hum Mol Genet* **4**(8): 1381-1386.
58. Kjaer S & Ibanez CF (2003) Intrinsic susceptibility to misfolding of a hot-spot for Hirschsprung disease mutations in the ectodomain of RET. *Hum Mol Genet* **12**(17): 2133-2144.
59. Mulligan LM, Eng C, Healey CS, Ponder MA, Feldman GL, Li P, Jackson CE & Ponder BA (1994) A de novo mutation of the RET proto-oncogene in a patient with MEN 2A. *Hum Mol Genet* **3**(6): 1007-1008.
60. Mulligan LM, Eng C, Healey CS, Clayton D, Kwok JB, Gardner E, Ponder MA, Frilling A, Jackson CE, Lehnert H, et al. (1994) Specific mutations of the RET proto-oncogene are related to disease phenotype in MEN 2A and FMTC. *Nature Genet* **6**(1): 70-74.
61. Wells SA Jr, Asa SL, Dralle H, Elisei R, Gagel RF, Lee N, Machens A, et al. (2015) Revised American Thyroid Association guidelines for the management of medullary thyroid carcinoma. *Thyroid* **25**(6): 567-610.

62. Grieco M, Santoro M, Berlingieri MT, Melillo RM, Donghi R, Bongarzone I, et al. (1990) PTC is a novel rearranged form of the ret proto-oncogene and is frequently detected in vivo in human thyroid papillary carcinomas. *Cell* **60**(4): 557-563.
63. Kohno T, Ichikawa H, Totoki Y, Yasuda K, Hiramoto M, Nammo T, Sakamoto H, Tsuta K, et al. (2012) KIF5B-RET fusions in lung adenocarcinoma. *Nat Med* **18**(3): 375-377.
64. Lipson D, Capelletti M, Yelensky R, Otto G, Parker A, Jarosz M, Curran JA, Balasubramanian S, et al. (2012) Identification of new ALK and RET gene fusions from colorectal and lung cancer biopsies. *Nat Med* **18**(3): 382-4. 117
65. Li F, Feng Y, Fang R, Fang Z, Xia J, Han X, Liu XY, Chen H, Liu H & Ji H (2012) Identification of RET gene fusion by exon array analyses in "pan-negative" lung cancer from never smokers. *Cell Res* **22**(5): 928-931.
66. Takeuchi K, Soda M, Togashi Y, Suzuki R, Sakata S, Hatano S, Asaka R, et al. (2012) RET, ROS1 and ALK fusions in lung cancer. *Nat Med* **18**(3): 378-81.
67. Ballerini P, Struski S, Cresson C, Prade N, Toujani S, Deswarte C, et al. (2012) RET fusion genes are associated with chronic myelomonocytic leukemia and enhance monocytic differentiation. *Leukemia* **26**(11): 2384-2389.
68. Romei C & Elisei R (2012) RET/PTC Translocations and Clinico-Pathological Features in Human Papillary Thyroid Carcinoma. *Front Endocrinol (Lausanne)* **3**: 54.
69. Ito Y, Okada Y, Sato M, Sawai H, Funahashi H, Murase T, Hayakawa T & Manabe T (2005) Expression of glial cell line-derived neurotrophic factor family members and their receptors in pancreatic cancers. *Surgery* **138**(4): 788-794.
70. Zeng Q, Cheng Y, Zhu Q, Yu Z, Wu X, Huang K, Zhou M, Han S & Zhang Q (2008) The relationship between overexpression of glial cell-derived neurotrophic factor and its RET receptor with progression and prognosis of human pancreatic cancer. *J Int Med Res* **36**(4): 656-664.
71. Essegir S, Todd SK, Hunt T, Poulsom R, Plaza-Menacho I, Reis-Filho JS & Isacke CM (2007) A role for glial cell derived neurotrophic factor induced expression by inflammatory cytokines and RET/GFR alpha 1 receptor up-regulation in breast cancer. *Cancer Res* **67**(24):11732-11741.
72. Gattelli A, Nalvarte I, Boulay A, Roloff TC, Schreiber M, Carragher N, Macleod KK, Schleder M, Lienhard S, Kenner L, Torres-Arzayus MI & Hynes NE (2013) Ret inhibition decreases growth and metastatic potential of estrogen receptor positive breast cancer cells. *EMBO Mol Med* **5**(9):1335-1350.
73. Plaza-Menacho I, Morandi A, Robertson D, Pancholi S, Drury S, Dowsett M, Martin LA & Isacke CM (2010) Targeting the receptor tyrosine kinase RET sensitizes breast cancer cells to tamoxifen treatment and reveals a role for RET in endocrine resistance. *Oncogene* **29**(33): 4648-4657.

74. Dykstra M, Cherukuri A, Sohn HW, Tzeng SJ & Pierce SK (2003) Location is everything: lipid rafts and immune cell signaling. *Annu Rev Immunol* **21**: 457-481.
75. Nagao M, Ishizaka Y, Nakagawara A, Kohno K, Kuwano M, Tahira T, Itoh F, Ikeda I & Sugimura T (1990) Expression of ret Proto-oncogene in Human Neuroblastomas. *Cancer Science* **81**(4): 309-312.
76. Narita N, Tanemura A, Murali R, Scolyer RA, Huang S, Arigami T, Yanagita S, Chong KK, Thompson JF, Morton DL & Hoon DS (2009) Functional RET G691S polymorphism in cutaneous malignant melanoma. *Oncogene* **28**(34): 3058-3068.
77. Barr J, Amato CM, Robinson SE, Kounalakis N & Robinson WA (2012) The RET G691S polymorphism is a germline variant in desmoplastic malignant melanoma. *Melanoma Res* **22**(1): 92-95.
78. Flavin R, Finn SP, Choueiri TK, Ingoldsby H, Ring M, Barrett C, Rogers M, Smyth P, et al. (2012) RET protein expression in papillary renal cell carcinoma. *Urol Oncol* **30**(6): 900-905.
79. Dawson DM, Lawrence EG, MacLennan GT, Amini SB, Kung HJ, Robinson D, Resnick MI, Kursh ED, Pretlow TP & Pretlow TG (1998) Altered expression of RET protooncogene product in prostatic intraepithelial neoplasia and prostate cancer. *J Natl Cancer Inst* **90**(7): 519-523. 118
80. Mulligan LM, Timmer T, Ivanchuk SM, Campling BG, Young LC, et al. (1998) Investigation of the genes for RET and its ligand complex GDNF/GFR $\alpha$ -1 in small cell lung carcinoma. *Genes Chromosomes Cancer* **21**(4): 326-332.
81. Luo Y, Tsuchiya KD, Park D, Fausel R, Kannurn S, et al. (2013) RET is a potential tumor suppressor gene in colorectal cancer. *Oncogene* **32**(16): 2037-2047.
82. Spanheimer PM, Cyr AR, Gillum MP, Woodfield GW, Askeland RW & Weigel RJ (2014) Distinct pathways regulated by RET and estrogen receptor in luminal breast cancer demonstrate the biological basis for combination therapy. *Ann Surg* **259**(4): 793- 799.
83. Wells SA, Robinson BG, Gagel RF, Dralle H, Fagin JA, Santoro M, et al. (2012) Vandetanib in patients with locally advanced or metastatic medullary thyroid cancer: a randomized, double-blind phase III trial. *J Clin Oncol* **30**(2): 134-141.
84. Schlumberger M, Elisei R, Muller S, Schoffski P, Brose MS, et al. (2015) Final overall survival analysis of EXAM, an international, double-blind, randomized, placebocontrolled phase III trial of cabozantinib (Cabo) in medullary thyroid carcinoma (MTC) patients with documented RECIST progression at baseline. *Journal of Clinical Oncology* **33**(15): S6012.
85. Carlomagno F, Vitagliano D, Guida T, Ciardiello F, et al. (2002) ZD6474, an orally available inhibitor of KDR tyrosine kinase activity, efficiently blocks oncogenic RET kinases. *Cancer Research* **62**(24): 7284-7290.

86. Wedge SR, Ogilvie DJ, Dukes M, Kendrew J, Chester R, et al. (2002) ZD6474 inhibits vascular endothelial growth factor signaling, angiogenesis, and tumor growth following oral administration. *Cancer Research* **62**(16): 4645–4655.
87. Joly A (2006) Simultaneous blockade of VEGF and HGF receptors results in potent antiangiogenic and anti-tumor effects. *Eur J Cancer Supplements* **4**: 35.
88. Song M (2015) Progress in Discovery of KIF5B-RET Kinase Inhibitors for the Treatment of Non-Small-Cell Lung Cancer. *J Med Chem* **58**(9): 3672-3681.
89. Viola D, Valerio L, Molinaro E, Agate L, Bottici V, Biagini A, Lorusso L, et al. (2016) Treatment of advanced thyroid cancer with targeted therapies: ten years of experience. *Endocr Relat Cancer* **23**(4): R185-205.
90. Zhang J, Yang PL & Gray NS (2009) Targeting cancer with small molecule kinase inhibitors. *Nature Reviews Cancer* **9**(1): 28-39
91. Andreucci E, Francica P, Fearn A, Martin LA, Chiarugi P, Isacke CM & Morandi A (2016) Targeting the receptor tyrosine kinase RET in combination with aromatase inhibitors in ER positive breast cancer xenografts. *Oncotarget* **7**(49): 80543-80553.
92. Jemal A, Bray F, Center MM, Ferlay J, Ward E & Forman D (2011) Global Cancer Statistics. *A Cancer Journal for Clinicians* **61**(2): 69 – 90.
93. Jung SY, Rosenzweig M, Sereika SM, Linkov F, Brufsky A & Weissfeld JL (2012) Factors associated with mortality after breast cancer metastasis. *Cancer Causes Control* **23**(1):103 – 112.
94. Ferlay J, Shin HR, Bray F, Forman D, Mathers C & Parkin DM (2008) GLOBOCAN 2008. *International Journal of Cancer* **127**(12): 2893 – 2917.
95. Canadian Cancer Society, Statistics Canada, Public Health Agency of Canada, Provincial/Territorial Cancer Registries (2017) *Canadian Cancer Statistics. Toronto, ON: Canadian Cancer Society.*
96. Swanton C, Burrell RA & Futreal PA (2011) Breast cancer genome heterogeneity: a challenge to personalized medicine? *Breast Cancer Research* **13**(1): 104. 119
97. Polyak K (2011) Heterogeneity in breast cancer. *The Journal of Clinical Investigation* **121**(10): 3786 – 3788.
98. Bertucci F & Birnbaum D (2008) Reasons for breast cancer heterogeneity. *Journal of Biology* **7**(2): 6.
99. Goldhirsch A, Wood WC, Coates AS, Gelber RD, Thurlimann B & Senn JH (2011) Strategies for subtypes – dealing with the diversity of breast cancer: highlights of the St Gallen International Expert Consensus on the Primary Therapy of Early Breast Cancer. *Annals of Oncology* **22**(8): 1736 – 1747.

100. Schnitt SJ (2010) Classification and prognosis of invasive breast cancer: from morphology to molecular taxonomy. *Modern Pathology* **23**(Suppl 2): S60–S64.
101. Anders CK, Johnson R, Litton J, Phillips M & Bleyer A (2010) Breast Cancer Before Age 40 Years. *Semin Oncol* **36**(3): 237-249.
102. Malhotra GK, Zhao X, Band H & Band V (2010) Histological, molecular and functional subtypes of breast cancers. *Cancer Biol Ther* **10**(10): 955-960.
103. Giuliano AE, Connolly JL, Edge SB, Mittendorf EA, et al. (2017) Breast Cancer - Major changes in the American Joint Committee on Cancer eighth edition cancer staging manual. CA: *A Cancer Journal for Clinicians* **67**(4): 290-303.
104. Shak S (1999) Overview of the trastuzumab (Herceptin) anti-Her2 monoclonal antibody clinical program in HER2-overexpressing metastatic breast cancer. *Seminars in Oncology* **26**(4 Suppl 12): 71-77.
105. Cheang MC, Chia SK, Voduc D, Gao D, Leung S, et al. (2009) Ki67 Index, Her2 Status, and Prognosis of patients with luminal B breast cancer. *Journal of the National Cancer Institute* **101**(10): 736-750.
106. Finetti P, Cervera N, Charafe-Jauffret E, Chabannon C, et al. (2008) Sixteen-kinase gene expression identifies luminal breast cancers with poor prognosis. *Cancer Research* **68**(3): 767-776.
107. Sorlie T, Perou C, Tibshirani R, Aas T, Geisler S, et al. (2001) Gene expression patterns of breast carcinomas distinguish tumor subclasses with clinical implications. *PNAS* **98**(19): 10869 – 10874.
108. Bergamaschi A, Kim YH, Wang P, Sorlie T, et al. (2006) Distinct patterns of DNA copy number alteration are associated with different clinicopathological features and geneexpression subtypes of breast cancer. *Genes Chromosomes Cancer* **45**(11): 1033-1040.
109. Chin K, DeVries S, Fridlyand J, Spellman PT, et al. (2006) Genomic and transcriptional aberrations linked to breast cancer pathophysiologies. *Cancer Cell* **10**(6): 529-541.
110. Vincent-Salomon A, Gruel N, Lucchesi C, MacGrogan G, et al. (2007) Identification of typical medullary breast carcinoma as a genomic sub-group of basal-like carcinomas, a heterogeneous new molecular entity. *Breast Cancer Res* **9**(2): R24.
111. Rakha EA, Reis-Filho JS & Ellis IO (2008) Basal-Like Breast Cancer: A Critical Review. *Journal of Clinical Oncology* **26**(15): 2568-2581.
112. Prat A, Parker JS, Karginova O, Fan C, Livasy C, et al. (2010) Phenotypic and molecular characterization of the claudin-low intrinsic subtype of breast cancer. *Breast Cancer Research* **12**(5): R68.

113. Perou CM (2011) Molecular Stratification of Triple-Negative Breast Cancers. *The Oncologist* **15**(Suppl 5): 39-48.
114. Boulay A, Breuleux M, Stephan C, Fux C, Brisken C, et al. (2008) The Ret receptor tyrosine kinase pathway functionally interacts with the ERalpha pathway in breast cancer. *Cancer Res* **68**(10): 3743-3751. 120
115. Unger K, Wienberg J, Riches A, Hieber L, Walch A, Brown A, et al. (2010) Novel gene rearrangements in transformed breast cells identified by high-resolution breakpoint analysis of chromosomal aberrations. *Endocr Relat Cancer* **17**(1): 87-98.
116. Kan Z, Jaiswal BS, Stinson J, Janakiraman V, Bhatt D, et al. (2010) Diverse somatic mutation patterns and pathway alterations in human cancers. *Nature* **466**(7308): 869-873.
117. Nikolsky YS, Sviridov E, Yao J, et al. (2008) Genome-wide functional synergy between amplified and mutated genes in human breast cancer. *Cancer Research* **68**(22): 9532- 9540.
118. Morandi A, Martin LA, Gao Q, Pancholi S, Mackay A, et al. (2013) GDNF-RET signaling in ER-positive breast cancers is a key determinant of response and resistance to aromatase inhibitors. *Cancer Res* **73**(12): 3783-3795.
119. Kang J, Perry JK, Pandey V, Fielder GC, Mei B, et al. (2009) Artemin is oncogenic for human mammary carcinoma cells. *Oncogene* **28**(19): 2034-2045.
120. Stine ZE, McGaughey DM, Bessling SL, Li S & McCallion AS (2011) Steroid hormone modulation of RET through two estrogen responsive enhancers in breast cancer. *Human Molecular Genetics* **20**(19): 3746–3756.
121. Spanheimer PM, Park JM, Askeland RW, Kulak MV, et al. (2014) Inhibition of RET increases the efficacy of antiestrogen and is a novel treatment strategy for luminal breast cancer. *Clinical Cancer Research* **20**(8): 2115-2125.
122. Ridley AJ, Schwartz MA, Burridge K, Firtel RA, et al. (2003) Cell Migration: Integrating Signals from Front to Back. *Science* **302**(5651): 1704-1709.
123. Cabodi S, del Pilar Camacho-Leal M, Di Stefano P & Defilippi P (2010) Integrin signalling adaptors: not only figurants in the cancer story. *Nature Reviews Cancer* **10**(12): 858-870.
124. Seguin L, Desgrosellier JS, Weis SM & Cheresch DA (2015) Integrins and cancer: regulators of cancer stemness, metastasis, and drug resistance. *Trends in Cell Biology* **2**(4): 234-240.
125. Yao ES, Zhang H, Chen YY, Lee B, Chew K, Moore D & Park C (2007) Increased  $\beta$ 1 integrin is associated with decreased survival in invasive breast cancer. *Cancer Research* **67**(2): 659-664.
126. Bokel C & Brown NH (2002) Integrins in development: moving on, responding to, and sticking to the extracellular matrix. *Developmental Cell* **3**(3): 311-321.

127. Ridley AJ, Schwartz MA, Burridge K, Firtel RA, Ginsberg MH, et al. (2003) Cell migration: integrating signals from front to back. *Science* **302**(5651): 1704-1709.
128. Mitra SK, Hanson DA & Schlaepfer DD (2005) Focal adhesion kinase: in command and control of cell motility. *Nature Reviews Molecular Cell Biology* **6**(1): 56-68.
129. Deakin NO, Pignatelli J & Turner CE (2012) Diverse roles for the paxillin family of proteins in cancer. *Genes & Cancer* **3**(5-6): 362-370.
130. Short SM, Yoder BJ, Tarr SM, Prescott NL, et al. (2007) The expression of the cytoskeletal focal adhesion protein paxillin in breast cancer correlates with HER2 overexpression and may help predict response to chemotherapy: a retrospective immunohistochemical study. *The Breast Journal* **13**(2): 130-139.
131. Delon I & Brown NH (2007) Integrins and the actin cytoskeleton. *Current Opinion in Cell Biology* **19**(1): 43-50.
132. Murakami H, Iwashita T, Asai N, et al. (1999) Rho-dependent and -independent tyrosine phosphorylation of focal adhesion kinase, paxillin and p130Cas mediated by Ret kinase. *Oncogene* **18**(11): 1975-1982. 121
133. Cockburn JG, Richardson DS, Gujral TS & Mulligan LM (2010) RET-Mediated Cell Adhesion and Migration Require Multiple Integrin Subunits. *J Clin Endocrinol Metab* **95**(11): E342-E346.
134. Sandilands E, Serrels B, Wilkinson S & Frame MC (2012) Src-dependent autophagic degradation of Ret in FAK-signalling-defective cancer cells. *EMBO Rep* **13**(8): 733-740.
135. Plaza-Menacho I, Morandi A, Mologni L, Boender P, et al. (2011) Focal adhesion kinase (FAK) binds RET kinase via its FERM domain, priming a direct and reciprocal RETFAK transactivation mechanism. *J Biol Chem* **286**(19): 17292-17302.
136. Funahashi H, Takeyama H, Sawai H, Furuta A, et al (2003) Alteration of integrin expression by glial cell line-derived neurotrophic factor (GDNF) in human pancreatic cancer cells. *Pancreas* **27**(2): 190-196.
137. Soba P, Han C, Zheng Y, Perea D, et al. (2015) The Ret receptor regulates sensory neuron dendrite growth and integrin mediated adhesion. *Elife* **4**: p. e05491.
138. van Agthoven T, van Agthoven TL, Dekker A, van der Spek PJ, Vreede L & Dorssers LC (1998) Identification of BCAR3 by a random search for genes involved in antiestrogen resistance of human breast cancer cells. *EMBO J* **17**(10): 2799-2808.
139. Cai D, Clayton LK, Smolyar A & Lerner A (1999) AND-34, a Novel p130Cas-Binding Thymic Stromal Cell Protein Regulated by Adhesion and Inflammatory Cytokines. *J Immunol* **163**(4): 2104-2112.

140. Lu Y, Brush J & Stewart TA (1999) NSP1 defines a novel family of adaptor proteins linking integrin and tyrosine kinase receptors to the c-Jun N-terminal kinase/stress-activated protein kinase signalling pathway. *Journal of Biological Chemistry* **274**(15): 10047-10052.
141. Cai D, Iyer A, Felekis KN, Near RI, Luo Z, et al. (2003) AND-34/BCAR3, a GDP exchange factor whose overexpression confers antiestrogen resistance, activates Rac, PAK1, and the cyclin D1 promoter. *Cancer Res* **63**(20): 6802-6808.
142. Mace PD, Wallez Y, Dobaczewska MK, et al (2011) NSP-Cas protein structures reveal a promiscuous interaction module in cell signaling. *Nat Struct Mol Biol* **18**(12): 1381-1387.
143. Vervoort VS, Roselli S, Oshima RG & Pasquale EB (2007) Splice variants and expression patterns of SHEP1, BCAR3 and NSP1, a gene family involved in integrin and receptor tyrosine kinase signaling. *Gene* **391**(1-2):161-170.
144. Near RI, Smith RS, Toselli PA, Freddo TF, Bloom AB, et al. (2009) Loss of AND34/BCAR3 expression in mice results in rupture of the adult lens. *Molecular Vision* **15**: 685-699.
145. Dorssers LC, van Agthoven T, Dekker A, van Agthoven TL & Kok EM (1993) Induction of antiestrogen resistance in human breast cancer cells by random insertional mutagenesis using defective retroviruses: Identification of bcar-1, a common integration site. *Molecular Endocrinology* **7**(7): 870-878.
146. Brinkman A, van der Flier S, Kok EM & Dorssers LC (2000) BCAR1, a human homologue of the adapter protein p130Cas, and antiestrogen resistance in breast cancer cells. *Journal of the National Cancer Institute* **92**(2):112-120.
147. Cai D, Felekis KN, Near RI, O'Neill GM, et al. (2003) The GDP exchange factor AND34 is expressed in B cells, associates with HEF1, and activates Cdc42. *J Immunol* **170**(2): 969-78.
148. Sun G, Cheng SYS, Chen M, Lim CJ & Pallen CJ (2012) Protein tyrosine phosphatase alpha phosphotyrosyl-789 binds BCAR3 to position Cas for activation at integrin-mediated focal adhesions. *Mol Cell Biol* **32**(18): 3776-3789.
149. Oh MJ, van Agthoven T, Choi JE, Jeong YJ, Chung YH, et al. (2008) BCAR3 regulates EGF-induced DNA synthesis in normal human breast MCF-12A cells. *Biochemical and Biophysical Research Communications* **375**(3): 430-434.
150. Li C, Wang S, Xing Z, Lin A, Liang K, et al. (2017) A ROR1-HER3-lncRNA signalling axis modulates the Hippo-YAP pathway to regulate bone metastasis. *Nat Cell Biol.* **19**(2): 106-119.
151. Rufanova VA & Sorokin A (2006) CrkII associates with BCAR3 in response to endothelin-1 in human glomerular mesangial cells. *Experimental Biology and Medicine* **231**(6): 752-756.
152. Wilson AL, Schrecengost RS, Guerrero MS, Thomas KS & Bouton AH (2013) Breast Cancer Antiestrogen Resistance 3 (BCAR3) Promotes Cell Motility by Regulating Actin

Cytoskeletal and Adhesion Remodeling in Invasive Breast Cancer Cells. *PLoS ONE* **8**(6): e65678.

153. Near RI, Zhang Y, Makkinje A, Vanden Borre P & Lerner A (2007) AND-34/BCAR3 differs from other NSP homologs in induction of anti-estrogen resistance, cyclin D1 promoter activation and altered breast cancer cell morphology. *J Cell Physiol* **212**(3): 655-665.

154. Guo J, Canaff L, Rajadurai CV, Fils-Aime N, Tian J, et al. (2014) Breast cancer antiestrogen resistance 3 inhibits transforming growth factor beta/Smad signaling and associates with favorable breast cancer disease outcomes. *Breast Cancer Res* **16**(6): 476.

155. van Agthoven T, Sieuwerts AM, Meijer-van Gelder ME, Look MP, et al. (2009) Relevance of breast cancer antiestrogen resistance genes in human breast cancer progression and tamoxifen resistance. *Journal of Clinical Oncology* **27**(4): 542-549.

156. Cross AM, Wilson AL, Guerrero MS, Thomas KS, et al. (2016) Breast cancer antiestrogen resistance 3-p130Cas interactions promote adhesion disassembly and invasion in breast cancer cells. *Oncogene* **35**(45): 5850-5859.

157. Vanden Borre P, Near RI, Makkinje A, Mostoslavsky G & Lerner A (2011) BCAR3/AND-34 can signal independent of complex formation with CAS family members or the presence of p130Cas. *Cellular Signalling* **23**(6): 1030-1040.

158. Felekis KN, Narsimhan RP, Near R, Castro AF, et al. (2005) AND-34 activates phosphatidylinositol 3-kinase and induces anti-estrogen resistance in a SH2 and GDP exchange factor-like domain-dependent manner. *Mol Cancer Res* **3**(1): 32-41.

159. Felekis KN, Narsimhan RP, Near R, Castro AF, Zheng Y, Quilliam LA & Lerner A (2005) AND-34 Activates Phosphatidylinositol 3-Kinase and Induces Anti-Estrogen Resistance in a SH2 and GDP Exchange Factor-Like Domain-Dependent Manner. *Molecular Cancer Research* **3**(1): 32-41.

160. Wallez Y, Riedl SJ & Pasquale EB (2014) Association of the Breast Cancer Antiestrogen Resistance Protein 1 (BCAR1) and BCAR3 Scaffolding Proteins in Cell Signaling and Antiestrogen Resistance. *Journal of Biological Chemistry* **289**(15): 10431-10444.

161. Schuh NR, Guerreo MS, Schrecengost BS & Bouton AH (2010) BCAR3 regulates Src/p130 Cas association, Src kinase activity, and breast cancer adhesion signaling. *J Biol Chem* **285**(4): 2309-17.

162. Rufanova VA, Alexanian A, Wakatsuki T, Lerner A & Sorokin A (2009) Pyk2 mediates endothelin-1 signaling via p130Cas/BCAR3 cascade and regulates human glomerular mesangial cell adhesion and spreading. *Journal of Cellular Physiology* **219**(1): 45-56.

163. Ibrahim R, Lemoine A, Bertoglio J & Raingeaud J (2015) Human enhancer of filamentation 1-induced colorectal cancer cell migration: Role of serine phosphorylation 123 and interaction with the breast cancer anti-estrogen resistance 3 protein. *Int J Biochem Cell Biol* **64**: 45-57.

164. Green YS, Kwon S & Christian JL (2016) Expression pattern of bcar3, a downstream target of Gata2, and its binding partner, bcar1, during *Xenopus* development. *Gene Expr Patterns* **20**(1): 55-62.
165. Pennekamp P, Feldner S, Seesing FJ, Psathaki OE, Scholer HR, Wieacker P, Dworniczak B (2011) Bcar3 is expressed in sertoli cells and germ cells of the developing testis in mice. *Sex Dev* **5**(4): 197-204.
166. Kondo T, Nakamori T, Nagai H, Takeshita A, Kusakabe KT & Okada T (2016) A novel spontaneous mutation of BCAR3 results in extrusion cataracts in CF#1 mouse strain. *Mammalian Genome* **27**(9-10): 451-459.
167. Koytiger G, Kaushanksy A, Gordus A, Rush J, Sorger PK & MacBeath G (2013) Phosphotyrosine Signaling Proteins that Drive Oncogenesis Tend to be Highly Interconnected. *Molecular & Cellular Proteomics* **12**(5):1204-1213.
168. Oh MJ, van Agthoven T, Choi JE, Jeong YJ, Chung YH, et al. (2008) BCAR3 regulates EGF-induced DNA synthesis in normal human breast MCF-12A cells. *Biochem Biophys Res Commun* **375**(3): 430-434.
169. Schrecengost RS, Riggins RB, Thomas KS, Guerrero MS & Bouton AH (2007) Breast cancer antiestrogen resistance-3 expression regulates breast cancer cell migration through promotion of p130Cas membrane localization and membrane ruffling. *Cancer Res* **67**(13): 6174-6182.
170. Oh MJ, Yi SJ, Kim HS, Kim JH, Jeong YH, van Agthoven T & Jhun BH (2013) Functional roles of BCAR3 in the signaling pathways of insulin leading to DNA synthesis, membrane ruffling and GLUT4 translocation. *Biochem Biophys Res Commun* **441**(4): 911-916.
171. Attie-Bitach T, Abitbol M, Gerard M, Delezoide AL, et al. (1998) Expression of the RET proto-oncogene in human embryos. *Am J Med Genet* **80**(5): 481-486.
172. Arighi E, Borrello MG & Sariola H (2005) RET tyrosine kinase signaling in development and cancer. *Cytokine Growth Factor Rev* **16**(4-5): 441-467.
173. Morandi A, Plaza-Menacho I & Isacke CM (2011) RET in breast cancer: functional and therapeutic implications. *Trends Mol Med* **17**(3): 149-157.
174. Ginsburg OB, Bray F, Coleman MP, Vanderpuye V, Eniu A, et al. (2017) The global burden of women's cancers: a grand challenge in global health. *The Lancet* **389**(10071): 847-860.
175. Prat A & Perou CM (2011) Deconstructing the molecular portraits of breast cancer. *Molecular Oncology* **5**(1): 5-23.
176. Goodman, SL & Picard M (2012) Integrins as therapeutic targets. *Trends Pharmacol Sci.* **33**(7): 405-412.

177. dos Santos PB, Zanetti JS, Riberio-Silva A & Beltrao EI (2012) Beta 1 integrin predicts survival in breast cancer: a clinicopathological and immunohistochemical study. *Diagn Pathol* **7**: 104.
178. Ginzinger DG (2002) Gene quantification using real-time quantitative PCR: an emerging technology hits the mainstream. *Exp Hematol* **30**(6): 503-512.
179. Neve RM, Chin K, Fridlyand J, Yeh J, Baehner FL, et al. (2006) A collection of breast cancer cell lines for the study of functionally distinct cancer subtypes. *Cancer Cell* **10**(6): 515-527.
180. Naveilhan P, Baudet C, Mikaelis A, Shen L, Westphal H & Ernfors P (1998) Expression and regulation of GFRalpha3, a glial cell line-derived neurotrophic factor family receptor. *Proc Natl Acad Sci U S A* **95**(3): 1295-1300.
181. Watanabe T, Ichihara M, Hashimoto M, et al. (2002) Characterization of gene expression induced by RET with MEN2A or MEN2B mutation. *Am J Pathol* **161**(1): 249-256.
182. Califano D, Monaco C, de Vita G, D'Alessio A, et al. (1995) Activated RET/PTC oncogene elicits immediate early and delayed response genes in PC12 cells. *Oncogene* **11**(1): 107-112.
183. Griseri P, Garrone O, Lo Sardo A, Monteverde M, et al. (2016) Genetic and epigenetic factors affect RET gene expression in breast cancer cell lines and influence survival in patients. *Oncotarget* **7**(18): 26465-26479.
184. Ivanchuk SM, Myers SM & Mulligan LM (1998) Expression of alternatively spliced RET transcripts in the developing human kidney and Wilms tumor. *Oncogene* **16**(8): 991-996.
185. Melloni GEM, Mazzarella L, Bernard L, Bodini M, et al. (2017) A knowledge-based framework for the discovery of cancer-predisposing variants using large-scale sequencing breast cancer data. *Breast Cancer Res* **19**(1): p. 63.
186. Ban K, Feng S, Shao L & Ittmann M (2017) RET Signaling in Prostate Cancer. *Clin Cancer Res* **23**(16): 4885-4896.
187. Eng C, Mulligan LM, Smith DP, Healey CS, Frilling A, et al (1995) Mutation of the RET protooncogene in sporadic medullary thyroid carcinoma. *Genes Chrom Canc* **12**(3): 209- 212.
188. Oh MJ, Yi SJ, Kim HS, Kim JH, et al. Functional roles of BCAR3 in the signaling pathways of insulin leading to DNA synthesis, membrane ruffling and GLUT4 translocation. *Biochemical and Biophysical Research Communications* **441**(4): 911-916.
189. Makkinje A, Vanden Borre P, Near RI, Patel PS & Lerner A (2012) Breast cancer antiestrogen resistance 3 (BCAR3) protein augments binding of the c-Src SH3 domain to Crk-associated substrate (p130cas) *Journal of Biological Chemistry* **287**(33): 27703- 27714.
190. Schrecengost RS, Riggins RB, Thomas KS, Guerrero MS & Bouton AH (2007) Breast cancer antiestrogen resistance-3 expression regulates breast cancer cell migration through

promotion of p130Cas membrane localization and membrane ruffling. *Cancer Research* **67**(13): 6174-6182.

191. Brantley MA Jr, Jain S, Barr EE, Johnson EM Jr & Milbrandt J (2008) Neurturin-mediated RET activation is required for retinal function. *J Neurosci* **28**(16): 4123-4135.

192. Laukaitis, CM, Webb DJ, Donais K & Horwitz AF (2001) Differential dynamics of alpha 5 integrin, paxillin, and alpha-actinin during formation and disassembly of adhesions in migrating cells. *J Cell Biol* **153**(7): 1427-1440.

193. Bhatt A, Kaverina I, Otey C & Huttenlocher A (2002) Regulation of focal complex composition and disassembly by the calcium-dependent protease calpain. *J Cell Sci* **115**(Pt 17): 3415-3425.

194. Janostiak R, Brabek J, Auernheimer V, et al. (2014) CAS directly interacts with vinculin to control mechanosensing and focal adhesion dynamics. *Cell Mol Life Sci* **71**(4): 727- 744.

195. Gujral TS, Singh VK, Jia Z & Mulligan LM (2006) Molecular Mechanisms of RET Receptor-Mediated Oncogenesis in Multiple Endocrine Neoplasia 2B. *Cancer Res* **66**(22): 10741-10749.

196. Crupi MJ, Yoganathan P, Bone LN, Lian E, Fetz A, Antonescu CN & Mulligan LM (2015). Distinct Temporal Regulation of RET Isoform Internalization: Roles of Clathrin and AP2. *Traffic* **16**(11):1155-1173.

197. Bustin SA (2002) Quantification of mRNA using real-time reverse transcription PCR (RT-PCR): trends and problems. *J Mol Endocrinol* **29**(1): 23-39.

198. Gorelik R & Gautreau A (2014) Quantitative and unbiased analysis of directional persistence in cell migration. *Nat Protoc* **9**(8): 1931-1943.

199. Luckert K, Gujral TS, Chan M, Sevecka M, et al. (2013) A dual array-based approach to assess the abundance and post-translational modification state of signaling proteins. *Sci Signal* **5**(206): pI1.

200. Richardson DS, Gujral TS, Peng S, Asa SL & Mulligan LM (2009) Transcript level modulates the inherent oncogenicity of RET/PTC oncoproteins. *Cancer Res* **69**(11): 4861-4869.

201. Wallez Y, Mace PD, Pasquale EB & Riedl SJ (2012) NSP-CAS Protein Complexes: Emerging Signaling Modules in Cancer. *Genes Cancer* **3**(5-6): p. 382-393.

202. Maruyama I. (2014) Mechanisms of activation of receptor tyrosine kinases: monomers or dimers. *Cells* **3**(2): 304-330.

203. Ignatiadis M & Sotiriou C (2013) Luminal breast cancer: from biology to treatment. *Nature Reviews Clinical Oncology* **10**: 494-506.

204. Hatem R, Labiod D, Chateau-Joubert S, et al. (2016) Vandetanib as a potential new treatment for estrogen receptor-negative breast cancers. *Int J Cancer* **138**(10): 2510-2521.
205. Toledo RA, Hatakana R, Lourenco DM Jr, Lindsey SC, et al. (2015) Comprehensive assessment of the disputed RET Y791F variant shows no association with medullary thyroid carcinoma susceptibility. *Endocr Relat Cancer* **22**(1): 65-76.
206. Abmayr SM, Yao T, Parmely T & Workman JL (2006) Preparation of Nuclear and Cytoplasmic Extracts from Mammalian Cells. *Current Protocols in Molecular Biology* **75**:12.1:12.1.1-12.1.10.
207. Banerjee A, Wu ZS, Qian P, Kang J, et al. (2011) Artemin synergizes with TWIST1 to promote metastasis and poor survival outcome in patients with ER negative mammary carcinoma. *Breast Cancer Res* **13**(6): R112.
208. Ibrahim R, Lemoine A, Bertoglio J & Raingeaud J (2015) Human enhancer of filamentation 1-induced colorectal cancer cell migration: Role of serine phosphorylation and interaction with the breast cancer anti-estrogen resistance 3 protein. *The International Journal of Biochemistry & Cell Biology* **64**: 45-57.
209. Bianchini G, Balko JM, Mayer IA, Sanders ME & Gianni L (2016) Triple-negative breast cancer: challenges and opportunities of a heterogeneous disease. *Nat Rev Clin Oncol* **13**(11): 674-690.
210. Delahaye LJMJ, Drukker CA, Dreezen C, Witteveen A, et al. (2017) A breast cancer gene signature for indolent disease. *Breast Cancer Res Treat* **164**(2): 461-466.
211. Wang C, Mayer JA, Mazumdar A & Brown PH (2012) The rearranged during transfection/papillary thyroid carcinoma tyrosine kinase is an estrogen-dependent gene required for the growth of estrogen receptor positive breast cancer cells. *Breast Cancer Res Treat* **133**(2): 487-500.
212. Tolaney SN, Nechushtan H, Ron IG, Schoffski P, et al. (2016) Cabozantinib for metastatic breast carcinoma: results of a phase II placebo-controlled randomized discontinuation study. *Breast Cancer Res Treat* **160**(2): 305-312.
213. Rosell, R & Karachaliou N (2016) RET inhibitors for patients with RET fusion-positive and RET wild-type non-small-cell lung cancer. *The Lancet Oncology* **17**(12): 1623-1625.
214. Chau, NG & Haddad RI (2013) Vandetanib for the treatment of medullary thyroid cancer. *Clin Cancer Res* **19**(3): 524-529.
215. de Boer RH (2013) Vandetanib in advanced non small cell lung cancer: a promise unfulfilled. *Transl Lung Cancer Res* **2**(1): E7-E9.
216. Middleton GP, Palmer DH, Greenhalf W, Ghaneh P, et al. (2017) Vandetanib plus gemcitabine versus placebo plus gemcitabine in locally advanced or metastatic pancreatic

carcinoma (ViP): a prospective, randomised, double-blind, multicentre phase 2 trial. *Lancet Oncol* **18**(4): 486-499.

217. Mogni L (2016) RET Kinase Inhibitors: A review of recent patents (2012-2015). *Expert Opin Ther Pat* **27**(1): 91-99.